

Final Seismic Shake Table Test Plan

Spent Fuel and Waste Disposition

***Prepared for
US Department of Energy
Spent Fuel and Waste Science and
Technology
Elena Kalinina, Doug Ammerman,
Kevin Stovall, and Byron
Demosthenous
Sandia National Laboratories
Taylor Mason
Pacific Northwest National Laboratory
September 13, 2023
Milestone Number M3SF-23SN010202024
SAND2023-10436 R***

DISCLAIMER

This information was prepared as an account of work sponsored by an agency of the U.S. Government. Neither the U.S. Government nor any agency thereof, nor any of their employees, makes any warranty, expressed or implied, or assumes any legal liability or responsibility for the accuracy, completeness, or usefulness, of any information, apparatus, product, or process disclosed, or represents that its use would not infringe privately owned rights. References herein to any specific commercial product, process, or service by trade name, trade mark, manufacturer, or otherwise, does not necessarily constitute or imply its endorsement, recommendation, or favoring by the U.S. Government or any agency thereof. The views and opinions of authors expressed herein do not necessarily state or reflect those of the U.S. Government or any agency thereof.



Sandia National Laboratories

Sandia National Laboratories is a multi-mission laboratory managed and operated by National Technology & Engineering Solutions of Sandia, LLC., a wholly owned subsidiary of Honeywell International, Inc., for the U.S. Department of Energy's National Nuclear Security Administration under contract DE-NA0003525.



APPENDIX E
NFCSC DOCUMENT COVER SHEET¹

Name/Title: Seismic Shake Table Final Test Plan

Deliverable/Milestone/Revision No.: M3SF-23SN0102020224

Work Package Title and Number: External Loads, M3SF-23SN01020202

Work Package WBS Number: 1.08.01.02.02

Responsible Work Package Manager: Elena Kalinina



(Name/Signature)

Date Submitted: 09-13-23

| | | | | |
|--|---|--------------------------------|---|---|
| Quality Rigor Level for Deliverable/Milestone ² | <input type="checkbox"/> QRL-1 <input type="checkbox"/> Nuclear Data | <input type="checkbox"/> QRL-2 | <input checked="" type="checkbox"/> QRL-3 | <input type="checkbox"/> QRL-4 Lab QA Program ³ |
|--|---|--------------------------------|---|---|

This deliverable was prepared in accordance with

_____ (Participant/National Laboratory Name)

QA program which meets the requirements of

- DOE Order 414.1 NQA-1 Other

This Deliverable was subjected to:

- Technical Review Peer Review

Technical Review (TR)

Review Documentation Provided

- Signed TR Report or,
 Signed TR Concurrence Sheet or,
 Signature of TR Reviewer(s) below

Peer Review (PR)

Review Documentation Provided

- Signed PR Report or,
 Signed PR Concurrence Sheet or,
 Signature of PR Reviewer(s) below

Name and Signature of Reviewers

Hector Mendoza

NOTE 1: Appendix E should be filled out and submitted with the deliverable. Or, if the PICS:NE system permits, completely enter all applicable information in the PICS:NE Deliverable Form. The requirement is to ensure that all applicable information is entered either in the PICS:NE system or by using the NFCSC Document Cover Sheet.

- In some cases there may be a milestone where an item is being fabricated, maintenance is being performed on a facility, or a document is being issued through a formal document control process where it specifically calls out a formal review of the document. In these cases, documentation (e.g., inspection report, maintenance request, work planning package documentation or the documented review of the issued document through the document control process) of the completion of the activity, along with the Document Cover Sheet, is sufficient to demonstrate achieving the milestone.

NOTE 2: If QRL 1, 2, or 3 is not assigned, then the QRL 4 box must be checked, and the work is understood to be performed using laboratory QA requirements. This includes any deliverable developed in conformance with the respective National Laboratory / Participant, DOE or NNSA-approved QA Program.

NOTE 3: If the lab has an NQA-1 program and the work to be conducted requires an NQA-1 program, then the QRL-1 box must be checked in the work Package and on the Appendix E cover sheet and the work must be performed in accordance with the Lab's NQA-1 program. The QRL-4 box should not be checked.

This page is intentionally left blank.

EXECUTIVE SUMMARY

The Spent Fuel Waste Disposition (SFWD) program is planning to conduct a full-scale seismic shake table test on the dry storage systems of spent nuclear fuel (SNF) to close the gap related to seismic loads on fuel assemblies in dry storage systems. This test will allow for quantifying the strains and accelerations on surrogate fuel assembly hardware and cladding during earthquakes of different magnitudes and frequency content.

Full-scale testing is needed because a dry storage system is a complex and highly nonlinear system making it hard to predict (model) the responses to seismic excitations. The non-linearity arises from the multiple spatial gaps in the system – between fuel rods and the basket, between the basket and dry storage canister, between the dry storage canister and the storage cask (overpack), and ventilation gaps. The non-linearities pose significant limitations on the value of tests with scaled systems.

This report documents the final test plan of the seismic shake table test. The major purpose of this report is to provide:

- Recommendations for selection of acceleration time histories (THs) to be implemented in the shake table test,
- Update regarding the test unit hardware,
- Update regarding the concrete slab to be installed on the shake table,
- Update regarding instrumentation, and
- A description of the test activities and schedule.

This page left intentionally blank.

ACKNOWLEDGEMENTS

The authors would like to express their appreciation to Ned Larson (DOE NE) who has been providing continuing support for the External Loads work. Because of his support, we will be able to close the gap related to the integrity of spent nuclear fuel (SNF) in extended dry storage. The authors would also like to thank the UCSD professors José Restrepo, Joel Conte, and Koorosh Lotfizadeh. Their suggestions were essential for the development of the test plan.

This page is intentionally left blank.

CONTENTS

| | |
|--|------|
| EXECUTIVE SUMMARY | v |
| ACKNOWLEDGEMENTS | vii |
| LIST OF FIGURES | xi |
| LIST OF TABLES | xiii |
| ACRONYMS | xvi |
| 1. INTRODUCTION | 18 |
| 2. RECOMMENDATIONS FOR SELECTING ACCELERATION TIME HISTORIES | 22 |
| 2.1 Proposed Acceleration Time Histories for the CEUS Hard Rock Sites | 23 |
| 2.2 Results of Soil-Structure Interaction Analyses | 25 |
| 2.3 Proposed Acceleration Time Histories for the CEUS Soil and Soft Rock Sites | 30 |
| 2.4 Proposed Acceleration Time Histories for the WUS Soil and Soft Rock Sites | 31 |
| 2.5 Shake Table Simulations | 33 |
| 2.6 Shake Table Training | 36 |
| 3. TEST UNIT HARDWARE | 38 |
| 3.1 NUHOMS 32 PTH2 Dry Storage Canister | 38 |
| 3.2 Dummy Assemblies and Surrogate Assemblies | 41 |
| 3.2.1 Dummy Fuel Assemblies | 41 |
| 3.2.2 Surrogate Fuel Assemblies | 45 |
| 3.2.3 Dummy and Surrogate Assemblies Loading Map | 49 |
| 3.3 Dry Storage Overpacks | 51 |
| 3.3.1 Vertical Storage Overpack | 51 |
| 3.3.2 Horizontal Storage Overpack | 56 |
| 3.4 Safety Rigging | 57 |
| 4. CONCRETE SLAB ON THE SHAKE TABLE | 60 |
| 4.1 Recommended Concrete Surface Finish | 60 |
| 4.2 Proposed Concrete Slab Configuration | 64 |
| 5. INSTRUMENTATION AND PHOTOMETRICS | 66 |
| 5.1 Summary of Results Important for Instrumentation | 66 |
| 5.2 Surrogate and Dummy Assembly Instrumentation | 67 |
| 5.2.1 Surrogate Assemblies | 67 |
| 5.2.2 Dummy Assemblies | 71 |
| 5.3 Canister, Cask, and Trough Instrumentation | 72 |
| 5.4 Instrumentation Summary | 73 |
| 5.5 Data Acquisition System | 74 |
| 5.6 Photometrics | 76 |
| 6. TEST ACTIVITIES AND SCHEDULE | 80 |
| 6.1 Pre-Test Activities | 80 |
| 6.2 Test Activities | 82 |

| | | |
|-------|------------------------|----|
| 6.2.1 | Prerequisites | 82 |
| 6.2.2 | Activity Details | 82 |
| 6.3 | Test Schedule | 88 |
| 7. | REFERENCES | 90 |

LIST OF FIGURES

| | | |
|--------------|---|----|
| Figure 1-1. | Seismic shake table test roadmap. | 18 |
| Figure 2-1. | Conceptual representation of a dry storage system located on hard rock and soft rock/soil for the shake table test..... | 23 |
| Figure 2-2. | Mineral (VA) earthquake time histories, containment basemat [18]..... | 25 |
| Figure 2-3. | Model of an ISFSI pad with vertical casks. | 26 |
| Figure 2-4. | Model of an ISFSI pad with HSMs..... | 27 |
| Figure 2-5. | Response of the top of the pad with vertical casks (Configuration 1) compared to the free-field in CEUS soil scenario 1 (M 5.5, D 15 km, PGA 0.56 g, TH1). | 27 |
| Figure 2-6. | Peak amplification frequencies in CEUS and WUS soil and soft rock scenarios..... | 28 |
| Figure 2-7. | Amplifications in scenario 4, CEUS soft rock, magnitude 5.5, distance 15 km, PGA 0.25 g. | 29 |
| Figure 2-8. | Locations on the pad with the maximum Z acceleration in CEUS soil scenarios. | 29 |
| Figure 2-9. | Scenario 1, X-direction, RMSE between the target and achieved time histories (left) and response spectra (right). | 35 |
| Figure 3-1. | NUHOMS 32 PTH2 Schematics. | 38 |
| Figure 3-2. | NUHOMS 32 PTH2 Basket..... | 39 |
| Figure 3-3. | NUHOMS 24 PTH egg crate basket design. | 40 |
| Figure 3-4. | NUHOMS 32 PTH2 basket tube measurement. | 40 |
| Figure 3-5. | NUHOMS 32 PTH2 dry storage canisters at the SNL facility. | 41 |
| Figure 3-6. | Four aluminum plates bolted to the steel tube in one of five locations..... | 42 |
| Figure 3-7. | Dummy assembly overall view..... | 42 |
| Figure 3-8. | Dummy assembly main components. | 43 |
| Figure 3-9. | Statistics of the dummy assembly actual weights..... | 45 |
| Figure 3-10. | Dummy assembly in the delivery truck (left) and unloaded at the LHPOST (right). | 45 |
| Figure 3-11. | KNF's 16 x 16 CE PLUS7 surrogate assembly. | 46 |
| Figure 3-12. | KNF's 17 x 17 Westinghouse ACE7 surrogate assembly. | 46 |
| Figure 3-13. | Photos of 16 x 16 CE PLUS7 (left) and 17 x 17 Westinghouse ACE7 (right). | 47 |
| Figure 3-14. | SNL 17x17 surrogate assembly (left) and closeup of the spacer grid (right). | 48 |
| Figure 3-15. | New full-scale surrogate assembly photo. | 49 |
| Figure 3-16. | Canister loading map for the tests with the vertical cask..... | 50 |
| Figure 3-17. | Canister loading map for the tests with the trough. | 51 |
| Figure 3-18. | Vertical cask over all view and cross-sectional view. | 52 |
| Figure 3-19. | Cask arrival to LHPOST (UCSD)..... | 53 |
| Figure 3-20. | Pouring concrete into the cask (top and bottom left) and filled with concrete cask (bottom right). | 54 |
| Figure 3-21. | Completed vertical cask covered with the tarp (left) and concrete samples (right). | 55 |
| Figure 3-22. | Vertical cask mockup (left) and HI-STORM 100 vertical overpack (right). | 56 |
| Figure 3-23. | AHSMs base units at SONGS..... | 56 |
| Figure 3-24. | Mockup of the AHSM (trough design) and Trough Frame at the Manufacturing Facility. | 57 |

| | | |
|--------------|--|----|
| Figure 3-25. | Proposed design of the safety rigging..... | 58 |
| Figure 4-1. | Surface roughness levels and corresponding concrete profile per CSP classification by ICRI. | 61 |
| Figure 4-2. | Static friction between steel plate and different concrete finishes..... | 61 |
| Figure 4-3. | Steel block used in push-off friction tests..... | 62 |
| Figure 4-4. | Static friction between steel block and unfinished concrete surfaces..... | 62 |
| Figure 4-5. | Static friction coefficients from the friction tests and literature. | 63 |
| Figure 4-6. | Concrete slab position on the shake table. | 64 |
| Figure 4-7. | Anchoring Trough to the Shake Table..... | 65 |
| Figure 4-8. | Anchoring vertical cask to the shake table..... | 65 |
| Figure 5-1. | 3D distribution of peak strains on the rods in CEUS hard rock (left) and soil scenario (right), seismic hazard 5×10^{-5} from [32]..... | 66 |
| Figure 5-2. | 3D distribution of peak strains on the rods and guide tubes in WUS soft rock Diablo Canyon scenario..... | 67 |
| Figure 5-3. | Surrogate assembly rod to be instrumented. | 68 |
| Figure 5-4. | Strain gauge CEA-03-062UW-350 (left, not actual size) and accelerometer 727-2K (right, not actual size)..... | 69 |
| Figure 5-5. | Surrogate assembly instrumentation diagram..... | 69 |
| Figure 5-6. | Pressure paper locations and specifications..... | 70 |
| Figure 5-7. | Taping down the fiber sensor starting from the termination..... | 71 |
| Figure 5-8. | Block of three uniaxial accelerometers and its location on the dummy assembly..... | 72 |
| Figure 5-9. | Locations of tri-axial and bi-axial accelerometers on the dummy assemblies..... | 72 |
| Figure 5-10. | Sensor locations on the canister, vertical cask, and trough..... | 73 |
| Figure 5-11. | Althen LCF-3000 digital inclinometer..... | 73 |
| Figure 5-12. | New LHPOST data acquisition system..... | 75 |
| Figure 5-13. | Schematic diagram of a single DAQ node..... | 75 |
| Figure 5-14. | Triggering mechanism connecting the MTS 469D shake table controller to the video capture and DAQ systems..... | 76 |
| Figure 5-15. | Setup for the vertical cask tests in north–south direction. | 77 |
| Figure 5-16. | Setup for the vertical cask tests in west-east direction..... | 78 |
| Figure 5-17. | Overhead view of the vertical cask setup. | 78 |
| Figure 5-18. | Overhead view of the trough setup. | 79 |
| Figure 6-1. | Assembly Restraining Fixture..... | 81 |
| Figure 6-2. | Shake table test schedule. | 89 |

LIST OF TABLES

| | | |
|-------------|--|----|
| Table 2-1. | Classification of the CEUS sites. | 22 |
| Table 2-2. | Proposed time histories for CEUS hard rock conditions. | 24 |
| Table 2-3. | PGAs in Mineral (VA) earthquake compared to the design based PGA [17]. | 25 |
| Table 2-4. | Soil and soft rock SSI scenarios..... | 26 |
| Table 2-5. | Proposed time histories for CEUS soil conditions..... | 30 |
| Table 2-6. | Proposed time histories for CEUS soft rock conditions. | 31 |
| Table 2-7. | Proposed time histories for WUS soil conditions. | 32 |
| Table 2-8. | Proposed time histories for WUS soft rock conditions..... | 33 |
| Table 2-9. | Performance characteristics of LHPOST6 shake table. | 34 |
| Table 2-10. | Shake table simulation results..... | 35 |
| Table 3-1. | NUHOMS 32 PTH2 specifications..... | 39 |
| Table 3-2. | Aluminum plate thickness. | 42 |
| Table 3-3. | Dummy assembly target and actual weights..... | 44 |
| Table 3-4. | KNF’s surrogate assembly specifications. | 47 |
| Table 3-5. | The proposed distribution of the dummy assembly weights in the canister basket. | 50 |
| Table 3-6. | Estimated weight of the cask different parts. | 52 |
| Table 3-7. | Concrete samples data. | 53 |
| Table 3-8. | Specifications of the vertical cask mockup and HI-STORM vertical overpack. | 55 |
| Table 5-1. | Fujifilm pressure paper specifications. | 70 |
| Table 5-2. | Instrumentation summary. | 74 |
| Table 6-1. | Concrete slab installation activities. | 83 |
| Table 2-1. | Classification of the CEUS sites. | 22 |
| Table 2-2. | Proposed time histories for CEUS hard rock conditions. | 24 |
| Table 2-3. | PGAs in Mineral (VA) earthquake compared to the design based PGA [17]. | 25 |
| Table 2-4. | Soil and soft rock SSI scenarios..... | 26 |
| Table 2-5. | Proposed time histories for CEUS soil conditions..... | 30 |
| Table 2-6. | Proposed time histories for CEUS soft rock conditions. | 31 |
| Table 2-7. | Proposed time histories for WUS soil conditions. | 32 |
| Table 2-8. | Proposed time histories for WUS soft rock conditions..... | 33 |
| Table 2-9. | Performance characteristics of LHPOST6 shake table. | 34 |
| Table 2-10. | Shake table simulation results..... | 35 |
| Table 3-1. | NUHOMS 32 PTH2 specifications..... | 39 |
| Table 3-2. | Aluminum plate thickness. | 42 |
| Table 3-3. | Dummy assembly target and actual weights..... | 44 |
| Table 3-4. | KNF’s surrogate assembly specifications. | 47 |
| Table 3-5. | The proposed distribution of the dummy assembly weights in the canister basket. | 50 |
| Table 3-6. | Estimated weight of the cask different parts. | 52 |
| Table 3-7. | Concrete samples data. | 53 |
| Table 3-8. | Specifications of the vertical cask mockup and HI-STORM vertical overpack. | 55 |
| Table 5-1. | Fujifilm pressure paper specifications. | 70 |

| | | |
|------------|---|----|
| Table 5-2. | Instrumentation summary. | 74 |
| Table 6-1. | Concrete slab installation activities. | 83 |

This page intentionally left blank.

ACRONYMS

| | |
|---------|---|
| 3D | 3-dimensions |
| AHSM | advanced horizontal storage modules |
| CEUS | Central Eastern U.S. |
| DAQ | data acquisition |
| ENSA | Equipos Nucleares S.A. |
| FY | Fiscal Year |
| GMRS | ground motion response spectra |
| HSMs | horizontal storage modules |
| ICRI | International Concrete Repair Institute |
| ISFSI | independent spent fuel storage installation |
| KNF | Korean Nuclear Fuel |
| LHPOST6 | large capacity high-performance outdoor shake table |
| MTS | material test system |
| NPP | nuclear power plant |
| PGA | peak ground acceleration |
| PGD | peak ground displacement |
| PNNL | Pacific Northwest National Laboratory |
| RMSE | root mean square error |
| SFWD | Spent Fuel Waste Disposition |
| SNF | spent nuclear fuel |
| SNL | Sandia National Laboratory |
| SONGS | San Onofre Nuclear Generation Station |
| SSI | soil-structure interaction |
| TH | time history |
| UCSD | University of California, San Diego |
| UHRS | unified hazard response spectra |
| UNM | University of New Mexico |
| WUS | Western U.S. |

This page is intentionally left blank.

SPENT FUEL AND WASTE DISPOSITION FINAL SEISMIC SHAKE TABLE TEST PLAN

1. INTRODUCTION

The Spent Fuel Waste Disposition (SFWD) program is planning to conduct a full-scale seismic shake table test of the dry storage systems of spent nuclear fuel (SNF) to close the gap related to seismic loads on fuel assemblies in dry storage systems. This test will allow for quantifying the strains and accelerations on surrogate fuel assembly hardware and cladding during earthquakes of different magnitudes and frequency content.

Full-scale testing is needed because a dry storage system is a complex and highly nonlinear system making it hard to predict (model) the responses to seismic excitations. The non-linearity arises from the multiple gaps in the system – between fuel rods and the basket, between the basket and dry storage canister, between the dry storage canister and the storage cask (overpack), and ventilation gaps. The non-linearities pose significant limitations on the value of tests with scaled systems.

This report documents the final test plan of the seismic shake table test. Figure 1-1 displays the shake table test roadmap. A brief discussion of Fiscal Year 2021 (FY21) to FY24 work shown in the roadmap is provided below.

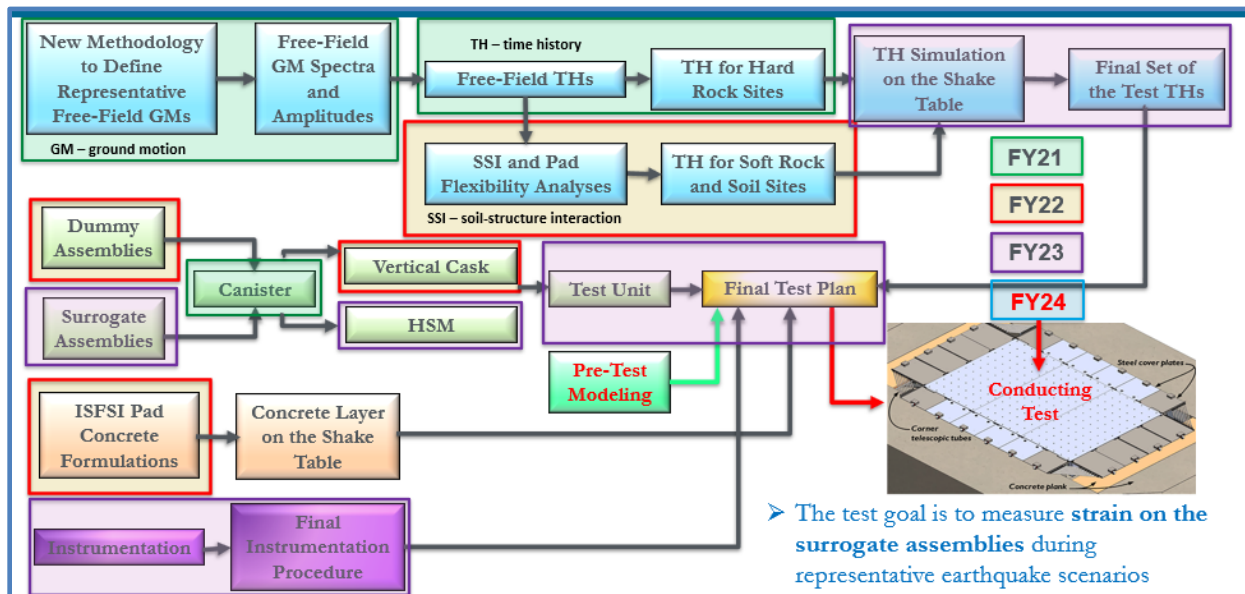


Figure 1-1. Seismic shake table test roadmap.

At the end of FY20, DOE transferred NUHOMS canisters from San Onofre Nuclear Generation Station (SONGS) to a few national labs, including Sandia National Laboratory (SNL). At that moment, an idea to conduct a shake table test of the full-scale dry storage systems of SNF was born. One of the NUHOMS 32 PTH2 canisters was designated for the test.

Shortly after, a preliminary agreement to conduct the test was made with the world's largest outdoor earthquake simulator, the large capacity high-performance outdoor shake table (LHPOST6), operated by the structural engineering department at the University of California in San Diego (UCSD). LHPOST6

has the largest payload capacity in the world of 2,040 tonnes. The LHPOST6 is the only shake table in the United States that can accommodate the large size and weight of the full-scale dry storage systems.

The preliminary concepts of conducting seismic shake table tests were developed at the end of FY20 and are documented in [1].

FY21 Work

The major research focus of the FY21 work was on developing free-field ground motions for hard rock, soil, and soft rock sites in the Central Eastern U.S. (CEUS) and Western U.S. (WUS) that would be representative of the range of seismotectonic and other conditions that any site might entail. This task was challenging because of the large number of independent spent fuel storage installation (ISFSI) sites and variety of seismotectonic and site conditions. The work was conducted in collaboration with SC Solutions. Dr. Norm Abrahamson, the renowned expert in this field, led the SC Solution team. Two reports ([2] and [3]) document this work. The preliminary concepts defined in [1] and the free-field ground motion work were used to develop a preliminary test plan documented in [4].

FY22 Work

In FY22, the major research focus was on soil-structure interaction (SSI) and pad flexibility analysis. At the hard rock sites, the pad motions can be assumed the same as the free-field ground motions as demonstrated in the initial SSI analysis [5]. At the soft rock and soil sites, the pad motions differ from the free-field ground motions due to the amplification or attenuation in the soft rock/soil and to the SSI. The SSI analysis was conducted in collaboration with SC Solutions. The pad motions, which account for SSI, were determined from modeling representative ISFSI pads with vertical casks for soil and soft rock sites in CEUS and WUS. This work is documented in [6] and is included in the updated test plan report [7].

A number of decisions were made about the test hardware. The design of a simplified mockup of the vertical cask (similar in weight and dimensions to the HI STORM 100) was developed. The mockup (referred to as the vertical cask further in this report) steel shell was manufactured in Colorado Springs (CO) and transported to LHPOST in May of 2022. The steel shell was filled with concrete in June 2022. The dummy assembly design was developed, and the manufacturing began in Spain under the supervision of the Spanish company Equipos Nucleares S.A. (ENSA).

A concrete slab will be installed on the shake table, before the tests with the dry storage systems, to simulate conditions representative of an ISFSI. The concrete surface will be in contact with the steel bottom of the cask during the test. A series of experiments were conducted at the University of New Mexico (UNM) to determine the friction coefficients between the steel plate (same steel finish as the bottom of the cask) and concrete samples with different surface finishes. The friction experiment is documented in [8]. The recommendations for the concrete surface finish to be used in the shake table test were made based on the results of the friction experiment data analysis.

FY23 Work

In FY23, the SSI analysis continued to include an ISFSI pad with horizontal storage modules (HSMs). The pad motions with account for SSI were determined from modeling representative ISFSI pad with HSMs for soil and soft rock sites in CEUS and WUS. The modeling work is documented in [9], and the analysis of modeling results is presented in [10].

The results of the ground motion work conducted in FY21-FY23 are the X, Y, and Z time histories (THs) for the representative earthquake scenarios for:

- Hard rock sites in CEUS - free-field ground motions (there are no ISFSIs located on hard rock sites in WUS)

- Soft rock sites in CEUS and WUS – ground motions with account for SSI (vertical casks and HSMs)
- Soil sites in CEUS and WUS – ground motions with account for SSI (vertical casks and HSMs)

Five THs were generated for each earthquake scenario. The number of THs proposed in the previous test plans [4] and [7] is very large (~150). The goal of the FY23 work was to define an optimal set of THs (~50) to be used in the shake table test. The modeling work was conducted at Pacific Northwest National Laboratory (PNNL) to guide the selection of the THs. This work was summarized in [11]. The details are documented in [12].

In parallel, the selected THs with high peak ground accelerations (PGAs) are being simulated by the UCSD to provide feedback on any problems with implementing these THs during the actual test.

The friction experiment data were analysed, and the appropriate test friction coefficient for the shake table test concrete surface was selected. This work is documented in [13].

The manufacturing of the dummy assemblies in Spain started in FY22. The dummy assemblies were fabricated at the end of 2022 and were delivered to LHPOST in February 2023.

A collaboration agreement was established with Korean Nuclear Fuel (KNF) in FY21. This agreement is supported by a non-disclosure agreement (NDA) between SNL, PNNL, and KNF and letter of intents, one signed by SNL and another one signed by KNF. As a part of this collaboration, KNF provided two surrogate assemblies for the shake table test. The assemblies were shipped to SNL in December 2022.

In spring 2023, a decision was made to design a simplified mockup of an HSM. The mockup (referred to as the trough further in this report) was designed and the contract for fabrication of its steel frame in Colorado Springs (CO) was placed. The steel frame will be transported to LHPOST in November 2023. It will be embedded in a concrete box on site.

The instrumentation of the different elements of the test units was revised. This concerns the location, number, and types of sensors. New fibre optics sensors were added to the instrumentation.

The preliminary test procedures and schedule was developed in collaboration with the UCSD.

FY24 Work

The shake table test will be conducted in spring and summer of 2024.

The final recommendations regarding the test will be made in winter of 2024.

The trough will be completed in the beginning of 2024.

The data collected during the test will be summarized in the FY24 report.

Pre-Test Modeling Work

In parallel with the work described above, the pre-test modeling has been conducted in FY21-FY23 by PNNL. The pre-test modeling provided important inputs for instrumentation, canister loading map, and for selecting final THs for the shake table test. This work is documented in [14] and [15]. The final pre-test modeling results are documented in [12].

Purpose of this Report

The major purpose of this report is to provide:

- Recommendations for selection of acceleration THs to be implemented in the shake table test.
- Updates regarding the test unit hardware.
- Updates regarding the concrete slab to be installed on the shake table.
- Updates regarding instrumentation.
- Description of the test activities and schedule.

The details about the previous work can be found in references [1] – [12]. The information from these references is presented in this report only to the extent needed to understand the updated test plan described in this report.

2. RECOMMENDATIONS FOR SELECTING ACCELERATION TIME HISTORIES

Prior to running representative acceleration time histories on the shake table, a test with a simple acceleration time history, such a sine sweep, is recommended. This test will allow for determining the damping of the test unit. It will be significantly harder to determine damping from the complex time histories.

The shake table inputs (acceleration time histories) must be representative of the range of seismotectonic and other conditions that any site in the CEUS or WUS might encounter. Representative earthquake scenarios were developed for the CEUS and WUS and details about the scenarios and supporting data are documented in [2].

For the CEUS, the representative earthquake scenarios were defined as:

- Local event with magnitude 5.5 at 15 km (9.32 mi)
- Moderate event with magnitude 6.5 at 40 km (24.85 mi)
- Large magnitude distant event with magnitude 7.8 at 200 km (124.27 mi)

For each representative earthquake scenario, the free-field horizontal and vertical acceleration spectral shapes corresponding to the 1E-04 seismic hazard level, were developed for general hard rock, soft rock, and soil sites. All three categories of sites are present in CEUS. A total of nine spectral shape sets (3 scenarios x 3 categories) were developed. For each spectral shape set, five THs were developed using candidate seed THs. The candidate seed THs were selected given the time history database from the NGA-West2 program [16]. The same selected candidate seed THs were used for hard rock, soft rock, and soil for a given earthquake scenario. A total of 45 THs were developed.

The grouping of CEUS nuclear power plant (NPP) sites was performed based on the average shear velocity within the top 30 m (98.42 ft) (V_{s30}) values. Table 2-1 provides the summary of this grouping. Twenty-four sites were classified as hard rock sites; 11 sites were classified as soft rock sites; and 16 sites were classified as soil sites.

Table 2-1. Classification of the CEUS sites.

| Site Classification | Average V_{s30} (m/sec) | Average V_{s30} (ft/sec) | Number of Sites |
|---------------------|------------------------------|-------------------------------|--------------------|
| Soil | 320.7 | 1052.2 | 16 |
| Soft Rock | 698.7 | 2292.3 | 11 |
| Hard Rock | 1868.3 | 6129.2 | 24 |

For the WUS the representative earthquake scenarios were defined as:

- Local event with magnitude 6.25 at 10 km (6.21 mi)
- Large magnitude local event with magnitude 7.5 at 5 km (3.11 mi)
- Large magnitude distant event with magnitude 7.5 at 200 km (124.27 mi)

At the WUS sites, two categories are present, soft rock and soil. The first two scenarios are applicable to the Diablo Canyon and Hanford NPP sites. Both sites have V_{s30} equal to 760 m/sec (2,493.44 ft/sec) which is representative of soft rock conditions. The first and third scenarios are applicable to the Palo

Verde site. This site has V_{s30} equal to 344 m/sec (1,128.61 ft/sec) which is representative of soil conditions.

A total of four spectral shape sets (2 scenarios x 2 categories) were developed. For each spectral shape set, five acceleration THs were developed using candidate seed THs. Different candidate seed THs were used for soft rock and soil sites for a given earthquake scenario. A total of 20 THs were developed.

The free-field acceleration THs for CEUS and WUS were calculated for the 1E-04 hazard level. The scaling coefficients were developed to scale the THs to the desirable level of seismic hazard. In accordance with RG1.208 [17], the site-specific ground motion response spectra (GMRS) must be defined based on 1E-04 unified hazard response spectra (UHRS) adjusted using 1E-05 UHRS. The resulting GMRS, with few exceptions, approximately correspond to the 5E-05 seismic hazard level. Consequently, it is proposed to scale the developed free-field THs to the 5E-05 seismic hazard level. The lower seismic hazard level (5E-04) represents smaller, but more frequently occurring earthquakes. It is proposed to scale a few THs to 5E-04 hazard level to collect data required for model validation of smaller seismic loads.

At the hard rock sites, the pad motions can be assumed the same as the free-field ground motions as demonstrated in the initial SSI analysis [5]. At the soft rock and soil sites, the pad motions differ from the free-field ground motions due to the SSI and pad flexibility. Note, that due to non-linearity, the amplifications are functions of the applied seismic load. Figure 2-1 shows the conceptual differences between the sites located on hard rock and the sites located on soft rock and soil.

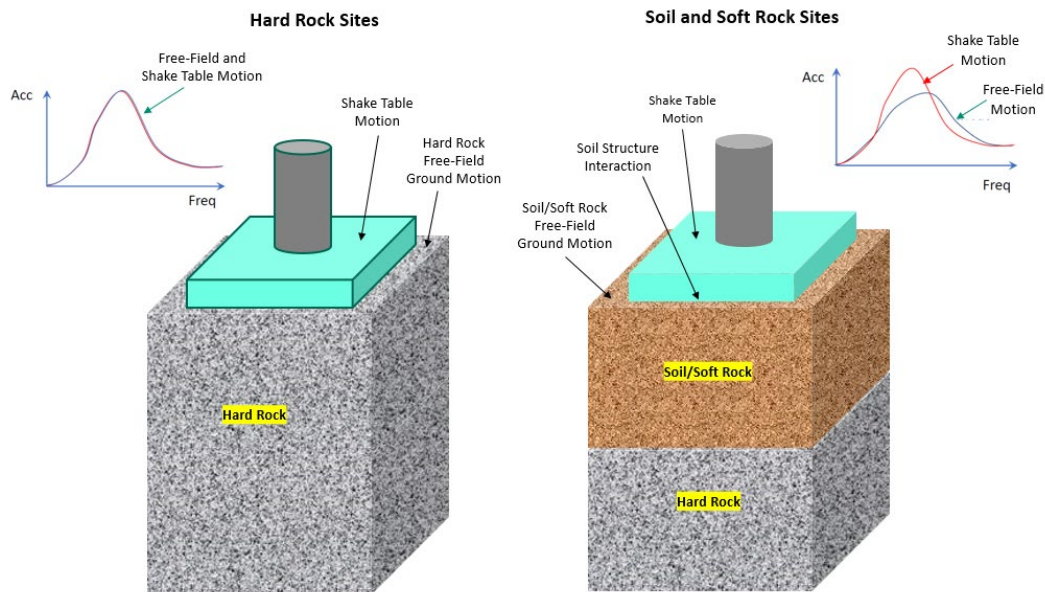


Figure 2-1. Conceptual representation of a dry storage system located on hard rock and soft rock/soil for the shake table test.

2.1 Proposed Acceleration Time Histories for the CEUS Hard Rock Sites

Because at the hard rock sites the pad motion can be assumed the same as the free-field ground motion, the free-field THs developed for hard rock conditions can be used as direct input into the shake table. These inputs are representative of 24 hard rock sites in CEUS. The same acceleration THs can be used in tests with the vertical cask and the trough.

The pre-test modeling demonstrated that strains on the surrogate assembly rods were very small (30-50 microstrain) when the hard rock free-field THs were scaled to a 5E-04 hazard level [15]. The strains on the rods were noticeably higher (up to 200 microstrain) when the THs were scaled to a 5E-05 hazard level. It is recommended to scale the hard rock THs to the 5E-05 hazard level. The pre-test modeling results for hard rock conditions are summarized in Table 2-2. Each TH selected based on the pre-test modeling is assigned a priority level. A total of 30 THs were recommended with six for hard rock and the remaining being for soil and soft rock. Also provided in this table is the information on the earthquake selected as a seed for each earthquake scenario. To provide statistical representation, it is recommended to use five THs for each earthquake scenario. As a result, 15 THs shown in Table 2-2 were proposed for the test.

Table 2-2. Proposed time histories for CEUS hard rock conditions.

| Earthquake Scenario | TH ID | Modeling Result | Priority | Earthquake | Year | Station Name |
|------------------------------|-------|--------------------------------------|----------|------------------------------------|------|---------------------------------|
| 5.5 at 15 km (9.32 mi) | 1 | | | L'Aquila (aftershock 1) Italy | 2009 | L'Aquila - V. Aterno - Ferriera |
| | 2 | Highest pad and basket acceleration | 24 | Coalinga-02 | 1983 | SGT (temp) |
| | 3 | | | Chalfant Valley-03 | 1986 | Bishop - Paradise Lodge |
| | 4 | Lowest rod/guide tube strain | 30 | Whittier Narrows-01 | 1987 | Pomona - 4th & Locust FF |
| | 5 | Highest (M5.5) rod/guide tube strain | 25 | Umbria Marche (aftershock 1) Italy | 1997 | Nocera Umbra-Salmata |
| 6.5 at 40 km (24.85 mi) | 6 | | | Imperial Valley-06 | 1979 | Victoria |
| | 7 | | | San Fernando | 1971 | Pearblossom Pump |
| | 8 | Highest rod strain | 9 | Chi-Chi, Taiwan-05 | 1999 | TCU140 |
| | 9 | | | Chuetsu-oki, Japan | 2007 | NIGH12 |
| | 10 | ~150 uE rod strain | 15 | Tottori, Japan | 2000 | OKY002 |
| 7.8 at 200 km (124.27 mi) | 11 | | | Tabas, Iran | 1978 | Sedeh |
| | 12 | | | Denali, Alaska | 2002 | TAPS Pump Station #08 |
| | 13 | Highest (M7.8) rod/guide tube strain | 26 | Kocaeli, Turkey | 1999 | Tekirdag |
| | 14 | | | Chi-Chi, Taiwan | 1999 | TAP046 |
| | 15 | | | Landers | 1992 | Tarzana - Cedar Hill |
| 5.8 at 17.7 km (11 mi) | N/A | | | Mineral, VA | 2011 | North Ana NPP |

One more case will be added to the CEUS hard rock scenarios, an actual 5.8 magnitude earthquake that occurred at 1:51 pm on August 23, 2011 in the vicinity of the North Anna Nuclear Plant. The earthquake's epicenter was 11 miles southwest of the station in Mineral, VA. As a result of this earthquake, the vertical casks at the North Anna ISFSI moved from 1 to 4 inches on the pad. It was determined [18] that the recorder data at the containment base-mat of Unit 1 provided the most reliable data of the earthquake characteristics. The corrected acceleration time-histories reproduced from [18] are shown in Figure 2-2 for the East-West, North-South and the vertical orientations. The earthquake duration was about 18 seconds.

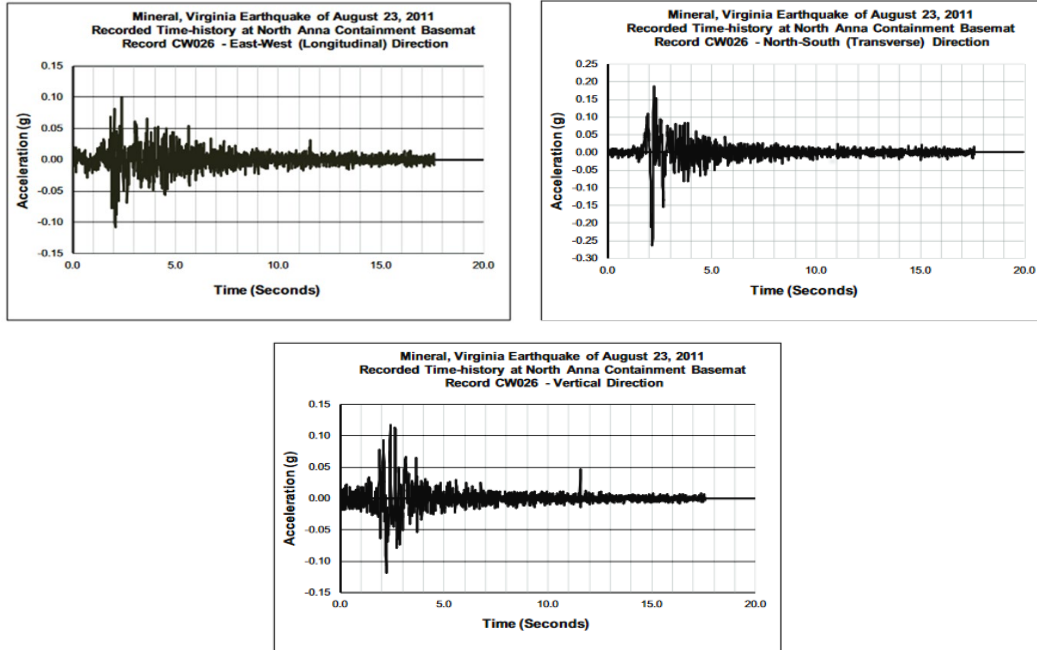


Figure 2-2. Mineral (VA) earthquake time histories, containment basemat [18].

The PGAs observed at the containment basemat during the Mineral (VA) earthquake and the design-based PGAs are shown in Table 2-3 reproduced from [18]. The observed horizontal N-S PGA and vertical PGA exceeded the original design-based values. The re-evaluated design-based horizontal N-S PGA is 0.572 g.

Table 2-3. PGAs in Mineral (VA) earthquake compared to the design based PGA [18].

| Component | Design Based PGAs (g) | Observed PGAs (g) |
|----------------|-----------------------|-------------------|
| Horizontal N-S | 0.12 | 0.264 |
| Horizontal E-W | 0.12 | 0.109 |
| Vertical | 0.08 | 0.118 |

2.2 Results of Soil-Structure Interaction Analyses

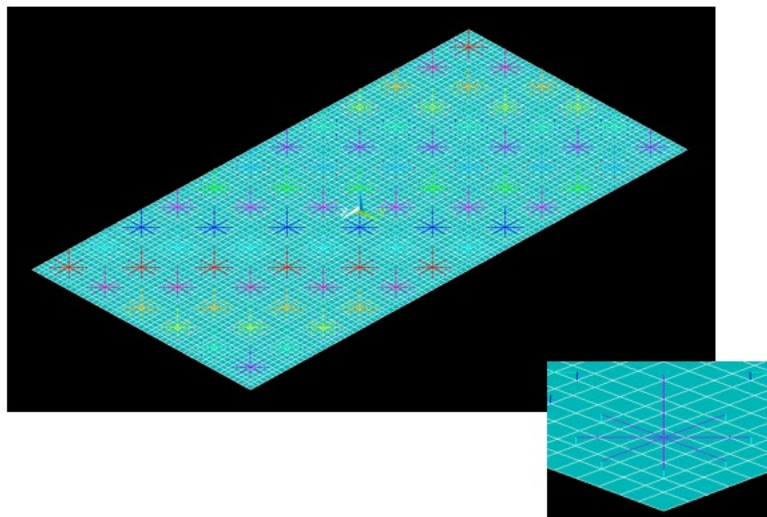
At the soft rock and soil sites, the pad motions differ from the free-field ground motions due to SSI and pad flexibility. The SSI analyses were conducted using SASSI software for the representative ISFSI pads with vertical casks and HSMs. The free-field soil and soft rock THs developed for CEUS and WUS were used as an input into the SSI models. The free-field THs were scaled to the PGAs shown in Table 2-4. Table 2-4 describes the earthquake scenarios and pad configurations considered in the SSI analyses. Two pad loading configurations were used in each case with the vertical casks. In configuration 1, the pad was fully loaded. In configuration 4, there were a few casks placed in the corner of the pad. The number of casks in configuration 4 is shown in parentheses in Table 2-4. Five THs were used in each scenario. For CEUS, a total of 105 modeling cases were considered - 70 (35x2 configurations) for the pad with vertical casks and 35 for the pad with HSMs. For WUS, a total of 80 modeling cases was considered - 70 (35x2 configurations) for the pad with vertical casks and 10 for the pad with HSMs. The details regarding the models and modeling results are provided in [5], [9], and [10].

Table 2-4. Soil and soft rock SSI scenarios.

| Scenario ID | Site Conditions | PGA (g) | Earthquake Parameters | Seismic Hazard | Pad Configuration | |
|-------------|-----------------|---------|-----------------------|----------------|-------------------|------|
| | | | | | Casks | HSMs |
| 1 | CEUS Soil | 0.56 | M 5.5, D 15 | GMRS | 2 x 6 (3) | 2x16 |
| 2 | CEUS Soil | 0.31 | M 6.5, D 40 | 5E-05 | 2 x 6 (3) | 2x16 |
| 3 | CEUS Soil | 0.1 | M 7.8, D 200 | 5E-04 | 2 x 6 (3) | 2x16 |
| 4 | CEUS Soft Rock | 0.25 | M 5.5, D 15 | 5E-05 | 6 x 12 (7) | 2x16 |
| 5 | CEUS Soft Rock | 0.08 | M 6.5, D 40 | 5E-04 | 6 x 12 (7) | 2x16 |
| 6 | CEUS Soft Rock | 0.29 | M 5.5, D 15 | GMRS | 6 x 12 (7) | 2x16 |
| 7 | CEUS Soft Rock | 0.18 | M 7.8, D 200 | 5E-05 | 6 x 12 (7) | 2x16 |
| 8 | WUS Soil | 0.23 | M 6.25, D 10 | 5E-05 | 2 x 15 (3) | N/A |
| 9 | WUS Soil | 0.14 | M 7.5, D 200 | 5E-05 | 2 x 15 (3) | N/A |
| 10 | WUS Soil | 0.09 | M 6.25, D 10 | 5E-04 | 2 x 15 (3) | N/A |
| 11 | WUS Soft Rock | 0.22 | M 6.25, D 10 | 5E-04 | 2 x 15 (6) | N/A |
| 12 | WUS Soft Rock | 0.52 | M 7.5, D 5 | 5E-05 | 2 x 15 (6) | N/A |
| 13 | Diablo Canyon | 0.92 | M 7.5, D 5 | GMRS | 5 x 28 (6) | 2x16 |
| 14 | Diablo Canyon | 1.3 | M 7.5, D 5 | 5E-05 | 5 x 28 (6) | 2x16 |

Note: M is magnitude and D is distance in km; number in parentheses is the number of casks in configuration 4.

The CEUS ISFSI pads representative of soil and soft rock sites with vertical casks were 2 x 6 and 6 x 12 respectively. The WUS ISFSI pads representative of soil were 2 x 15, and representative of soft rock were 2 x 15 and 5 x 28 (Diablo Canyon). The model of the 6 x 12 pad with the vertical casks is shown in Figure 2-3 as an example. The loaded cask weight was 335,952 lbs. The center of gravity height was 103". The ISFSI pad representative of soil and soft rock sites with HSMs was 2 x 16 (Figure 2-4). The loaded HSM weight was 348,955 lbs. The center of gravity height was 115.72".



Note: This pad configuration was used for soft rock conditions.

Figure 2-3. Model of an ISFSI pad with vertical casks.

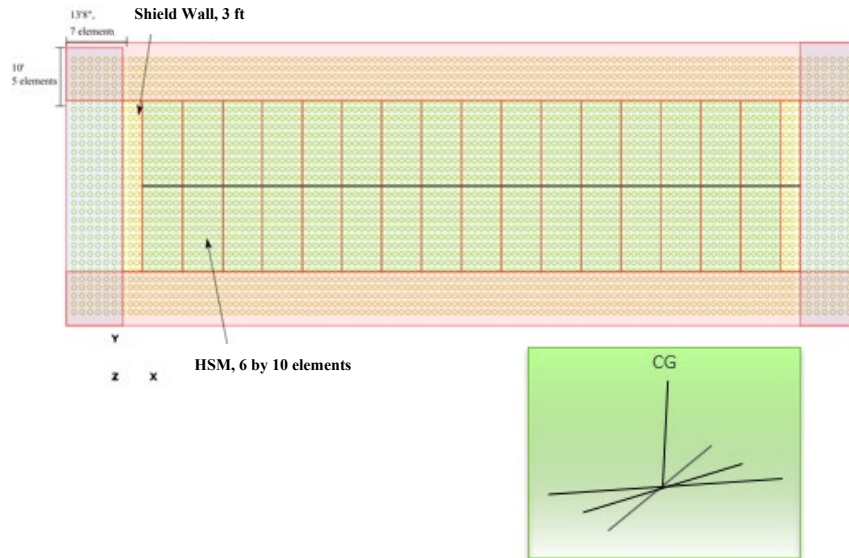
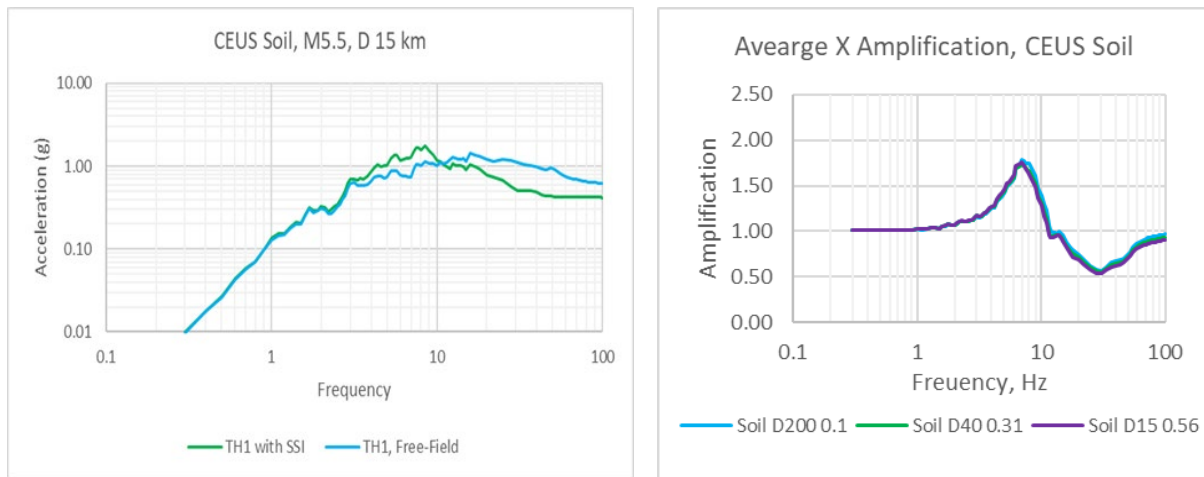


Figure 2-4. Model of an ISFSI pad with HSMs.

As a result of SSI, the acceleration spectra on the top of the pad differs from the free-field acceleration spectra. An example of this is illustrated in Figure 2-5 (horizontal direction X) for the CEUS soil scenario 1 (M 5.5, D 15 km, PGA 0.56 g, TH1) with vertical casks (configuration 1). There is an amplification within frequency band 3 to 10 Hz and attenuation within frequency band 10 to 100 Hz. The effect on the PGA is small. The amplifications are very similar in all CEUS soil scenarios as evident from Figure 2-5 (right).



Note: The accelerations (amplifications) are for horizontal direction X.

Figure 2-5. Response of the top of the pad with vertical casks (Configuration 1) compared to the free-field in CEUS soil scenario 1 (M 5.5, D 15 km, PGA 0.56 g, TH1).

Figure 2-6 compares average peak amplification frequencies in X, Y, and Z directions in CEUS and WUS soil and soft rock scenarios. All scenarios have higher peak frequency in Z direction compared to X and Y directions and similar peak frequency in X and Y directions. The WUS soil scenarios have the lowest peak frequencies – 2.1 to 3.7 Hz. The WUS soft rock scenarios have the highest X and Y peak frequencies – 8.4 and 9.7 Hz. The CEUS soil scenarios have the highest Z peak frequency – 12.5 Hz.

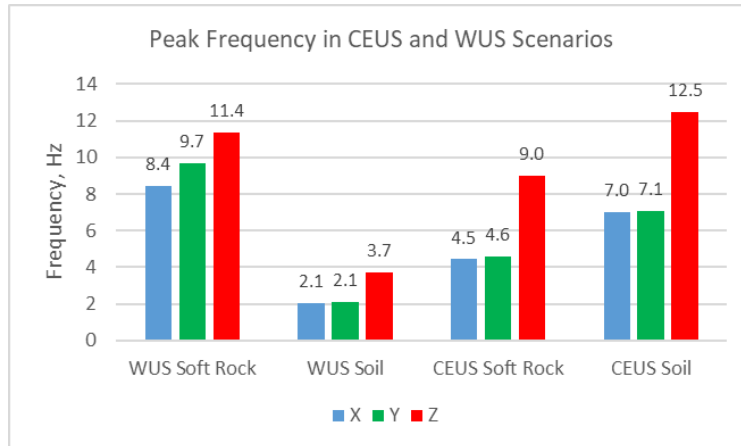


Figure 2-6. Peak amplification frequencies in CEUS and WUS soil and soft rock scenarios.

The modeling results were analyzed to identify the locations on the pad with the maximum amplifications. Analysis of the spectral accelerations in the X and Y directions demonstrated they are very similar in all locations on the pad. However, the spectral accelerations in the Z direction are different at different locations on the pad. Because the accelerations in X and Y directions vary very little at different locations on the pad, the points of interest are the ones with the maximum Z accelerations. The locations where the maximum most frequently occurs are at the corners of the pad. This same trend was observed for soil and soft rock scenarios for the pads with the vertical casks and HSMs. The differences between the amplifications in configurations 1 and 4 (pad with the vertical casks) in the locations with maximum Z acceleration were small in all scenarios.

The amplifications on the pad with the HSMs were compared to the amplifications on the pad with the vertical casks. The amplifications in the different earthquake scenarios with HSMs in the X, Y, and Z directions were compared to the amplifications in the corresponding earthquake scenarios with the vertical casks. The comparisons were done for the locations on the pad with the maximum Z acceleration. The amplifications are very similar for the cask and HSM in X, Y, and Z directions above ~3 Hz. The other soil and soft rock scenarios exhibit similar trends. This is illustrated in Figure 2-7 that compares amplifications in scenario 4, CEUS soft rock, magnitude 5.5, distance 15 km, PGA 0.25 g.

This comparison demonstrates that the configuration of the pad and the parameters of the dry storage system (cask versus HSM) have very small impact on the pad response in scenarios, except WUS Diablo Canyon scenario. The pad response is dominated by the type of geologic medium (soil and soft rock) and pad flexibility. Consequently, the same acceleration THs can be used for all soil and soft rock earthquake scenarios for both vertical cask and HSM in the shake table tests. In the Diablo Canyon scenario, the amplification shapes are very similar for the cask and HSM, but the amplification magnitude is higher in the case of vertical casks.

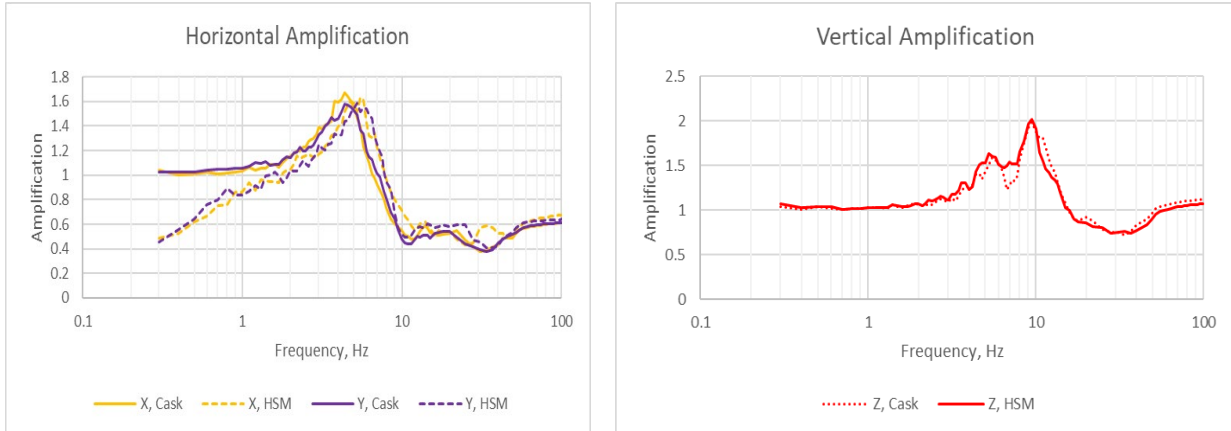


Figure 2-7. Amplifications in scenario 4, CEUS soft rock, magnitude 5.5, distance 15 km, PGA 0.25 g.

The THs with SSI obtained for CEUS and WUS soil and soft rock scenarios (both configurations 1 and 4 were considered) were used as a boundary condition on the top of the pad in the pre-test modeling. The pre-test model first calculated the response of the vertical cask and basket. The response of the basket was then used as a boundary condition in the detailed model of the fuel assemblies [15]. Accelerations were obtained on the cask, basket, and assembly while strains were obtained on the assembly rods. The modeling results were analyzed to determine the scenarios that have higher priority for implementing in the shake table test. The details are documented in [12].

The location selected based on the highest response (strain on the assembly rod and pad acceleration) is compared in Figure 2-8 to the locations with the maximum vertical accelerations on the pad in the CEUS soil scenarios. It can be concluded that the locations are similar.

The conclusions from the SSI analyses and pre-test modeling are used in Sections 2.3 and 2.4 to recommend THs for the shake table test.

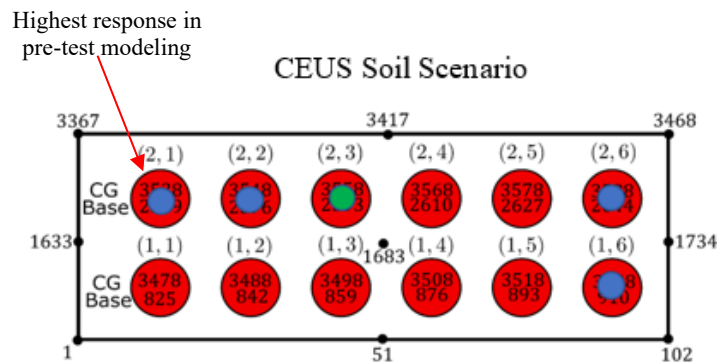


Figure 2-8. Locations on the pad with the maximum Z acceleration in CEUS soil scenarios.

2.3 Proposed Acceleration Time Histories for the CEUS Soil and Soft Rock Sites

It is recommended to use five THs in the shake table test to represent the CEUS soil conditions. The THs are for the earthquake scenario with 5.5 magnitude at 15 km (9.3 mi) and PGA of 0.56 g. Table 2-5 provides information on the free-field TH IDs, ID of the selected node on the pad, seed earthquake name, year, and station. Also provided in this table are the selection reasons based on the pre-test modeling. TH1, TH3, and node on the pad (shown in red font) were selected based on modeling. It is recommended to use all five THs to provide sufficient statistical representation. The nodes on the pad for TH2, TH4, and TH5 were selected based on the highest Z acceleration on the pad. The proposed THs are the same for the shake table tests with the vertical cask and the trough.

Table 2-5. Proposed time histories for CEUS soil conditions.

| Earthquake Scenario | Free-Field TH ID | Model Node ID | Modeling Result | Priority | Earthquake | Year | Station Name |
|---|------------------|---------------|--------------------------------------|----------|------------------------------------|------|---------------------------------|
| 5.5 at 15 km (9.32 mi) PGA 0.56 g GMRS | 1 | (2,1) | Highest pad acceleration | 4 | L'Aquila (aftershock 1) Italy | 2009 | L'Aquila - V. Aterno - Ferriera |
| | 2 | (1,6) | | | Coalinga-02 | 1983 | SGT (temp) |
| | 3 | (2,1) | Highest rod strain in soil scenarios | 13 | Chalfant Valley-03 | 1986 | Bishop - Paradise Lodge |
| | 4 | (1,6) | | | Whittier Narrows-01 | 1987 | Pomona - 4th & Locust FF |
| | 5 | (2,6) | | | Umbria Marche (aftershock 1) Italy | 1997 | Nocera Umbra-Salmata |

It is recommended to use 12 THs in the shake table test to represent the CEUS soft rock conditions. Five THs are for the earthquake scenarios with 5.5 magnitude at 15 km (9.3 mi) and PGA of 0.56 g. Five THs are for the earthquake scenarios with 7.8 magnitude at 200 km (124.27 mi) and PGA of 0.28g. Two THs are for the earthquake scenarios with 6.5 magnitude at 40 km (24.85 mi) and PGA of 0.08 g. Table 2-6 provides information on the free-field TH IDs, ID of the selected node on the pad, seed earthquake name, year, and station. Also provided in this table are the selection reasons based on the pre-test modeling. The nodes on the pad shown in red font were selected based on modeling. It is recommended to use all five THs for the first and second scenarios to provide sufficient statistical representation. The nodes on the pad for the corresponding THs were selected based on the highest Z acceleration on the pad. The 3rd scenario was selected based on lowest response. It is assumed that sufficient data for the post-test modeling can be collected with two THs selected based on the pre-test modeling. The proposed THs are the same for the shake table tests with the vertical cask and the trough.

Table 2-6. Proposed time histories for CEUS soft rock conditions.

| Earthquake Scenario | Free-Field TH ID | Node ID | Modeling Result | Priority | Earthquake | Year | Station Name |
|--|------------------|----------|--|----------|------------------------------------|------|---------------------------------|
| 5.5 at 15 km (9.32 mi) PGA 0.56 g GMRS | 1 | (6,1) | | | L'Aquila (aftershock 1) Italy | 2009 | L'Aquila - V. Aterno - Ferriera |
| | 2 | (1,12) | | | Coalinga-02 | 1983 | SGT (temp) |
| | 3 | (2,7) | Representative case for this scenario | 27 | Chalfant Valley-03 | 1986 | Bishop - Paradise Lodge |
| | 4 | (1,12) | | | Whittier Narrows-01 | 1987 | Pomona - 4th & Locust FF |
| | 5 | (6,12) | | | Umbria Marche (aftershock 1) Italy | 1997 | Nocera Umbra-Salmata |
| 7.8 at 200 km (124.27 mi) PGA 0.18g 5E-05 | 11 | (6,7) | Highest CEUS SR FR/GT strain | 28 | Tabas, Iran | 1978 | Sedeh |
| | 12 | (1,6) | | | Denali, Alaska | 2002 | TAPS Pump Station #08 |
| | 13 | (6,1) c4 | Midrange rod strain | 10 | Kocaeli, Turkey | 1999 | Tekirdag |
| | 14 | (1,6) | | | Chi-Chi, Taiwan | 1999 | TAP046 |
| | 15 | (4,2) | Highest pad/cask acceleration in soft rock scenarios | 29 | Landers | 1992 | Tarzana - Cedar Hill |
| 6.5 at 40 km (24.85 mi) PGA 0.08 g 5E-04 | 6 | (1,1) c4 | Lowest rod strain | 7 | Imperial Valley-06 | 1979 | Victoria |
| | 7 | (6,6) c4 | Lowest pad/cask acceleration | 23 | San Fernando | 1971 | Pearblossom Pump |

2.4 Proposed Acceleration Time Histories for the WUS Soil and Soft Rock Sites

It is recommended to use 10 THs in the shake table test to represent the WUS soil conditions. Five THs are for the earthquake scenarios with 7.5 magnitude at 200 km (124.27 mi) and PGA of 0.14 g. Five THs are for the earthquake scenarios with 6.25 magnitude at 10 km (6.21 mi) and PGA of 0.23g. Table 2-7 provides information on the free-field TH IDs, ID of the selected node on the pad, seed earthquake name, year, and station. Also provided in this table are the selection reasons based on the pre-test modeling. The nodes on the pad shown in red font were selected based on modeling. It is recommended to use all five THs for both earthquake scenarios to provide sufficient statistical representation. The nodes on the pad for the corresponding THs were selected based on the highest Z acceleration on the pad. The proposed THs are only applicable to the shake table tests with the vertical cask.

Table 2-7. Proposed time histories for WUS soil conditions.

| Earthquake Scenario | Free-Field TH ID | Node ID | Modeling Result | Priority | Earthquake | Year | Station Name |
|---|------------------|----------|--|----------|--------------------------|------|---------------------------------|
| 7.5 at 200 km (124.27 mi) PGA 0.14 g 5E-05 | 31 | (1,5) | | | Tabas, Iran | 1978 | Sedeh |
| | 32 | (2,1) c4 | Midrange rod strain | 8 | Hector Mine | 1999 | Castaic - Hasley Canyon |
| | 33 | (2,4) | | | Kocaeli, Turkey | 1999 | Balikesir |
| | 34 | (1,12) | | | Landers | 1992 | Chatsworth - Devonshire |
| | 35 | (1,7) | Highest rod strain in WUS soil scenarios | 12 | El Mayor-Cucapah, Mexico | 2010 | Santa Ana - Grand & Santa Clara |
| 6.25 at 10 km (6.21 mi) PGA 0.23 g 5E-05 | 21 | (2,15) | | | Chalfant Valley-02 | 1986 | Bishop - LADWP South St |
| | 22 | (1,4) | Highest rod strain in this earthquake scenario | 14 | L'Aquila, Italy | 2009 | GRAN SASSO (Assergi) |
| | 23 | (1,1) c4 | ~350 uE rod strain | 16 | Coalinga-01 | 1983 | Pleasant Valley P.P. - bldg. |
| | 24 | (2,15) | | | Chi-Chi Taiwan-06 | 1999 | TCU076 |
| | 25 | (2,1) | | | Mammoth Lakes-01 | 1980 | Long Valley Dam (Upr L Abut) |

It is recommended to use 10 THs in the shake table test to represent the WUS soft rock conditions. Five THs are for the earthquake scenarios with 7.5 magnitude at 5 km (3.1 mi) and PGA of 0.52 g with hazard level 5E-05. Five THs are for the earthquake scenarios with 7.5 magnitude at 5 km (3.1 mi) and PGA of 1.3 g (GMRS for Diablo Canyon). Table 2-8 provides information on the free-field TH IDs, ID of the selected node on the pad, seed earthquake name, year, and station. Also provided in this table are the selection reasons based on the pre-test modeling. The nodes on the pad shown in red font were selected based on modeling. It is recommended to use all five THs for both earthquake scenarios to provide sufficient statistical representation. The nodes on the pad for the corresponding THs were selected based on the highest Z acceleration on the pad. The proposed THs for the first earthquake scenario are only applicable to the shake table tests with the vertical cask. The proposed THs for the second earthquake scenario are applicable to the shake table tests with the vertical cask and the trough.

Table 2-8. Proposed time histories for WUS soft rock conditions.

| Earthquake Scenario | Free-Field TH ID | Node ID | Modeling Result | Priority | Earthquake | Year | Station Name |
|--|------------------|----------|---------------------------------------|----------|--------------------------|------|-----------------------------|
| 7.5 at 5 km (3.1 mi) PGA 0.52 g 5E-05 | 26 | (1,1) c4 | High assembly acceleration | 5 | Tabas, Iran | 1978 | Tabas |
| | 27 | (1,2) | | | Kocaeli, Turkey | 1999 | Duzce |
| | 28 | (2,2) | Highest basket and cask accelerations | 2 | El Mayor-Cucapah, Mexico | 2010 | El Centro - Imperial & Ross |
| | 29 | (2,10) | Highest guide tube strain | 3 | Landers | 1992 | Desert Hot Springs |
| | 30 | (2,1) c4 | Highest rod strain | 1 | Chi-Chi, Taiwan | 1999 | TCU076 |
| 7.5 at 5 km (3.1 mi) PGA 0.92 g and 1.3 g Diablo Canyon | 26 | (3,27) | Effects of anchoring | 21 | Tabas, Iran | 1978 | Tabas |
| | 27 | (3,3) | Effects of anchoring | 20 | Kocaeli, Turkey | 1999 | Duzce |
| | 28 | (3,3) | Highest cask acceleration | 6 | El Mayor-Cucapah, Mexico | 2010 | El Centro - Imperial & Ross |
| | 29 | (3,21) | Effects of anchoring | 18 | Landers | 1992 | Desert Hot Springs |
| | 30 | (3,14) | Effects of anchoring | 19 | Chi-Chi, Taiwan | 1999 | TCU076 |

2.5 Shake Table Simulations

The THs defined in Sections 2.2 through 2.4 can be implemented on the LHPOST6 shake table only if they meet the shake table performance limits defined in Table 2-9. The limits are given for the bare table and the table with a 4.9 MN specimen (the test unit along with the concrete slab and safety structure is ~1.6 MN). A number of parameters control these limits as described below.

- Peak acceleration is controlled by the actuator force capacities in the control zero-position of the table.
- Acceleration limit is controlled by the reaction mass until further studies.
- Acceleration limit is controlled by the design strength of the steel honeycomb platen.
- Peak force is controlled by the vertical actuator force capacities and accounting for the hold-down forces in the control zero-position of the table.
- Force limit is controlled by the design strength of the steel honeycomb platen and accounting for the hold-down forces in the control zero-position of the table.

Table 2-9. Performance characteristics of LHPOST6 shake table.

Uniaxial performance characteristics of the LHPOST6
Sinusoidal motions - Bare table condition - Centered rigid payload of 4.9 MN (1,100 kips)

| | | | | | | |
|---------------------------------|---|---|---|--|---|---|
| Platen size | 12.2 m × 7.6 m (40 ft × 25 ft) | | | | | |
| Frequency Bandwidth | 0 – 33 Hz | | | | | |
| Vertical Payload Capacity | 20 MN (4,500 kip) | | | | | |
| | Sinusoidal motions - Bare table condition | | | Sinusoidal motions - Centered rigid payload of 4.9 MN (1,100 kips) | | |
| | Horizontal X (E-W) | Horizontal Y (N-S) | Vertical Z (-) | Horizontal X (E-W) | Horizontal Y (N-S) | Vertical Z (-) |
| Peak Translational Displacement | ±0.89 m (±35 in) | ±0.38 m (±15 in) | ±0.127 m (±5 in) | ±0.89 m (±35 in) | ±0.38 m (±15 in) | ±0.127 m (±5 in) |
| Peak Translational Velocity | 3.0 m/sec (118 in/sec) | 2.0 m/sec (80 in/sec) | 0.45 m/sec (17 in/sec) | 3.0 m/sec (118 in/sec) | 2.0 m/sec (80 in/sec) | 0.55 m/sec (21 in/sec) |
| Peak Translational Acceleration | (5.8 g) ⁽¹⁾ 3.7 g ⁽²⁾ | (4.7 g) ⁽¹⁾ 1.85 g ⁽²⁾ | -3.4 g +31.1 g ⁽¹⁾ +11.9 g ⁽³⁾ | (1.6 g) ⁽¹⁾ 1.0 g ⁽²⁾ | (1.25 g) ⁽¹⁾ 0.50 g ⁽²⁾ | -1.64 g +7.5 g ⁽¹⁾ +2.5 g ⁽²⁾ |
| Peak Translational Force | 10.6 MN ⁽¹⁾ (2,380 kip) ⁽¹⁾ 6.8 MN ⁽²⁾ (1,530 kip) ⁽²⁾ | 8.38 MN ⁽¹⁾ (1,890 kip) ⁽¹⁾ 3.4 MN ⁽²⁾ (765 kip) ⁽²⁾ | -4.3 MN ⁽⁴⁾ +57.0 MN ⁽⁵⁾ (+12,800 kip) ⁽⁵⁾ +22.9 MN ⁽⁶⁾ (+5,150 kip) ⁽⁶⁾ | 10.6 MN ⁽¹⁾ (2,380 kip) ⁽¹⁾ 6.8 MN ⁽²⁾ (1,530 kip) ⁽²⁾ | 8.38 MN ⁽¹⁾ (1,890 kip) ⁽¹⁾ 3.4 MN ⁽²⁾ (765 kip) ⁽²⁾ | -4.3 MN ⁽⁴⁾ +57.0 MN ⁽⁵⁾ (+12,800 kip) ⁽⁵⁾ +22.9 MN ⁽⁶⁾ (+5,150 kip) ⁽⁶⁾ |
| Peak Rotation | 2.22 deg ⁽⁷⁾ | 1.45 deg ⁽⁷⁾ | 3.8 deg | 2.22 deg ⁽⁷⁾ | 1.45 deg ⁽⁷⁾ | 3.8 deg |
| Overtopping Moment Capacity | 32.0 MN-m (23,600 kip-ft) | 35.0 MN-m (25,800 kip-ft) | | 45.1 MN-m (33,200 kip-ft) | 50.0 MN-m (36,900 kip-ft) | |

Three high PGA earthquake scenarios were modeled by the UCSD (this work will be documented at the end of FY23 in the contractor's report) using the shake table simulator to evaluate the table's ability to reproduce these scenarios. These scenarios were:

- (1). CEUS hard rock scenario, M 6.5, D 40 km, TH3 (CEUS_HR_M65R40_Set03-RSN3221)
- (2). CEUS soil scenario M 5.5, D 15 km, PGA 0.56 g, TH3, node 2559, configuration 4 (CEUS_Soil_D15_056g_Config4_th_s_accel_base_TH03_node2559)
- (3). WUS soft rock scenario M 7.5, D 5 km, PGA 0.52 g, TH5, node 1457, configuration 4 (WUS_SR_D5_052g_Config4_th_s_accel_base_TH05_node1457)

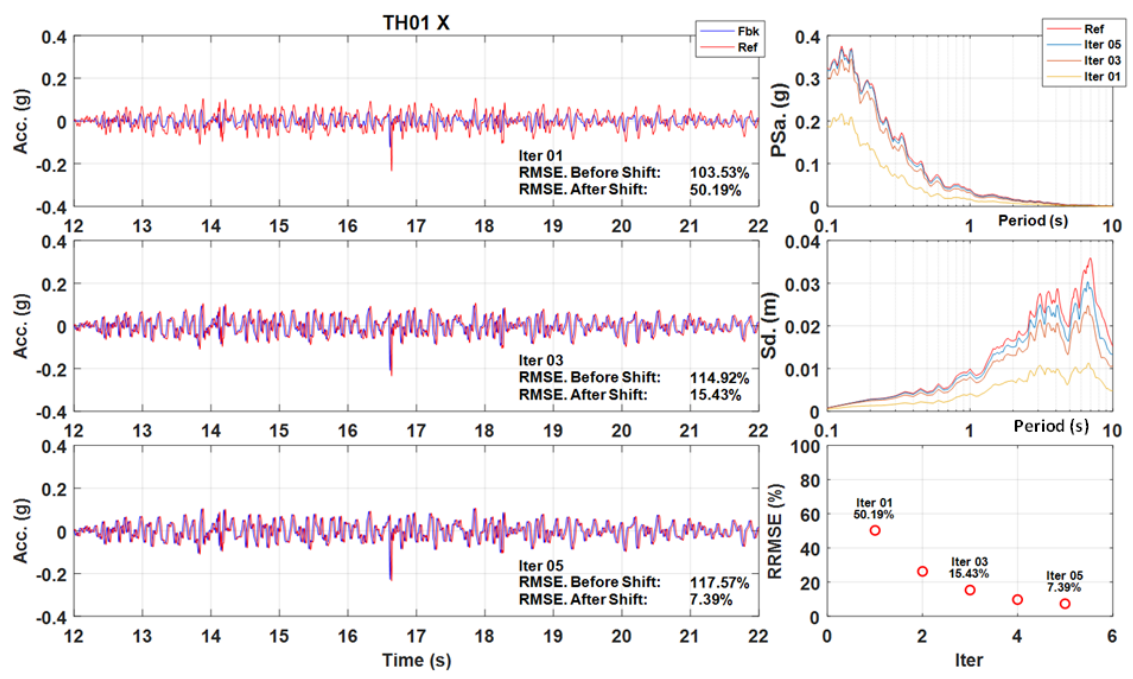
Shake table simulations results are summarized in Table 2-10. Scenario 3 resulted in exceeding peak ground displacement (PGD) in the vertical (Z) direction. The Scenario 3 THs were downscaled using 0.914 scaling factor (3 with scaling). The vertical PGD limit was met in this scenario. The Scenario 3 THs were filtered (3 with filter) using high pass filter at 0.12 Hz. The vertical PGD limit was met in this scenario as well. Either one or another adjustment will be required to run Scenario 3 on the shake table.

Table 2-10. Shake table simulation results.

| Scenario | PGA (g) | | | PGV (m/s; in/s) | | | PGD (mm; in) | | |
|----------------|---------|------|------|-----------------|-------|-------|--------------|--------|--------|
| | X | Y | Z | X | Y | Z | X | Y | Z |
| 1 | 0.24 | 0.19 | 0.13 | 0.04 | 0.07 | 0.03 | 9.87 | 22.66 | 7.83 |
| | | | | 1.58 | 2.89 | 1.16 | 0.39 | 0.89 | 0.31 |
| 2 | 0.35 | 0.87 | 0.39 | 0.11 | 0.16 | 0.06 | 9.38 | 11.25 | 12.8 |
| | | | | 4.45 | 6.3 | 2.22 | 0.37 | 0.44 | 0.5 |
| 3 | 0.58 | 0.53 | 0.4 | 0.63 | 0.34 | 0.41 | 368 | 140.43 | 136.83 |
| | | | | 24.86 | 13.46 | 15.95 | 14.49 | 5.53 | 5.39 |
| 3 with scaling | 0.53 | 0.48 | 0.36 | 0.57 | 0.31 | 0.36 | 331.2 | 126.39 | 123.15 |
| | | | | 22.37 | 12.12 | 14.36 | 13.04 | 4.98 | 4.85 |
| 3 with filter | 0.58 | 0.53 | 0.4 | 0.6 | 0.33 | 0.41 | 313.92 | 118.36 | 118.97 |
| | | | | 23.5 | 12.99 | 16.16 | 12.36 | 4.66 | 4.68 |

Note: PGV is peak ground velocity and PGD is peak ground displacement.

Another goal of the shake table simulations was to evaluate the achievable accuracy in implementing target THs. An iterative process was used to achieve better accuracy. Figure 2-9 provides illustration for Scenario 1, X direction. The three plots on the left of this figure show the root mean square error (RMSE) between the target and achieved accelerations for the 1st (top), 3rd (middle), and 5th (bottom) iterations. The RMSE changes from 50.19% (iteration 1) to 7.39% (iteration 5). The target and achieved response spectra for the three iterations are shown on the right top (accelerations) and middle (displacement). The bottom right plot shows RMSE versus iteration.



Note: Red curve (Ref) is target TH and blue curve (Fbk) is achieved TH.

Figure 2-9. Scenario 1, X-direction, RMSE between the target and achieved time histories (left) and response spectra (right).

2.6 Shake Table Training

As described in Section 2.5, a significantly better accuracy in reproducing the target THs on the shake table can be achieved using an iterative process. This iterative process will have to be implemented for each TH during the so called “table training”. The training will have to take place before the actual shake table tests with the vertical cask and trough. This is one of the most time-consuming test activities (Activity 2 in Section 6.2.2).

Table training is similar to a shake table simulation (Section 2.5). It is required because the shake table system is a closed-loop, nonlinear, dynamic system and the transfer function between the specified TH and the achieved table motion is not unity, as would be required for a perfect reproduction of the input TH. The controller of the shake table is tuned (trained) for each TH record that will be simulated on the table. The goal of the training is to optimize the tracking of the target/desired TH record by the shake table platen. This tuning process involves three main steps outlined below.

Step 1: The first step involves an iterative process in which the control parameters (feed-forward and feedback gains) of the three-variable controllers are manually adjusted iteratively in small increments while the table is in motion. Typically, this step is performed under a band-limited (e.g., 0.25–25 Hz) white noise input acceleration with an RMSE amplitude of 5-7%g to obtain a reliable estimate of the table 6 x 6 matrix transfer function between command and feedback accelerations. The parameter adjustment process continues until the table transfer function estimated recursively is deemed satisfactory (i.e., as close to unity as possible).

Step 2: The second step consists of obtaining an estimate of the inverse 6 x 6 matrix transfer function of the shake table. In the 469D controller of the LHPOST6, the inverse transfer function can be obtained using the adaptive inverse controller technique in which the parameters of the inverse transfer function are estimated by an adaptive inverse modeling process also known as adaptive controller “training” [19]. The quality of the estimated inverse model depends on the noise level, input amplitude level, and nonlinearities in the system. Transfer function estimation with an adaptive inverse controller is also performed under white noise acceleration with RMSE amplitude coinciding with that used in the first step to “fine-tune” the three-variable controller parameters.

Step 3: The third step in the tuning process involves the use of an iterative signal-matching technique. The iterative TH matching technique used in the 469D (LHPOST6 controller) software is called online iteration (OLI). It is a procedure that repeatedly modifies the command input to the shake table (e.g., a drive file containing a distorted version of the reference/target earthquake acceleration record to optimize the match between the achieved table motion (referred to as feedback signal) and the desired target/reference motion). This online iterative technique generates the next command to the table (i.e., the next drive file), by running the table in real-time with the current drive file as the command to the table, calculating offline the error between the desired and feedback (i.e., achieved motions, and updating the current drive file by adding to it a fraction determined by the iteration gain of the response error filtered through the inverse matrix transfer function of the shake table). The general trend of the response RMSE versus the iteration number was shown in Figure 2-9 (bottom right).

The iterative signal matching technique is needed to reduce as much as possible the effects of the shake table system nonlinearities on the signal distortion characteristics/properties of the shake table. Typically, Steps 1 through 3 are performed under bare table condition, or with the foundation of the specimen to be tested attached to the table platen.

Step 2 must be repeated with the test unit on the shake table to identify the 6 x 6 transfer function of the shake table-test unit combined system. This combined system transfer function is used to modify the drive files obtained in Step 3 under bare-table condition.

This page intentionally left blank.

3. TEST UNIT HARDWARE

Two test units will be used in the shake table test. The test units are simplified representations of a full-scale vertical dry storage cask and a full-scale horizontal dry storage module (trough). A major part of each test unit will be:

- NUHOMS 32PTH2 dry storage canister
- 28 dummy assemblies
- 4 surrogate assemblies

The NUHOMS 32 PTH2 canister with the dummy and surrogate assemblies will be placed first in the vertical cask and then in the trough for the shake table tests. The following sections provide the details regarding each element of the test units.

3.1 NUHOMS 32 PTH2 Dry Storage Canister

The NUHOMS 32 PTH2 and related NUHOMS canisters (Transnuclear, Inc.) have been used by many NPPs to store SNF assemblies. The canisters are placed in HSMs at the ISFSIs. The HSMs represent 39% of the current dry storage inventory of canisters. The vertical concrete casks (Holtec and NAC) represent 44% of the current dry storage inventory. The NUHOMS 32 PTH2 canister will be placed in the vertical cask and in the trough for the shake table test. The vertical cask was specially designed to accommodate the specific features of the NUHOMS 32 PTH2 canister (Section 3.3.1).

The NUHOMS 32 PTH2 dry storage canister schematics are shown in Figure 3-1. Note the grapple at the top of the canister. A niche was made in the vertical cask to accommodate the grapple. The NUHOMS 32 PTH2 canister specifications are provided in Table 3-1.

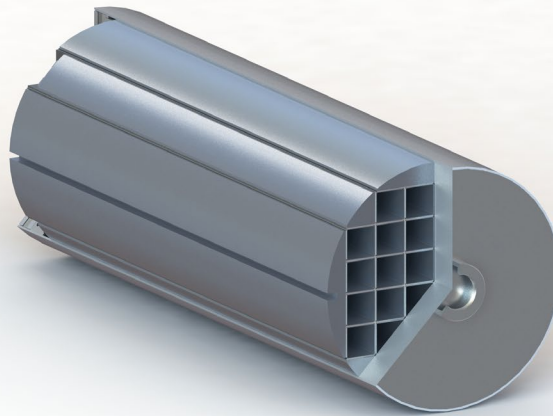
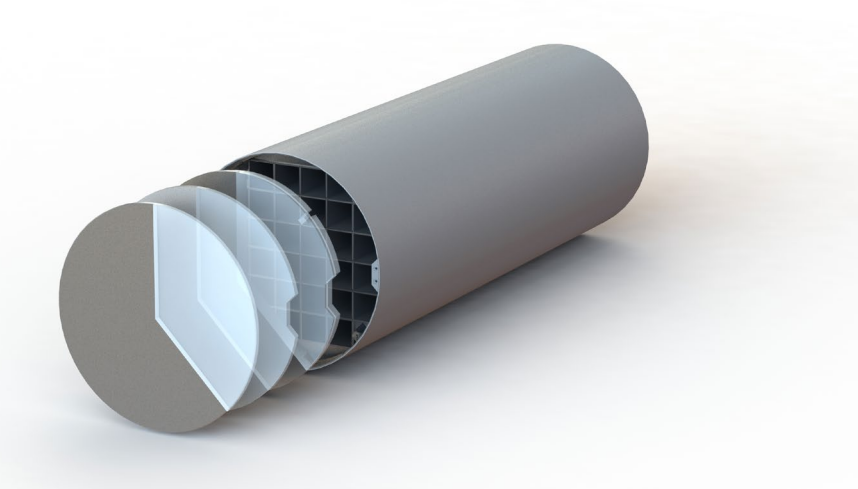


Figure 3-1. NUHOMS 32 PTH2 Schematics.

Table 3-1. NUHOMS 32 PTH2 specifications.

| Attribute | NUHOMS-32PTH2 | |
|---|-------------------------------|---------|
| a. Capacity (intact assemblies) | 32 pressurized water reactors | |
| b. Weight | lbs | kg |
| Empty | 56,170 | 22,501 |
| Loaded | 110,000 | 49,0 |
| c. Thermal | | |
| Design Heat Rejection (kW) | 37.2 | |
| Maximum Per Assy Heat Load (kW) | 1.5 | |
| Maximum Burnup (GWD/MTU) | 62.5 | |
| d. Shape | Cylindrical | |
| e. Dimensions | In | mm |
| Overall Length | 198.5 | 5,041.9 |
| Cross Section | 69.75 | 1,771.7 |
| Cavity Length | 178.65 | 4,537.7 |
| Wall Thickness | 0.63 | 16.0 |
| f. Materials of Construction | | |
| Canister Body | SS | |
| Basket | SS/Al/MMC | |
| Shield Plugs | Steel | |
| g. Cavity Atmosphere | He | |
| h. Maximum Leak Rate (atm-cm ³ /sec) | 1 x 10 ⁻⁷ | |

Figure 3-2 shows the canister internals.



Note: Square Openings are known as “basket tubes”.

Figure 3-2. NUHOMS 32 PTH2 Basket.

The main part of the canister is the basket. The basket consists of the slotted aluminum plates assembled into an "egg crate" configuration. The egg crates are held by stainless steel bands welded to the stainless-steel basket tubes (fuel compartments). The gap between the inside diameter of the canister and the basket tube grid is bridged by "transition rails" made from stainless steel and aluminum sections connected to the basket tube structure. The basket design of the NUHOMS 24 PTH canister is shown in Figure 3-3 reproduced from [20]. The NUHOMS 32 PTH2 basket geometry is similar to the egg crate basket geometry of the NUHOMS 24PTH canister.

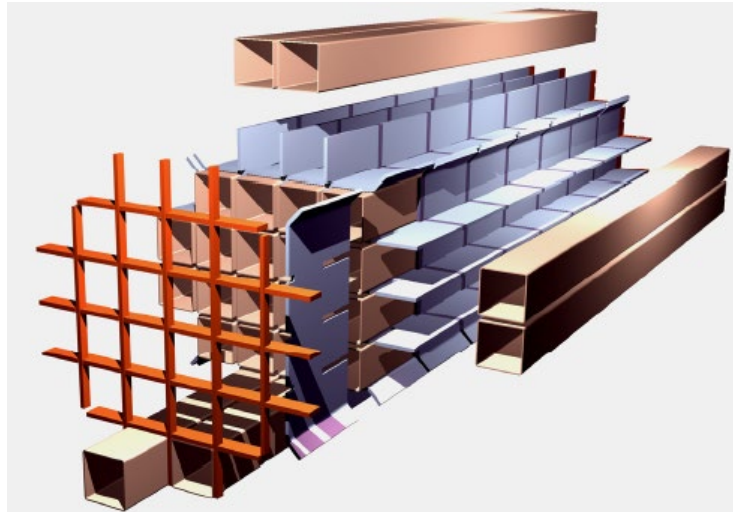


Figure 3-3. NUHOMS 24 PTH egg crate basket design.

The internal cross-section of each basket tube of the SNL canister was measured using a laser scanner (Figure 3-4). The average was 8.653" (219.79 mm). The NUHOMS canisters are designed for spent fuel assemblies such as 16 x 16 CE or Framatome ones. These assemblies are ~207 mm (8.15 in) in cross-section. Consequently, the average radial gap between the assembly and the basket tube is ~6.4 mm (0.25 in). The 17 x 17 assembly, such as a Westinghouse one, has cross-section of ~214 mm (8.42 in). It can fit into the basket tube, but the radial gap will be significantly smaller – 2.9 mm (0.11 in).

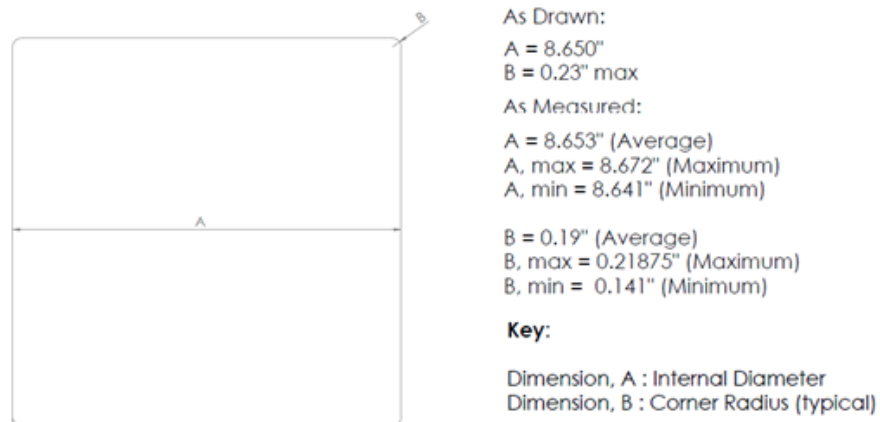


Figure 3-4. NUHOMS 32 PTH2 basket tube measurement.

Figure 3-5 shows NUHOMS 32 PTH2 dry storage canisters at the SNL test facility in Albuquerque, NM. In the seismic tests it will be important to be able to see the motion of the individual fuel assemblies within the basket, so the test will be performed without the three lids. In order to restrain the fuel assemblies (especially important for the horizontal tests) a restraint fixture will be designed that will keep the fuel assemblies from sliding out of the basket tubes but allow the motion within the tubes to be recorded via video.



Figure 3-5. NUHOMS 32 PTH2 dry storage canisters at the SNL facility.

3.2 Dummy Assemblies and Surrogate Assemblies

The NUHOMS 32 PTH2 canister will be loaded with 28 dummy assemblies and four surrogate assemblies. The following sections describe the dummy and surrogate assembly specifications.

3.2.1 Dummy Fuel Assemblies

In March 2022, a contract was placed with ENSA for manufacturing 30 dummy assemblies for the shake table test. In the test configuration with four surrogate assemblies, 28 dummy assemblies will be used. Two dummy assemblies are spare. The original dummy assembly design was developed in collaboration with PNNL [21]. The design was then revised to optimize manufacturing.

The main part of each dummy assembly is the 4,490 mm (176.77 in) long steel square tube with a 180 mm (7.09 in) cross-section and 12.5 mm (0.49 in) wall thickness. A 70 mm (2.76 in) diameter steel support rod with four rebars welded to it in five locations along its length was placed inside the square steel tube to provide reinforcement. The steel tube was filled with concrete. The concrete density was 146.7 lbs/ft³ – 148.6 lbs/ft³ (2,350 - 2,380 kg/m³). The bottom plate was placed on the bottom end and two angle irons were placed on the top end of the square tube. The length of the tube with the concrete is 4,284 mm (168.66 in). The remaining 206 mm (8.11 in) of the empty steel tube (instrumentation niche) will be used for instrumentation.

Twenty aluminum plates will be bolted to the steel tube, five plates along each surface. Figure 3-6 shows four aluminum plates bolted to the steel tube in one of five locations. The aluminum plate thickness is different for the different assembly types (Table 3-2). This design allows the dummy assemblies to achieve different cross-sections (width x height) while maintaining similar weights - 639.4 kg (Type I), 641.2 kg (Type II), and 643.4 kg (Type III). Type I (28 assemblies) has a cross-section of 207 mm (8.14 in), the same as the 16 x 16 surrogate assemblies. Type II (one assembly) has a cross-section of 210 mm (8.27 in). Type III (one assembly) has a cross-section of 214 mm (8.42 in), the same as the 17 x 17 surrogate assemblies. Using different cross-sections will allow for evaluating the effects related to the radial gap.

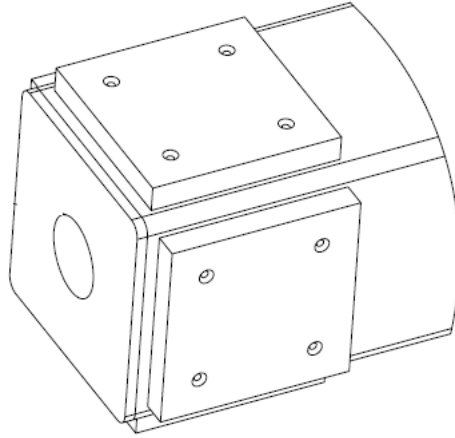


Figure 3-6. Four aluminum plates bolted to the steel tube in one of five locations.

Table 3-2. Aluminum plate thickness.

| Cross-Section (mm) | Aluminum Plate Thickness | |
|--------------------|--------------------------|-------|
| | mm | in |
| 207 | 16 | 0.630 |
| 210 | 17.5 | 0.689 |
| 214 | 19.5 | 0.768 |

The dummy assembly overall view is shown in Figure 3-7. The main components of the dummy assembly are shown in Figure 3-8.

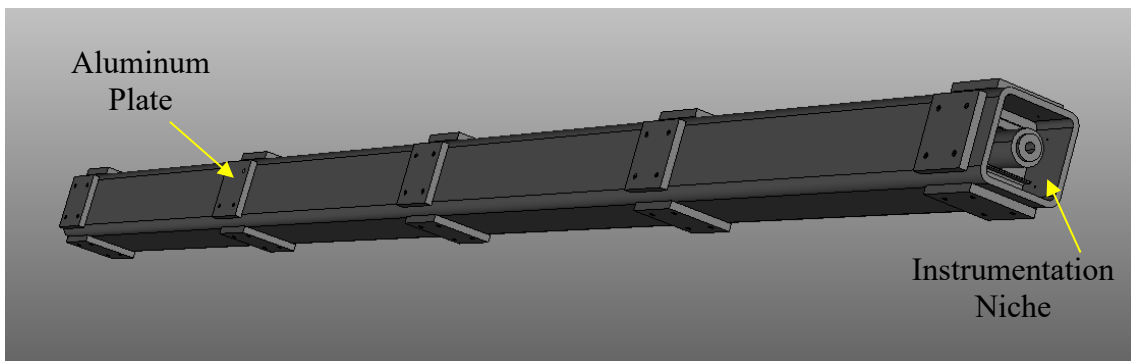


Figure 3-7. Dummy assembly overall view.

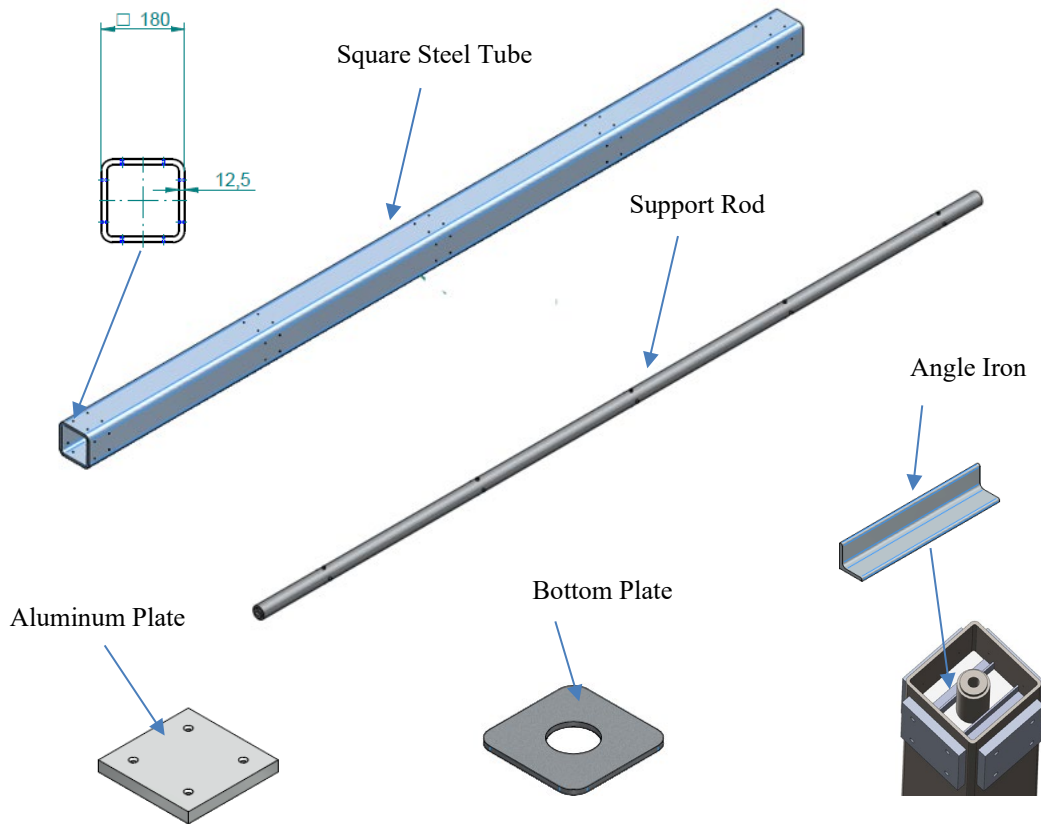


Figure 3-8. Dummy assembly main components.

The dummy assembly target and actual weights are provided in Table 3-3. The minimum dummy assembly weight is 625 kg (1,377 lbs) or 2% below the target weight. The maximum dummy assembly weight is 633 kg (1,394 lbs) or 1% below the target weight. The differences in weights are due to the variations in the achieved concrete densities. The box and whisker plot in Figure 3-9 provides the statistics of the actual dummy assembly weights.

Table 3-3. Dummy assembly target and actual weights.

| Dummy | ID | Cross-Section (mm) | Color | Weight | | |
|----------|----|--------------------|-------|-----------------|--------|--------|
| | | | | Per Design (kg) | Actual | |
| | | | | | (kg) | (lbs) |
| Type I | 1 | 207 | Green | 639.4 | 625 | 1376.7 |
| Type I | 2 | 207 | Green | 639.4 | 631 | 1389.9 |
| Type I | 3 | 207 | Green | 639.4 | 625 | 1376.7 |
| Type I | 4 | 207 | Green | 639.4 | 629 | 1385.5 |
| Type I | 5 | 207 | Green | 639.4 | 627 | 1381.1 |
| Type I | 6 | 207 | Green | 639.4 | 631 | 1389.9 |
| Type I | 7 | 207 | Green | 639.4 | 633 | 1394.3 |
| Type I | 8 | 207 | Green | 639.4 | 627 | 1381.1 |
| Type I | 9 | 207 | Green | 639.4 | 627 | 1381.1 |
| Type I | 10 | 207 | Green | 639.4 | 633 | 1394.3 |
| Type I | 11 | 207 | Green | 639.4 | 625 | 1376.7 |
| Type I | 12 | 207 | Green | 639.4 | 625 | 1376.7 |
| Type I | 13 | 207 | Green | 639.4 | 627 | 1381.1 |
| Type I | 14 | 207 | Green | 639.4 | 633 | 1394.3 |
| Type I | 15 | 207 | Green | 639.4 | 631 | 1389.9 |
| Type I | 16 | 207 | Green | 639.4 | 629 | 1385.5 |
| Type I | 17 | 207 | Green | 639.4 | 631 | 1389.9 |
| Type I | 18 | 207 | Green | 639.4 | 627 | 1381.1 |
| Type I | 19 | 207 | Green | 639.4 | 631 | 1389.9 |
| Type I | 20 | 207 | Green | 639.4 | 631 | 1389.9 |
| Type I | 21 | 207 | Green | 639.4 | 629 | 1385.5 |
| Type I | 22 | 207 | Green | 639.4 | 629 | 1385.5 |
| Type I | 23 | 207 | Green | 639.4 | 631 | 1389.9 |
| Type I | 24 | 207 | Green | 639.4 | 633 | 1394.3 |
| Type I | 25 | 207 | Green | 639.4 | 629 | 1385.5 |
| Type I | 26 | 207 | Green | 639.4 | 627 | 1381.1 |
| Type I | 27 | 207 | Green | 639.4 | 629 | 1385.5 |
| Type I | 28 | 207 | Green | 639.4 | 629 | 1385.5 |
| Type II | 1 | 210 | Gray | 641.2 | 633 | 1394.3 |
| Type III | 1 | 214 | Blue | 643.4 | 633 | 1394.3 |

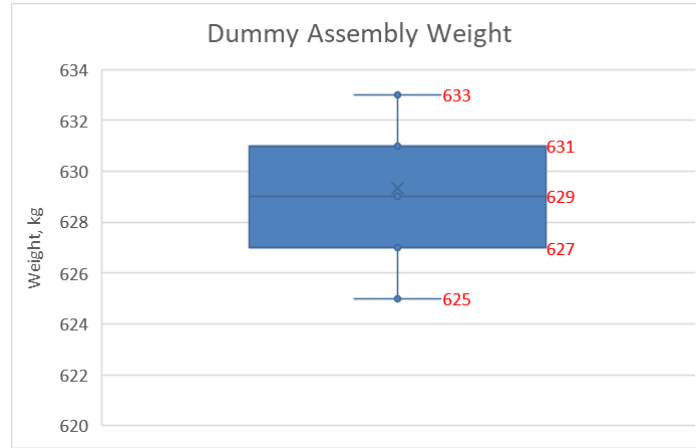


Figure 3-9. Statistics of the dummy assembly actual weights.

The dummy assemblies were delivered to LHPOST in February 2023. Figure 3-10 (left) shows the dummy assembly in the delivery truck at the moment of their arrival to the LHPOST. Figure 3-10 (right) shows the dummy assemblies in their storage location at LHPOST. The Type I assemblies (207 mm cross-section) are painted in green. The Type II assembly (210 mm cross-section) is painted in white. The Type III assembly (214 mm cross-section) is painted in blue.



Figure 3-10. Dummy assembly in the delivery truck (left) and unloaded at the LHPOST (right).

3.2.2 Surrogate Fuel Assemblies

Four surrogate assemblies will be used in the test to assess the differences related to the assembly type, radial gap, and condition (intact versus slightly damaged spacer grid) and its location in the basket.

Two surrogate assemblies will be a 16 x 16 CE PLUS7 and a 17 x 17 Westinghouse ACE7. These assemblies were provided for the shake table test by the KNF as a part the collaboration agreement. The assemblies were delivered to the SNL in Albuquerque (NM) in December 2022 where they will be instrumented along with the other two surrogate assemblies. The assembly rods are zirconium alloy tubes filled with the lead pellets The assembly schematics are shown in Figure 3-11 and Figure 3-12.

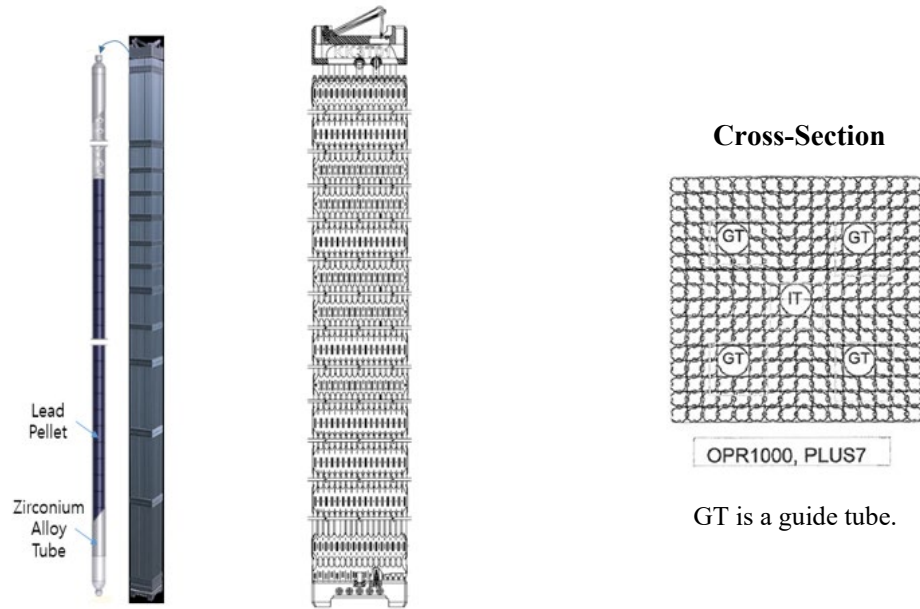


Figure 3-11. KNF's 16 x 16 CE PLUS7 surrogate assembly.

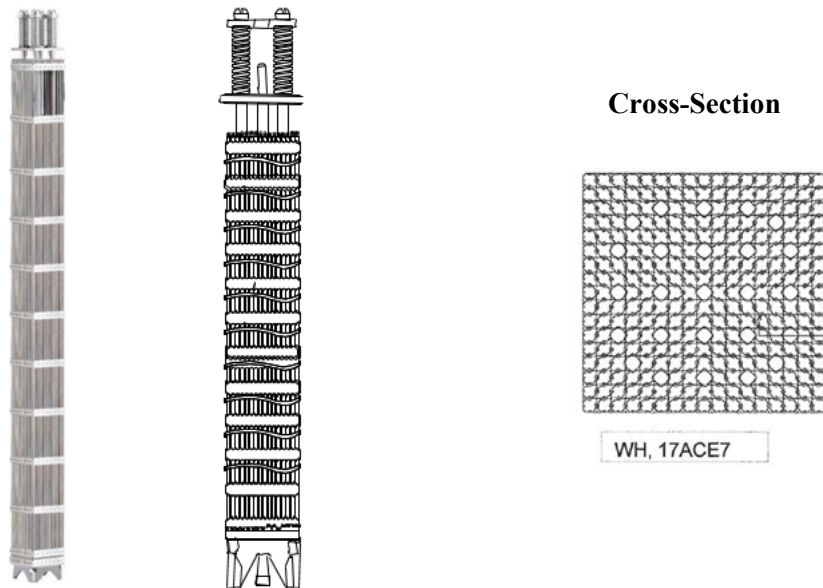


Figure 3-12. KNF's 17 x 17 Westinghouse ACE7 surrogate assembly.

The assembly specifications are provided in Table 3-4. The outer and inner diameters of the rods in these 16 x 16 and 17 x 17 surrogate assemblies are the same. The guide tube outer and inner diameter are about two times larger in the 16 x 16 assembly compared to the 17 x 17 assembly. Photos of the KNF surrogate assemblies are shown in Figure 3-13.

Table 3-4. KNF’s surrogate assembly specifications.

| Assembly Type | 16x16 CE PLUS7 | | 17x17 Westinghouse | |
|-------------------------|----------------|---------|--------------------|---------|
| Length (mm in) | 4,528 | 178.27 | 4,063 | 159.96 |
| Cross-section (mm in) | 207.264 | 8.16 | 213.97 | 8.42 |
| Weight (kg lbs) | 639 | 1408.75 | 673 | 1483.71 |
| Number of Rods | 236 | | 264 | |
| Number of guide tubes | 4 | | 24 | |
| Pitch (mm in) | 12.85 | 0.51 | 12.6 | 0.50 |

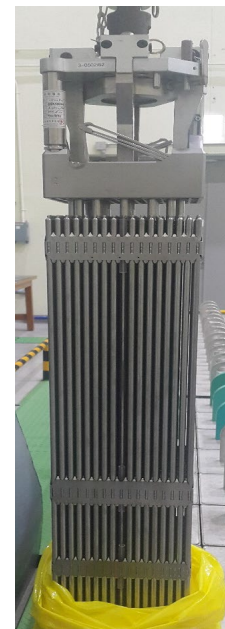


Figure 3-13. Photos of 16 x 16 CE PLUS7 (left) and 17 x 17 Westinghouse ACE7 (right).

The third assembly that will be used in the shake table test is SNL’s 17 x 17 Westinghouse surrogate assembly. This surrogate assembly was used in the 30 cm (11.81 in) drop test in 2020 [22]. The spacer grids were deformed up to 6.1 mm (0.24 in) in this test, but the rods and other hardware were not damaged. The assembly and the spacer grid with the largest deformation are shown in Figure 3-14.

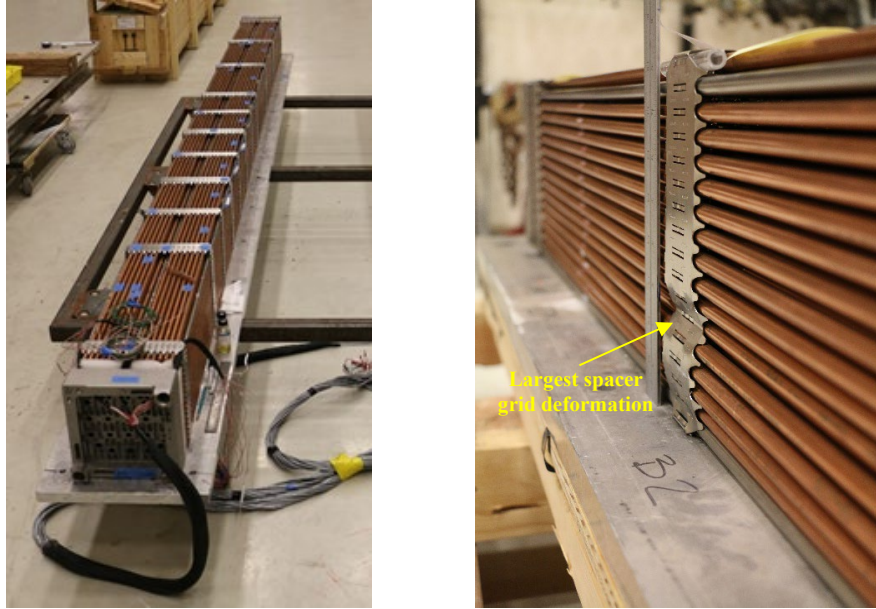


Figure 3-14. SNL 17x17 surrogate assembly (left) and closeup of the spacer grid (right).

All rods of the SNL surrogate assembly, except three, are copper tubes with lead rope inside (Figure 3-15). Three rods are zircaloy tubes, one with the lead rope, one with the lead pellets, and one with molybdenum pellets.

The weight of the surrogate assembly is 785 kg. A few photos of the pre-30cm-drop-test full-scale surrogate assembly with different level of details are shown in Figure 3-15. The locations of zircaloy tubes are identified on the bottom photo and the copper tube and its specifications are shown in the top photo.

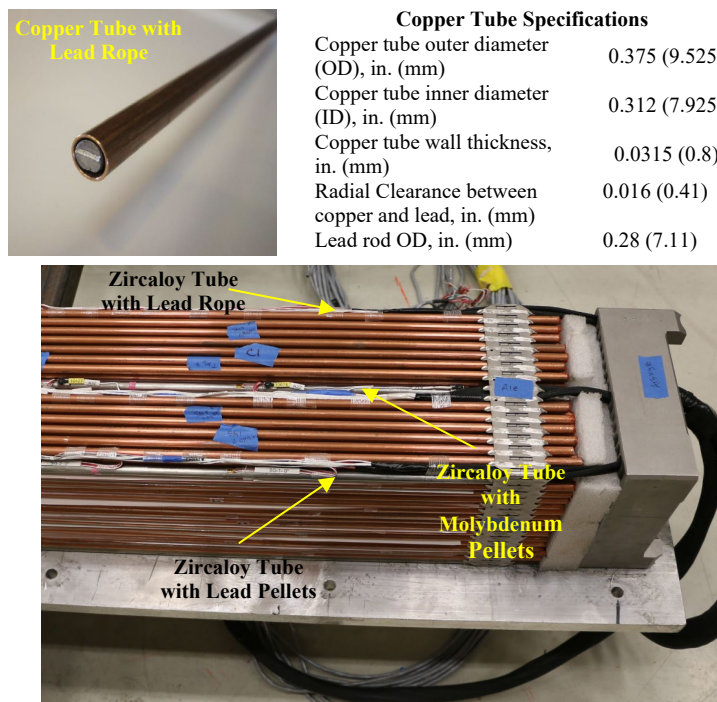


Figure 3-15. New full-scale surrogate assembly photo.

3.2.3 The contract for manufacturing the fourth surrogate assembly (16 x 16) was placed by PNNL with Framatome. The rods and the skeleton of the surrogate assembly will be delivered to SNL in March 2024. The rods will be inserted into the skeleton at SNL. Dummy and Surrogate Assemblies Loading Map

As was described in the previous sections, dummy and surrogate assemblies have different cross-sections and weights. The location of the surrogate assemblies in the basket of the canister are especially important because they need to cover the expected location related variations in the strains on the assembly rods. These locations were proposed based on modeling results [15]. Surrogate assembly A is placed in one of the center cells of the basket. Surrogate assembly B is placed in an outer cell. Surrogate assembly C is placed in a mid/corner cell. Surrogate assembly D is placed in an outer cell in the corner. The proposed locations will be confirmed (or revised) after the design of the fourth surrogate assembly is known. Note that D and B are aligned with the MMTT instrumented assembly locations.

The surrogate assembly are labeled as:

- A - PNNL 16 x 16 (to be manufactured)
- B - KNF 16 x 16 CE PLUS7
- C - KNF 17 x 17 Westinghouse ACE7
- D - SNL 17 x 17 Westinghouse

The locations of the dummy assemblies were selected by minimizing the deviation of the average dummy assembly weight in each row and in each column in the basket from the target weight of the dummy assembly (639.4 kg). The proposed distribution of the dummy assembly weights in the canister basket are provided in Table 3-5.

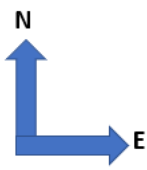
Table 3-5. The proposed distribution of the dummy assembly weights in the canister basket.

| | 1 | 2 | 3 | 4 | 5 | 6 | | Row Average | |
|----------------|-------|----------|----------|-------|------------|----------|---|-------------|-------|
| 1 | | 625 | 631 | 625 | 629 | | 1 | 627.5 | 98.1% |
| 2 | 627 | 631 | 633 | 627 | 627 | 633 | 2 | 629.6 | 98.5% |
| 3 | 625 | 625 | 633 | 627 | 633 | B | 3 | 628.6 | 98.3% |
| 4 | 631 | 629 | A | 633 | 631 | 627 | 4 | 630.2 | 98.6% |
| 5 | 631 | 631 | 629 | 629 | C | 631 | 5 | 630.2 | 98.6% |
| 6 | | D | 633 | 629 | 627 | | 6 | 629.6 | 98.5% |
| | 1 | 2 | 3 | 4 | 5 | 6 | | | |
| Column Average | 628.5 | 628.2 | 631.8 | 628.3 | 629.4 | 630.3 | | | |
| | 98.3% | 98.2% | 98.8% | 98.3% | 98.4% | 98.6% | | | |

Figure 3-16 shows the proposed canister loading map for the tests with the vertical cask. The dummy assembly are labeled as:

- # Type I Dummy (1 - 28), 207 mm cross-section
- T2 Type II Dummy, 210 mm cross-section
- T3 Type III Dummy, 214 mm cross-section

| | | | | | |
|---|----|-----------|-----------|----------|----------|
| | 10 | B | 18 | 23 | |
| 4 | 9 | 14 | 17 | C | 26 |
| 3 | 8 | 13 | T2 | 22 | 25 |
| 2 | 7 | T3 | A | 21 | 24 |
| 1 | 6 | 12 | 16 | 20 | D |
| | 5 | 11 | 15 | 19 | |


Figure 3-16. Canister loading map for the tests with the vertical cask.

For the tests with the trough, the canister has to be rotated 90 degrees counterclockwise. The rotated loading map is shown in Figure 3-17.



Figure 3-17. Canister loading map for the tests with the trough.

3.3 Dry Storage Overpacks

The NUHOMS 32 PTH2 canister loaded with 28 dummy assemblies and four surrogate assemblies will be placed first in the vertical cask for the shake table test and then in the HSM (trough). The following sections describe the vertical cask and the trough.

3.3.1 Vertical Storage Overpack

For the vertical test configuration, the original plan was to use either a MAGNASTOR or HI-STORM 100 cask as a dry storage overpack. Both casks can accommodate the NUHOMS 32 PTH2 canister even though they are designed for other types of dry storage canisters. The cost of acquiring these casks was significantly higher than the project could have afforded. A decision was made to manufacture a simplified model of a vertical concrete cask.

The drawings of the cask were developed in collaboration with PNNL [23]. The cask consists of a steel carcass filled with concrete. It is 5.6 m (18.37 ft) in height and 3.56 m (11.68 ft) in diameter. The cask is composed of the following main parts with the quantity shown in parentheses:

- Part #1 – Outer Shell (1)
- Part #2 - Baseplate (1)
- Part #3 - Pedestal (1)
- Part #4 – Inner Shell with Radial Plates (1)
- Part #5 – Concrete (4)

The overall view and cross-sectional view of the cask and the dimensions of main components are shown in Figure 3-18. The numbers in Figure 3-18 correspond to the part numbers in Table 3-6. The circular opening in the middle of the pedestal is for accommodating the NUHOMS 32 PTH2 grapple. The cask is lifted with four lugs/pins inserted into the lifting holes located on the top of the cask. The tapped holes in

the base plate are for mounting the anchor brackets. Most of the shake table tests will be performed with the cask free-standing. However, a few tests with the cask anchored to the shake table are planned to address the conditions that currently exist at two NPPs and might be the conditions at the other NPPs in the future.

The inner shell, outer shell, baseplate, and pedestal are made of carbon steel and are assembled into the cask carcass. The estimated weight of each part is provided in Table 3-6. The outer shell wall thickness is 0.25 in. The inner shell is 79.75 in in diameter with the wall thickness of 1 in. The total weight of the steel carcass is 54,564 lbs (24,342 kg).

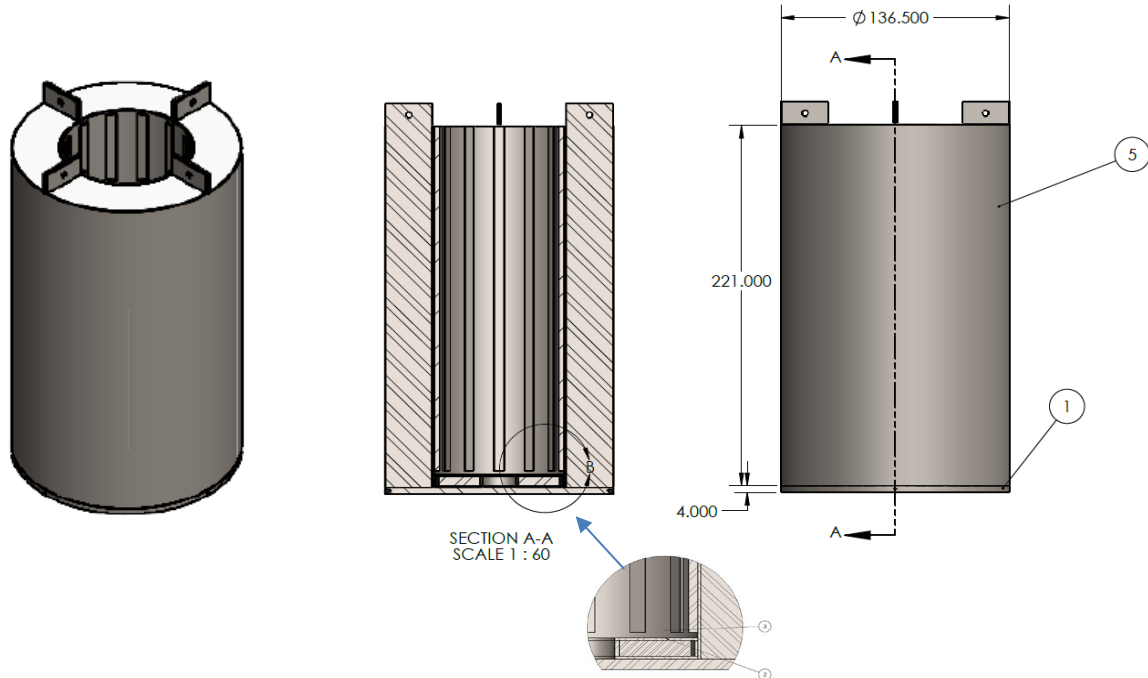


Figure 3-18. Vertical cask over all view and cross-sectional view.

The concrete is poured into four sections formed by the inner shell and outer shell. The total volume of the concrete is 1,204 ft³ (34 m³). The estimated concrete weight in Table 3-6 is based on the concrete density of 150 pcf (2,403 kg/m³).

The following were the requirements on the vertical cask materials: steel minimum yield strength 46 ksi (317 MPa) and concrete minimum compressive strength 4 ksi (28 MPa).

Table 3-6. Estimated weight of the cask different parts.

| Part NN | Part Name | Weight (lbs kg) | | Comments |
|---------|--------------------------------|-------------------|--------|---------------------------------|
| 1 | Outer Shell | 6,707 | 3,045 | Manufactured |
| 2 | Base Plate | 16,595 | 7,534 | Manufactured |
| 3 | Pedestal | 3,351 | 1,521 | Manufactured |
| 4 | Inner Shell with Radial Plates | 28,024 | 12,723 | Manufactured |
| 5 | Concrete (estimated) | 180,600 | 81,992 | Provided by concrete contractor |

| | | | | |
|--|-----------------------------------|---------|---------|--|
| | Cask Total Weight | 235,277 | 106,816 | |
| | Steel Carcass Total Weight | 54,677 | 24,823 | |

The vertical cask carcass was manufactured by Springs Fabrication, LLC located in Colorado Springs, CO in May 2022. It was delivered to LHPOST on June 10, 2022. A concrete pad was built at the LHPOST at the beginning of May next to the shake table to house the cask until the time of the test. Figure 3-19 shows the arrival of the cask to the shake table facility.



Figure 3-19. Cask arrival to LHPOST (UCSD).

The cask was filled with concrete on June 14, 2022. The local suppliers were limited to the concrete mix with the final concrete density. Three samples of concrete were collected into cylindrical test samples. The cylinder weights with the concrete and calculated concrete density are shown in Table 3-7. An empty cylinder weight is 0.33 kg (0.73 lbs).

Table 3-7. Concrete samples data.

| Sample ID | Weight (lbs) | Calculated Concrete Density | |
|----------------|--------------|-----------------------------|-------------------|
| | | pcf | kg/m ³ |
| Cylinder 1 | 28.38 | 140.8 | 2,255.7 |
| Cylinder 2 | 28.43 | 141.1 | 2,259.8 |
| Cylinder 3 | 28.92 | 143.6 | 2,299.7 |
| Average | | 141.8 | 2,271.7 |

Figure 3-20 shows the process of concrete pouring (top and bottom left) and the top of the cask at the end of concrete pouring (bottom right). Figure 3-21 shows the completed vertical cask (right) and 3 cylinders with concrete samples (left).



Figure 3-20. Pouring concrete into the cask (top and bottom left) and filled with concrete cask (bottom right).



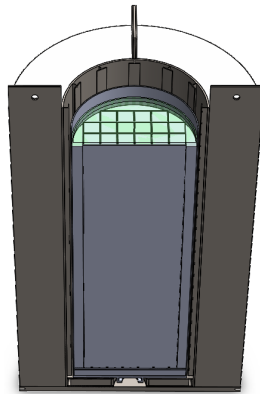
Figure 3-21. Completed vertical cask covered with the tarp (left) and concrete samples (right).

The total weight of the test unit assuming the average concrete density is 326,650 lbs (148,304 kg). The total weight of the test unit assuming the maximum concrete density is 328,587 lbs (149,178 kg). The vertical cask mockup is very similar to the HI-STORM 100 overpack with regard to the dimensions and empty and loaded weights. The mockup is built as steel-concrete-steel, which is similar to the HI-STORM 100 design. Figure 3-22 shows the schematics of the vertical cask mockup and the HI-STORM 100 vertical overpack. Table 3-8 compares the vertical cask mockup and HI-STORM 100 (Holtec) specifications.

Table 3-8. Specifications of the vertical cask mockup and HI-STORM vertical overpack.

| Specification | Vertical Cask Model | | Hi-STORM 100 Vertical Overpack | |
|-------------------------|---------------------|---------|--------------------------------|---------|
| Length (m in) | 225.00 | 5.72 | 231.25 | 5.87 |
| Outer diameter (in m) | 136.50 | 3.47 | 132.50 | 3.37 |
| Wall thickness (in m) | 28.43 | 0.72 | 29.50 | 0.75 |
| Empty weight (lbs kg) | 225,645 | 106,458 | 270,000 | 122,470 |
| Loaded weight (lbs kg) | 326,650 | 152,385 | 360,000 | 163,293 |

Vertical Cask Mockup



HI-STORM 100

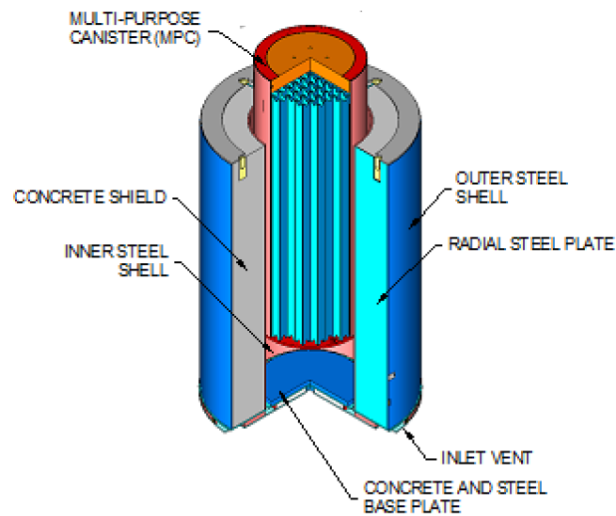


Figure 3-22. Vertical cask mockup (left) and HI-STORM 100 vertical overpack (right).

The vertical cask will be free standing on the shake table, except when the Diablo Canyon acceleration time histories are applied to the table. In the Diablo Canyon scenarios, the vertical cask will be anchored to the shake table as described in Section 4.2.

3.3.2 Horizontal Storage Overpack

The NUHOMS canisters are stored in NUHOMS advanced horizontal storage modules (AHSMs). The original plan was to use one of the AHSM base units available from SONGS. The base unit weight is 175,000 (79,450 kg) to 192,000 lbs (87,168 kg) depending on the model. Figure 3-23 shows the AHSMs at SONGS. The standard AHSM has a 3.625 in (92 mm) gap between the canister and the internal AHSM wall. The high seismic AHSM has a 9.125 in (232 mm) gap between the canister and the internal AHSM wall.



Figure 3-23. AHSMs base units at SONGS.

Because the proposed cost of transporting an AHSM to LHPOST was prohibitive, the decision was made to manufacture a mockup of an AHSM. The developed AHSM mockup (trough) design is shown in Figure 3-24 (left). The trough consists of the steel frame embedded into the concrete box. The total estimated weight of the trough is 144,000 lbs (65,376 kg). The actual weight will depend on the achieved density of the concrete.

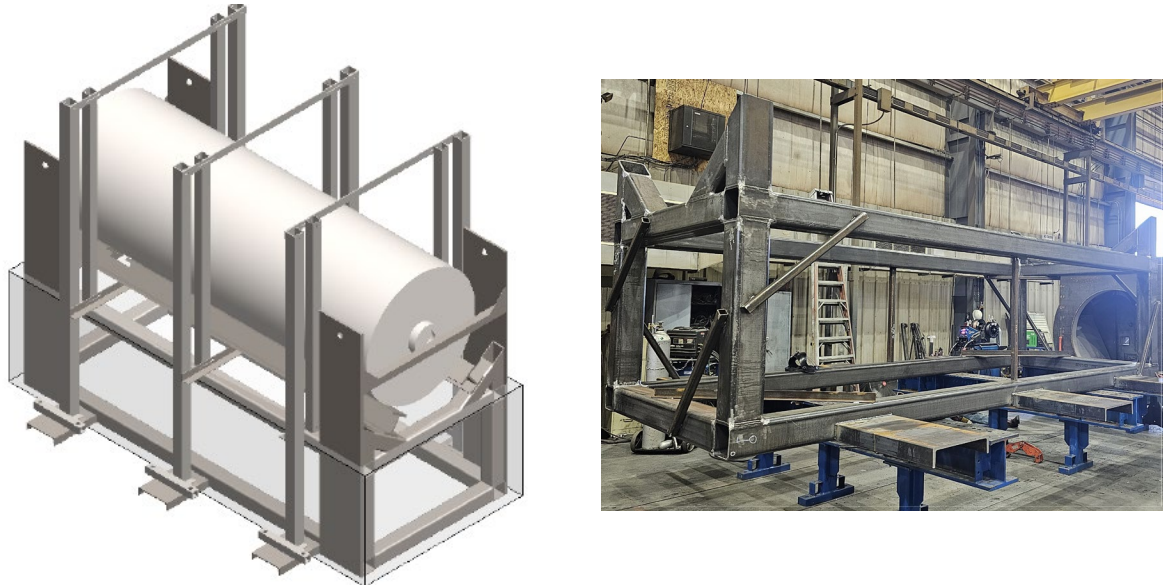


Figure 3-24. Mockup of the AHSM (trough design) and Trough Frame at the Manufacturing Facility.

The main part of the trough is the steel frame with the skids that hold the canister. The skids have cutouts for ease of lifting the canister in and out of the trough. The base frame dimensions are 216 in (5.49 m) (length) by 90.5 in (2.30 m) (width) by 58.8 in (1.49 m) (height). Four lifting plates are welded to the frame, two on each side. Six anchoring channels at the bottom of the frame, three on each side, are for anchoring the trough to the shake table. Six vertical columns, three on each side, are welded to the anchoring plates. Canister side restraint is provided by bolting an appropriate depth beam to the frame. This design allows for achieving different gaps between the canister and the side walls which is needed to represent both, regular AHSM and high seismic AHSM.

The frame is embedded into a concrete box. The concrete box dimensions are 228.125 in (5.79 m) (length) by 101 in (2.57 m) (width) by 61.5 in (1.56 m) (height).

The trough is being manufactured by Springs Fabrication, LLC located in Colorado Springs, CO. Figure 3-24 (right) shows the trough frame at the manufacturing facility. The frame will be transported to the LHPOST in November 2023. The trough will be embedded into the concrete box at the LHPOST.

3.4 Safety Rigging

The pre-test modeling indicated limited sliding of the free-standing cask (except Diablo Canyon scenario) and no tip over. However, to meet the LHPOST safety requirements, the safety rigging must be used in the tests with the vertical cask. The proposed design of the safety rigging is shown in Figure 3-25. This design will allow for sliding (if any) only within the concrete slab on the shake table and will prevent tipping over.

The safety rigging will be bolted to the shake table after the vertical cask is placed in the centre of the concrete slab. The rigging is reinforced by the angled supports on the long side of the shake table. On the short side the reinforcement is provided by the nylon straps because there is no room for the angled supports. Timbers will be attached to all the beams at the top part of the rigging. They will provide energy dissipation in case if the vertical cask slides and hits the safety rigging during one of the tests.

The design of the safety rigging will be finalized and a contract for manufacturing the safety rigging will be placed in October 2023. The safety rigging will be delivered from the manufacturer (TBD) to LHPOST. The expected time of completion is January 2024.

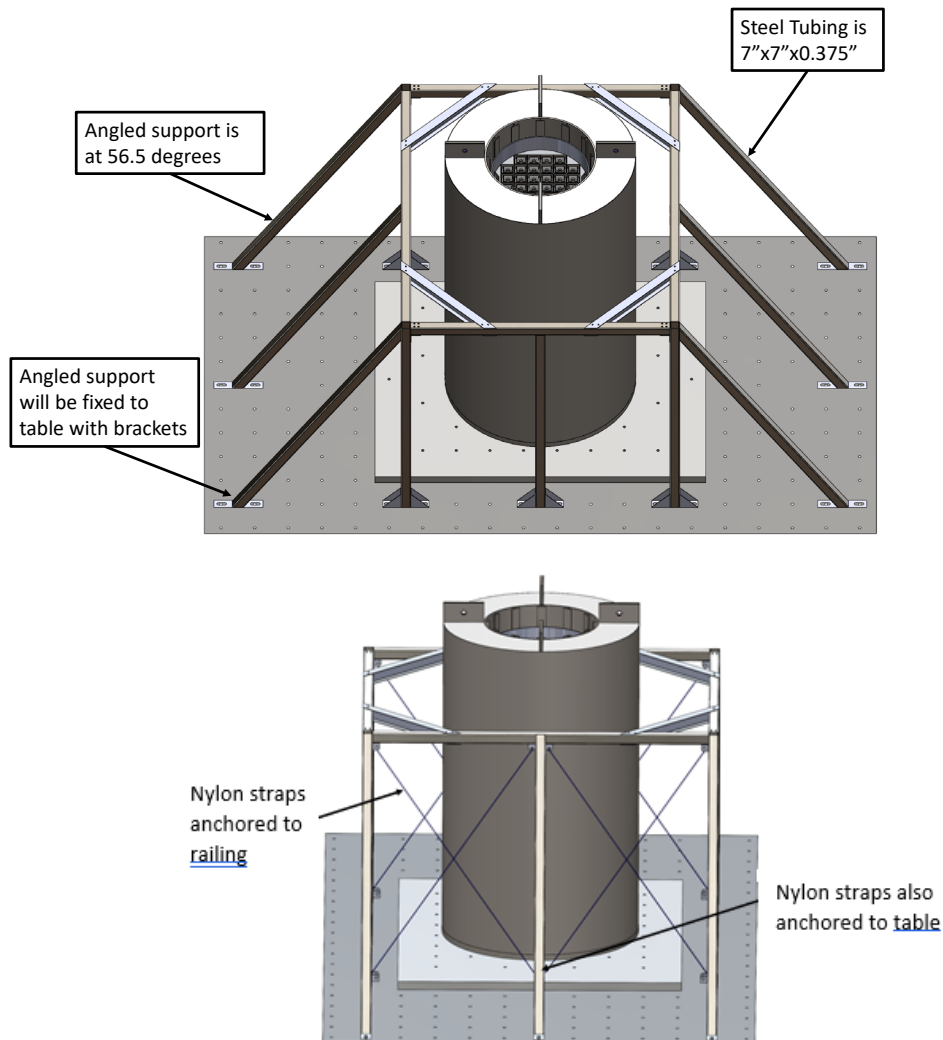


Figure 3-25. Proposed design of the safety rigging.

This page intentionally left blank.

4. CONCRETE SLAB ON THE SHAKE TABLE

A concrete slab will be installed on the shake table before the test to simulate ISFSI pad conditions. The concrete surface should be representative of an ISFSI pad. Section 4.1 provides recommendations for the concrete surface finish. Section 4.2 describes the configuration of the concrete slab. This information was very limited in the previous test plan report [7] because the analysis of the friction experiment data was not completed at that time.

4.1 Recommended Concrete Surface Finish

In the shake table tests with the vertical cask, the cask will be free-standing because this is representative of all, except two, ISFSIs in the U.S. with vertical casks. The static and dynamic friction coefficients between the steel bottom of the cask and the concrete layer on the shake table and the friction decay constant are important parameters that will affect cask behavior during the test. These parameters must be known for the pre- and post-test modelling, data analysis, and model validation. Note that in the tests with a HSM, the HSM will be anchored to the shake table and the friction parameters will not be relevant.

Limited data were available for the friction between concrete and steel. The ISFSI pad friction coefficient range assumed in NUREG/CR-6865 [24] was from 0.2 to 0.8 with an average of 0.53. The friction coefficient value used in the HI-STORM 100 FSAR [25] was 0.53. A construction report for the Grand Gulf ISFSI, performed experiments to verify friction coefficient and determined that it was 0.54 [26].

A friction experiment was conducted at the Engineering Department of UNM to determine the friction coefficients between a steel plate with the same finish as the bottom of the vertical cask and different concrete surfaces. The experiment is documented in [8]. The detailed data analysis is presented in [13].

Static and dynamic steel on concrete friction coefficients can be measured from the horizontal force versus displacement data. The approach taken was to fix the steel plate and to pull the concrete sample over the plate with a constant displacement rate using a material test system (MTS) machine. This allows for collecting continuous horizontal force data over the length of the steel plate. Four displacement rates were used: 3 mm/s, 5 mm/s, 7 mm/s, and 9 mm/s. Three vertical loads were applied: 182 N (41 lbs), 342 N (77 lbs), and 540 N (121 lbs). The tests were performed with four concrete samples having different surface finishes. The total number of tests was 48 (4 displacement rates x 3 loads x 4 concrete samples).

For ease of reproducibility and implementation in the field, a multi-use ABS plastic sheet liner (Spec Formliners, Inc., Santa Ana, CA) with a specific surface roughness was used to obtain the four surface roughness levels for the concrete blocks. Four selected surface roughness levels of concrete were: light sandblast, light to medium sandblast, medium bush hammer, and heavy sandblast. The surface roughness levels were related to the concrete roughness profiles as defined by the International Concrete Repair Institute (ICRI). Figure 4-1 illustrates the relationship between each surface roughness level and its corresponding concrete profile according to CSP classification by ICRI.

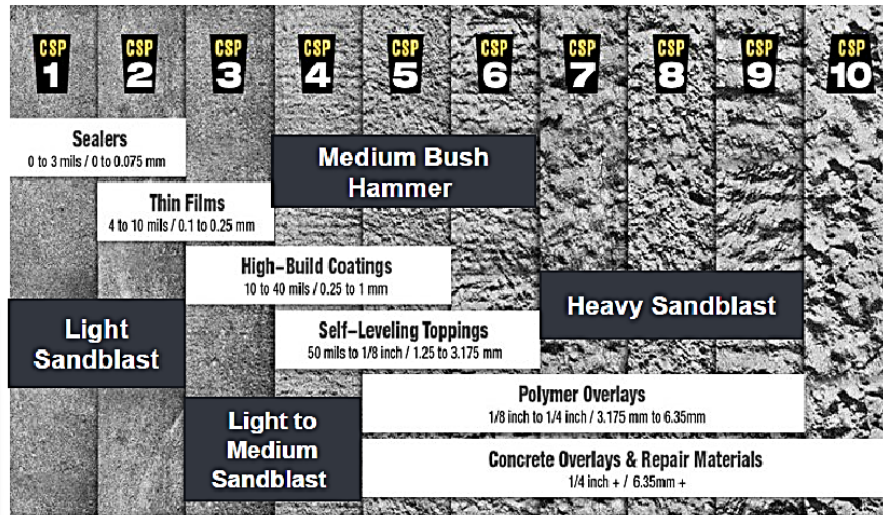


Figure 4-1. Surface roughness levels and corresponding concrete profile per CSP classification by ICRI.

The box and whisker plot in Figure 4-2 compares the statistics of the static coefficient of friction between the steel plate and different concrete finishes from 48 tests. The static friction coefficient decreases as the surface roughness increases from light sandblast to light to medium sandblast and to medium bush hammer. The dynamic friction coefficients are 15% to 18% lower than the static friction coefficients. The same trend of decreasing dynamic friction coefficients with increasing surface roughness was observed. The reason is believed to be related to the actual contact area between steel and concrete. As the surface roughness increases, the actual contact area decreases.

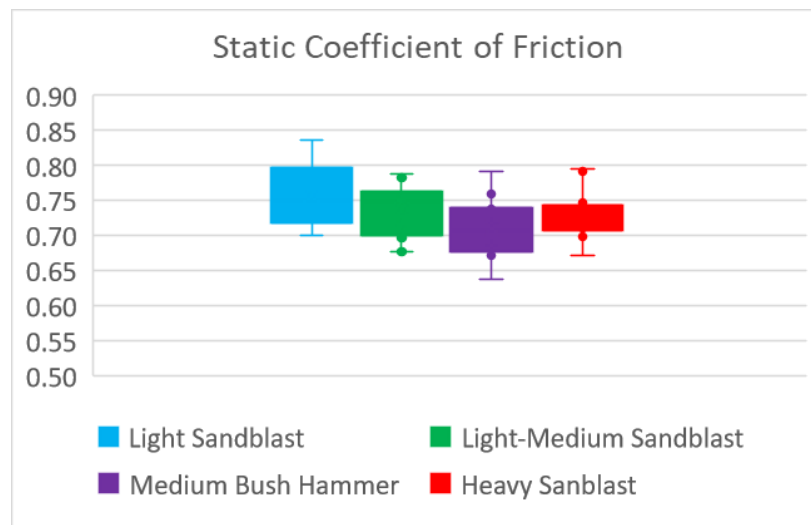


Figure 4-2. Static friction between steel plate and different concrete finishes.

A series of push-off friction tests were conducted to determine static friction coefficients on concrete surfaces without finish, such as a concrete pavement of a driveway (3 different surfaces were considered) and a concrete garage floor surface (one surface was considered). The test setup was similar to what is recommended in [25] for the steel on concrete push-off tests at an ISFSI with a HI-STORM 100 dry storage cask. The tests were conducted with a 42-lb steel block with the dimensions of 6"x6"x4". The steel block is shown in Figure 4-3. Three surfaces of the block used in the tests were: top face (6"x6") and

side face (4"x6") with unfinished steel surfaces and the bottom face (6"x6") with bead blasted surface generated following the instructions of an SSPC-SP2 type finish.



Note: The top of the block in this photo is the side face with the hook used to pull the block.

Figure 4-3. Steel block used in push-off friction tests.

For each concrete surface, 22 measurements were taken for each of three steel block faces. The total number of tests was 198 for driveway concrete surface and 66 for the garage floor concrete surface. The box and whisker plot in Figure 4-4 compares the statistics of the static coefficient of friction between the steel block and unfinished concrete surfaces. The coefficient of friction range is very similar for the driveway and garage floor concrete surfaces. The garage floor has a slightly smaller friction coefficient and smaller variation in the friction coefficient values due to a smoother surface.

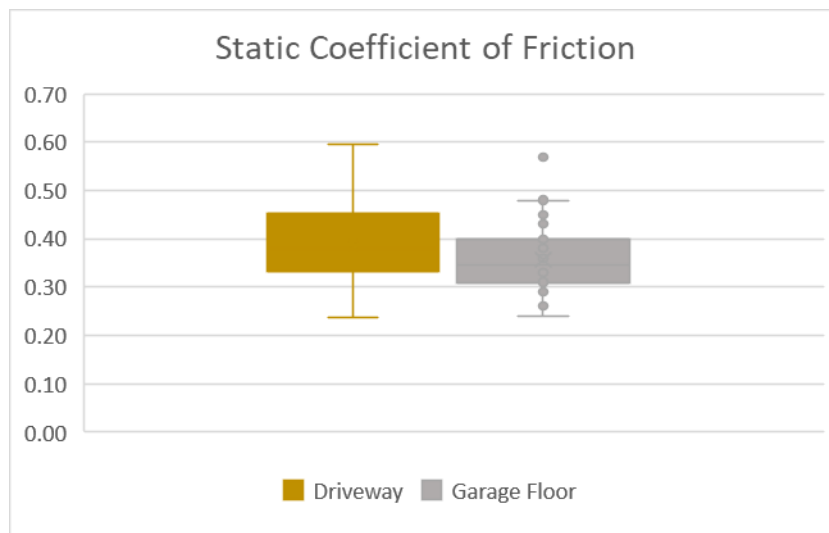


Figure 4-4. Static friction between steel block and unfinished concrete surfaces.

The results from the friction experiment and push-off tests are compared to the literature data in Figure 4-5.

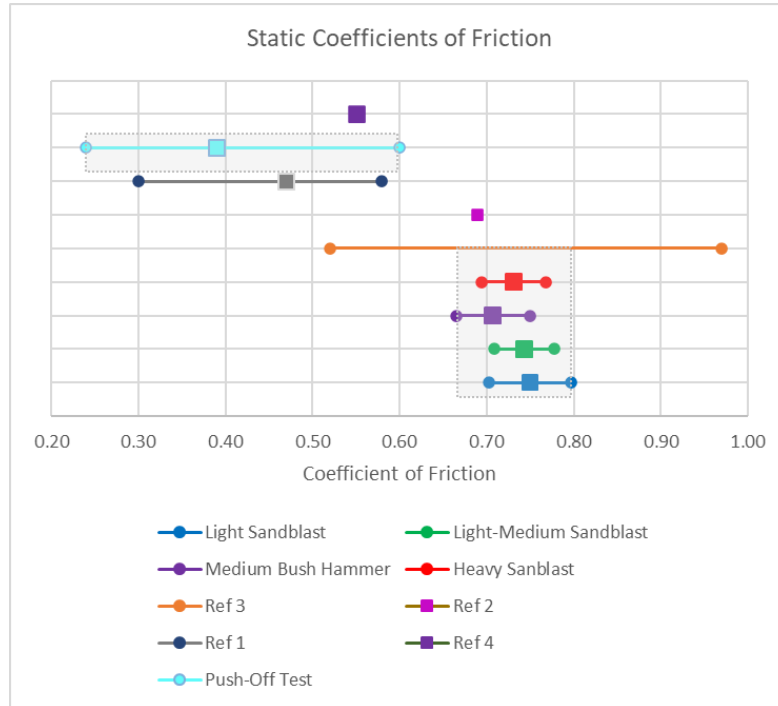


Figure 4-5. Static friction coefficients from the friction tests and literature.

“Ref 1” refers to the data from [27]. The average coefficient of friction between the machined mild steel and concrete was found to be 0.47 for stress levels between 1 and 68,000 psi.

“Ref 2” refers to the data from [28]. The data point is an average based on the results of fifteen push-off tests. The tests were conducted with a concrete block on a steel plate.

“Ref 3” in this figure refers to the data from [29]. This wide range covers three results from tests with varying concrete surface finishes.

“Ref 4” refers to the data from [30]. In this experiment the coefficient of static friction was calculated between a steel tube and three concrete blocks with varied surface finishes. The recommended static friction coefficient between the concrete and steel tube was 0.55.

The static friction from the friction experiment is within the range in Ref 2 and Ref 3. This is believed to be a range for concrete with a surface finish. The static friction from the push-off tests similar to the range in Ref 1 and Ref 4. This is believed to be a range for smooth concrete without surface finish.

Note that the ISFSI pad friction coefficient range assumed in NUREG/CR-6865 [24] was from 0.2 to 0.8. Based on the data obtained from the friction experiment and push-off tests it can be concluded that the static friction of 0.2 is unrealistic. The minimum value was 0.24, which was also confirmed by the literature data.

For the shake table test it is recommended to use concrete with light to medium sandblast finish. In the friction experiment, these surfaces resulted in the static friction coefficient of 0.74 (standard deviation 0.035) and dynamic friction coefficient of 0.60 (standard deviation 0.046).

The following are the reasons for this recommendation:

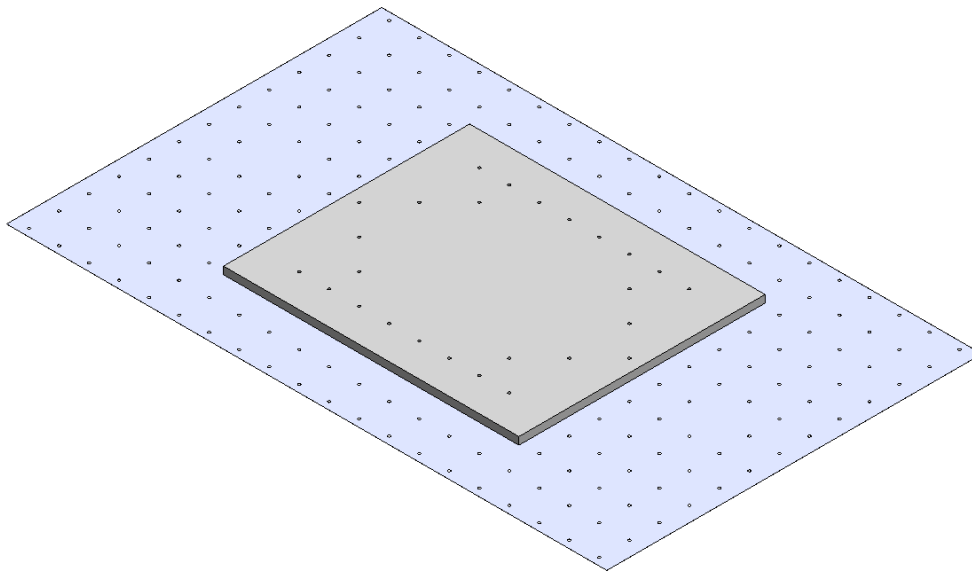
- This surface finish has lowest variation in static and dynamic friction coefficient values.

- The static friction is expected to decrease under the stress conditions (with the loaded cask) only slightly.
- If cask sliding occurs, the sliding velocity is not expected to affect the dynamic friction.
- The number of potential cases with cask sliding is small and is related to the limiting earthquakes scenarios in the WUS.
- Cask sliding absorbs energy so tests with a higher coefficient of friction will lead to higher loadings on the fuel assemblies.

After the concrete slab is installed and the concrete is cured, the push-off tests will be conducted with the same steel block (Figure 4-3) at multiple locations on the slab to obtain the static friction coefficients. The push-off test will be repeated after the shake table test with the vertical cask is completed to determine if there were any changes in friction coefficients.

4.2 Proposed Concrete Slab Configuration

The proposed concrete slab is 196.85" (5.0 m) wide, 236.22" (6.0 m) long and 6" (150 mm) thick. The position of the concrete slab on the shake table is shown in Figure 4-6.



Note: The holes shown on the concrete slab are needed for anchoring the trough and the vertical cask.

Figure 4-6. Concrete slab position on the shake table.

The concrete pad position on the shake table should take into account anchoring of the vertical cask and trough to the shake table. The shake table has multiple holes. The holes needed for anchoring should be accessible after the concrete slab is installed. The other holes that are located within the concrete slab will be used for studs for the slab reinforcement.

The design of the trough allows for an easy anchoring to the table as shown in Figure 4-7. Anchoring the vertical cask will require four clamps shown in Figure 4-8. The clamp system consists of two different configurations to match hole locations on the table. Every clamp plate is 0.5" (12.7 mm) thick. The height of the clamp system is 10" (254 mm).

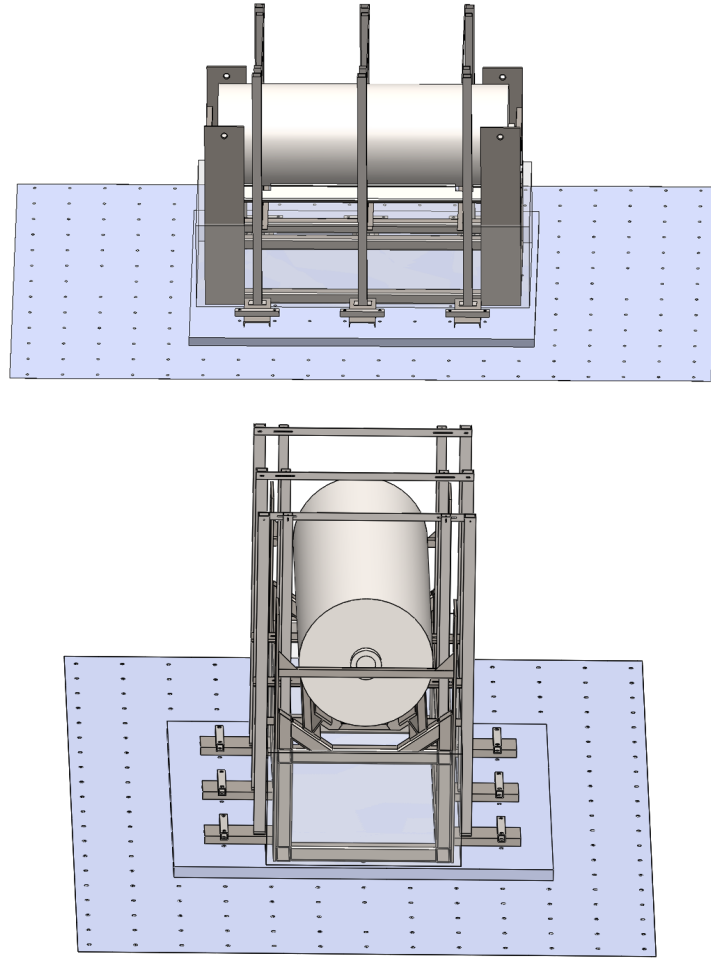


Figure 4-7. Anchoring Trough to the Shake Table.

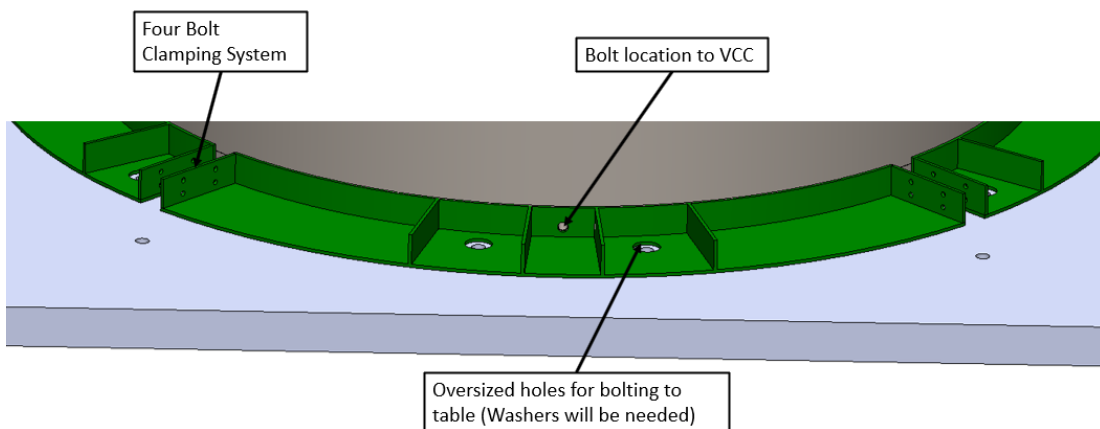


Figure 4-8. Anchoring vertical cask to the shake table.

5. INSTRUMENTATION AND PHOTOMETRICS

5.1 Summary of Results Important for Instrumentation

The instrumentation is guided by the results of the previous experiments ([31] and [22]) and the pre-test modeling in [14] and [32]. The latest pre-test modeling results will be documented in the report due at the end of FY23. These results provided guidance for selecting surrogate assembly rods and locations on the rods for instrumentation with accelerometers and strain gauges.

The discussion of the results from the previous experiments and pre-test modeling is provided in the previous test plan report [7]. Only a few important conclusions from [7] are included in this report.

Figure 5-1 shows 3D distribution of peak strains on the fuel assembly rods in CEUS hard rock scenario (left) and soil scenario (right) corresponding to seismic hazard 5×10^{-5} reproduced from [32]. The peak fuel rod strains occur at the top and bottom of the fuel assembly in the vicinity of the spacer grids. As explained in [32], the spacer grids add lateral stiffness to the fuel assembly and act as stress concentrations. The strains are larger at the bottom of the fuel assembly because the bending moments induced by the seismic excitation are highest toward the bottom. The high strains at the top of the fuel assembly are due to impact between the top nozzle and the basket. These results suggested that one strain gauge placed at the top and three strain gauges placed at the bottom part of the assembly should capture the largest strains on the rods. The peak strain values in nine different cases (calculated in [32]) ranged from 45 to 364 microstrain.

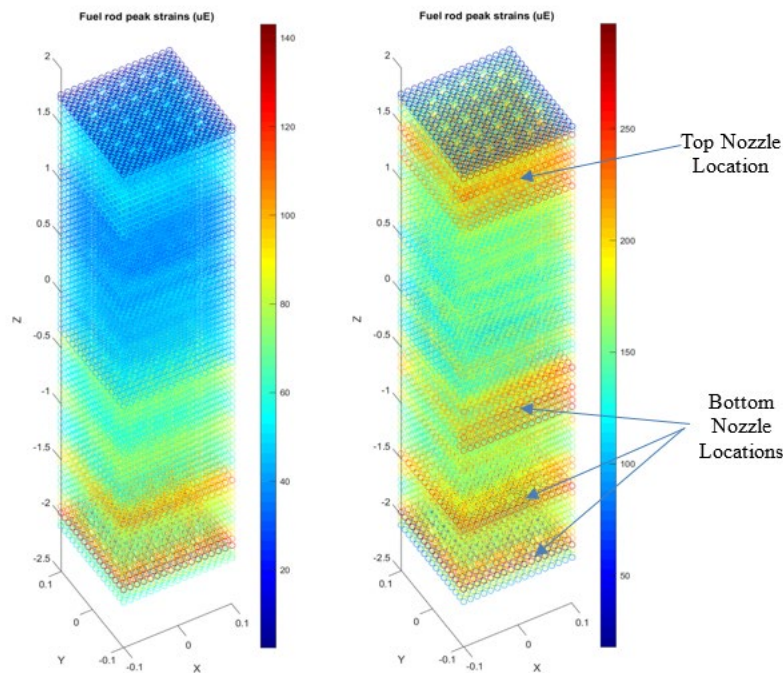


Figure 5-1. 3D distribution of peak strains on the rods in CEUS hard rock (left) and soil scenario (right), seismic hazard 5×10^{-5} from [32].

In FY23, the pre-test modeling extended to the WUS scenarios. The scenario that resulted in the highest strains was the WUS soft rock scenario for Diablo Canyon. The vertical cask in this scenario was free-standing. Figure 5-2 shows 3D distribution of peak strains on the fuel assembly rods and guide tubes in this most limiting scenario. The maximum strain on the rods was 843 microstrain. The maximum strain on the guide tubes was 1,554 microstrain. These results confirm that the previously proposed locations for

the strain gauges and accelerometers should capture the largest strains on the rods in both, CEUS and WUS earthquake scenarios.

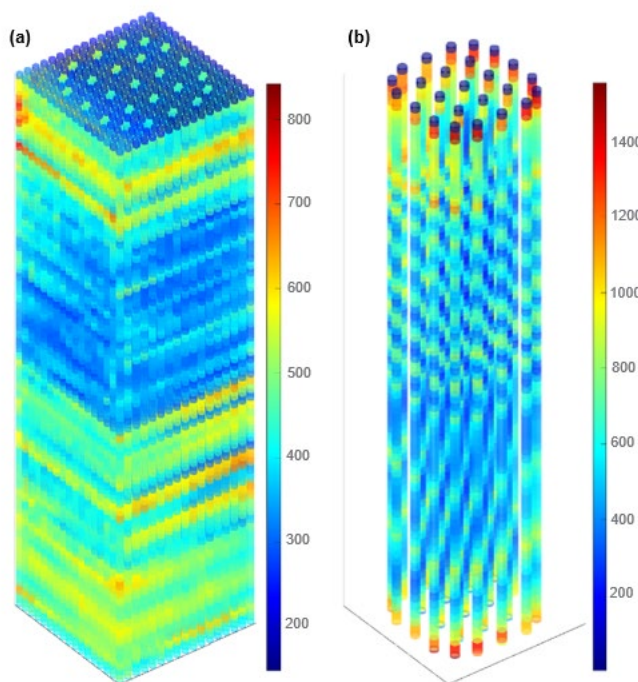


Figure 5-2. 3D distribution of peak strains on the rods and guide tubes in WUS soft rock Diablo Canyon scenario.

The observed strains on the rods within the short middle spans of the surrogate assembly in the 30 cm drop test were 400-600 microstrain [7]. The pressure paper inserted between the rods in these spans did not register rod-to-rod contact. The rod-to-rod contact was registered in the bottom and top long spans at the locations with the observed strain from 400 microstrain to 1,724 microstrain. The pre-test modeling predicted rod-to-rod contact in the Diablo Canyon scenario and WUS soft rock scenario, M 7.5, D 5 km, PGA 0.52 g. It is anticipated that the Diablo Canyon scenario will have to be downscaled to meet the shake table limits (Section 2.5). Consequently, the actual rod-to-rod contact forces will be significantly smaller than the predicted ones. The estimate of the contact pressure in the WUS soft rock scenario is less than 0.1 ksi. Placing pressure paper in the long spans of the surrogate assemblies will allow for registering the rod-to-rod contact if such contact occurs under any of the earthquake scenarios.

The movement of the free-standing vertical cask during the tests will be recorded by dynamic inclinometers. The pre-test modeling suggested that the inclination of the cask during the tests would not be detectable by an instrument with 0.05° resolution for most of the earthquake scenarios. Consequently, the resolution should be at least 0.01°. The most appropriate resolution would be 0.001°.

5.2 Surrogate and Dummy Assembly Instrumentation

5.2.1 Surrogate Assemblies

The major goal of the shake table test is **to measure strains on the surrogate assembly rods**. The pre-test modeling results demonstrated that one strain gauge placed on the rod at the top and three strain gauges placed on the rod at the bottom part of the assembly should capture the largest strains on the rods. To register the variations of responses as the fuel assembly impacts different faces of the basket wall, it is

proposed to instrument one rod on each side of the surrogate assembly. Two centrally located rods in the top row on each side of surrogate assembly were pulled to provide sufficient room for instrumenting one of the central rods in the second row as shown in Figure 5-3.

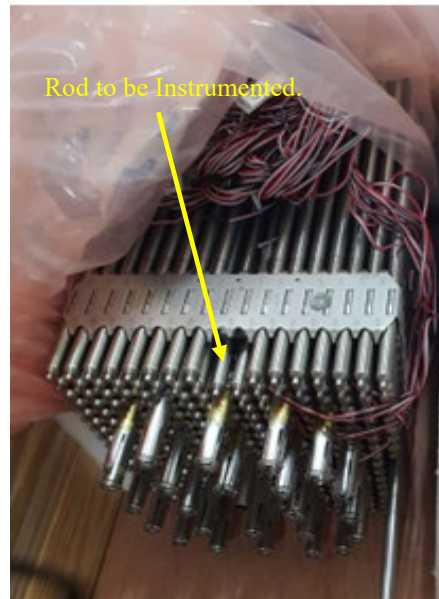


Figure 5-3. Surrogate assembly rod to be instrumented.

The strain gauges acquired for the test are CEA-03-062UW-350 (Figure 5-4, left). This is the same model as the one used in the 30 cm drop tests [33]. The inputs for this test were from the 30 cm drop test of 1/3 scale cask [22]. At each location on the rod, the strain gauges will be placed at 0 degrees and 90 degrees to pick up 3-dimensional vibrations. The total number of strain gauges will be 128 (2 strain gauges per location x 4 locations x 4 rods x 4 surrogate assemblies).

The accelerations on the surrogate assembly rods need to be recorded to provide the inputs for the post-test data analysis and modeling. The accelerometers acquired for the test are Endevco model 727-2K (Figure 5-4, right) with an acceleration range up to 2,000 g. This is the same model as the ones used in the 30 cm drop tests [33].

It is proposed to place uniaxial accelerometers on four rods of each surrogate assembly. These will be the same rods where the strain gauges will be placed. This will allow for filtering high frequency acceleration spikes that do not result in strain spikes. The accelerometers will be placed within the long spacer grid span near the top nozzle and bottom nozzle ends. On two rods (sides 1 and 3), uniaxial accelerometers will be placed at 0°. On the other two rods (sides 2 and 4) they will be placed at 90°. This placement will allow for adequate sampling of the 0° and 90° components. The total number of uniaxial accelerometers will be 32 (1 accelerometer x 2 locations x 4 rods x 4 surrogate assemblies).

One triaxial accelerometer (or uniaxial accelerometer block with three uniaxial accelerometers) will be installed on the top of the surrogate assembly on the tie plate. The top of the assembly banging against the basket is predicted to be a major loading indicator [14]. The purpose of these accelerometers is to track the motion of the surrogate assemblies and the timing of impacts.

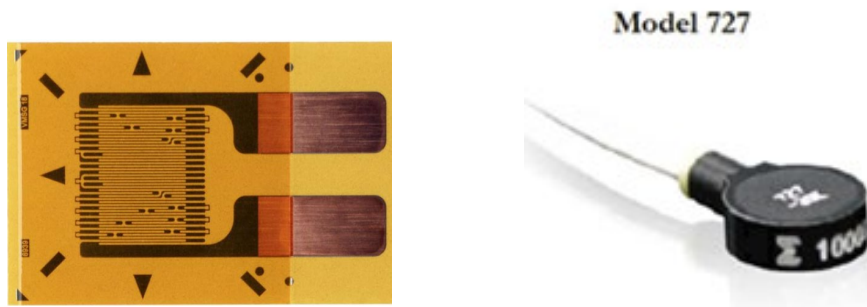


Figure 5-4. Strain gauge CEA-03-062UW-350 (left, not actual size) and accelerometer 727-2K (right, not actual size).

Figure 5-5 shows the locations of the strain gauges and accelerometers on four sides of one surrogate assembly. The other three surrogate assemblies will be instrumented following the same scheme.

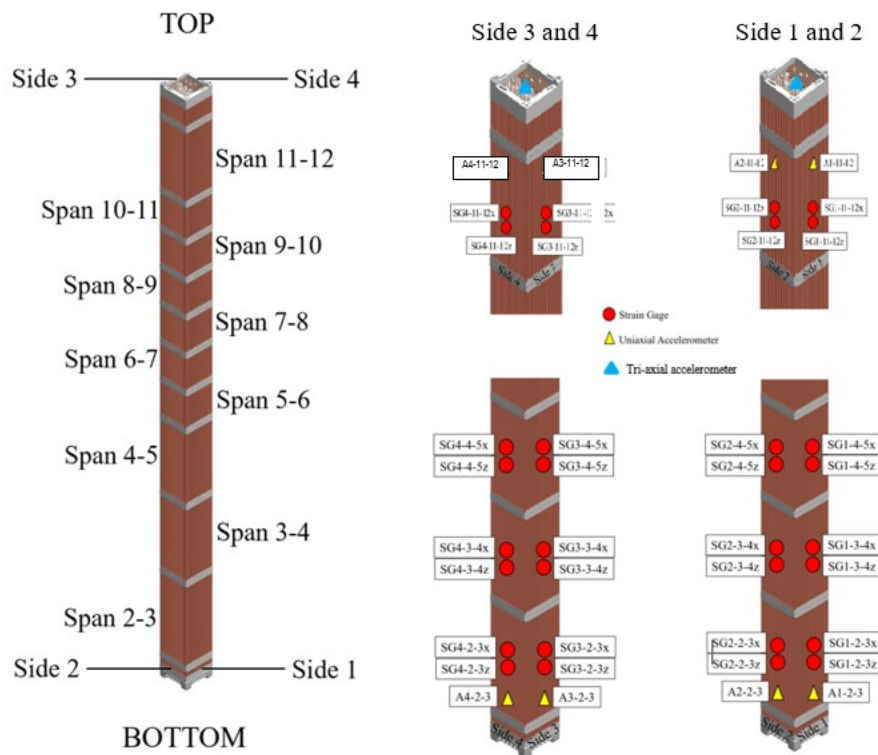


Figure 5-5. Surrogate assembly instrumentation diagram.

Pressure paper (Fujifilm) will be inserted between the rods of the two long spans, one near the assembly bottom and one near its top nozzle, of each surrogate assembly to register rod-to-rod contact if such contact occurs during the test. Table 5-1 shows the available types of the pressure paper. The types acquired for the 30 cm drop test [33] were: extreme low, super low, low, and medium. Because rod-to-rod contact predicted by modeling is below 100 psi, it is proposed to use ultra-low (A) and super low (B) pressure paper in the shake table test. This will cover the contact pressure range of 28 to 350 psi.

Table 5-1. Fujifilm pressure paper specifications.

| Table 1: Fujifilm Prescale® Specifications | | |
|--|---------------------------------|--|
| Film Type | Roll Dimensions | Pressure Range |
| Extreme Low (LLLLW/4LW) | 9.8 ft × 12.2in (3 m × 310mm) | 7.2–28 psi (0.5–1.97 kg/cm ²) |
| Ultra Low (LLLW) | 16.4 ft × 10.6in (5 m × 270mm) | 28–85 psi (2–6 kg/cm ²) |
| Super Low (LLW) | 19.7 ft × 10.6in (6 m × 270mm) | 70–350 psi (5–25 kg/cm ²) |
| Low (LW) | 39.4 ft × 10.6in (12 m × 270mm) | 350–1,400 psi (25–100 kg/cm ²) |
| Medium (MS) | 39.4 ft × 10.6in (12 m × 270mm) | 1,400–7,100 psi (100–500 kg/cm ²) |
| High (HS) | 39.4 ft × 10.6in (12 m × 270mm) | 7,100–18,500 psi (500–1,300 kg/cm ²) |
| Super High (HHS) | 39.4 ft × 10.6in (12 m × 270mm) | 18,500–43,200 psi (1,300–3,000 kg/cm ²) |

Figure 5-6 shows the sequence in which the pressure paper will be installed between the rods of the surrogate assemblies in two long spans. “A” will be installed in the middle rows. “B” will be installed between rod rows 2&3, 3&4, 4&5, and 4&6 and between the 4 bottom rod rows, except the last one and next to last one to leave sufficient room for the instrumentation. These locations were selected because the highest rod-to-rod contact pressures were observed in the top and bottom rows in the 30 cm drop test.

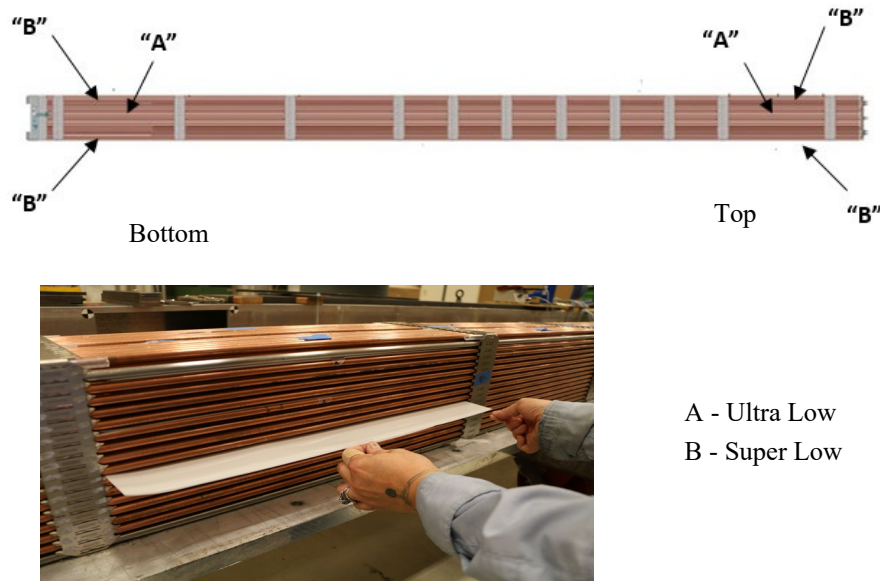


Figure 5-6. Pressure paper locations and specifications.

As discussed above, strain gauges will register the strain time histories in four locations on each instrumented surrogate assembly rod. The pre-test modeling suggested that these location allow for capturing the maximum strain values. To assess this finding, the rod adjacent to one of four instrumented rods on two surrogate assemblies will be instrumented with fiber optic sensors that can measure strain with high spatial resolution.

The selected system is Luna's ODiSI. It provides strain measurements along the entire length of a fiber sensor (up to 20 m long), at a millimeter-scale sensor spacing. These measurements are of strain in the direction of the fiber sensor. Compared to an equivalent solution made of fiber Bragg grating strain sensor arrays, the use of the ODiSI will be more straightforward, will use off-the-shelf sensors, reducing cost and lead-times, and provide much finer strain data, than having to custom design and fabricate fiber Bragg grating sensor arrays that would tend to be costly and call for a longer lead-time.

A single optical channel device would be required, simplifying the cost and the necessary optical connections and entry points into the test unit. This device (ODiSI 6102) with two channels enabled will be rented from Luna for the duration of the test.

Three ODiSI continuous strain-sensing 5 m long fiber sensors will be purchased for the shake table test. Two of them will be placed on the surrogate assembly rods. One of them will be spare. The fiber sensor will be attached using epoxy to the surface of the rod as illustrated in Figure 5-7 (reproduced from [34]).

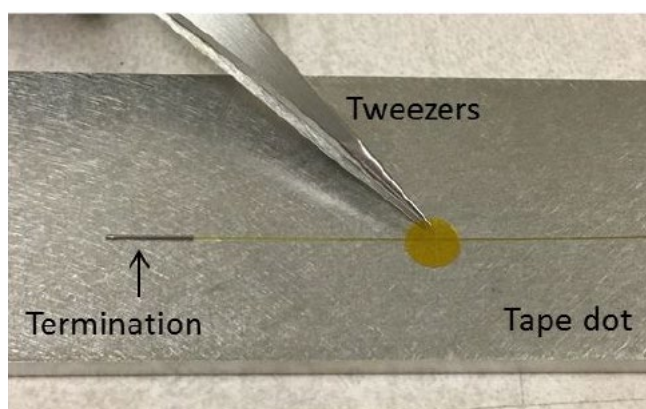


Figure 5-7. Taping down the fiber sensor starting from the termination.

It is expected that measurements can be made with a frequency up to 250 Hz with a 1-2 mm spatial resolution. Placing fiber sensor on the rod adjacent to the rod instrumented with strain gauges will allow for comparing discrete and continuous strain profiles. It is recommended to add two additional strain gauges on the two rods adjacent to the rods with the fiber sensors to enable a more accurate comparison.

5.2.2 Dummy Assemblies

A block of three or a block of two accelerometers (727-2K model) will be installed on the top of each dummy assembly. A tri-axial accelerometer block is shown in Figure 5-8 (right). The accelerometer block will be placed in the dummy assembly niche as shown in Figure 5-8 (left). The total number of blocks with three accelerometers will be 12. The total number of blocks with two accelerometers will be 16. The locations of the dummy assembly with 2-accelerometer and 3-accelerometer blocks are shown in Figure 5-9. This scheme will require 68 uniaxial accelerometers. The high cost of accelerometers precludes installation of 3-accelerometer blocks on each dummy assembly. All three dummy assemblies in the green zone in Figure 5-9 have 3-accelerometer blocks because they are of three different types and have different cross-sections. Around 40% of the assemblies (dummy and surrogate) in the orange and grey areas have 3-accelerometer blocks.

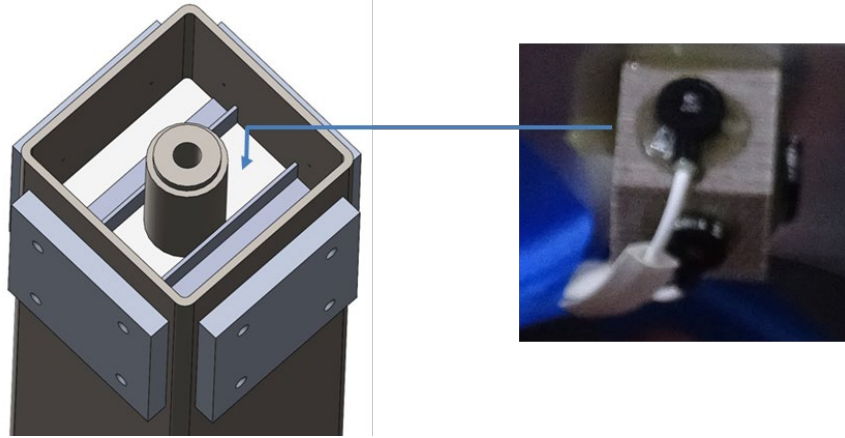


Figure 5-8. Block of three uniaxial accelerometers and its location on the dummy assembly.

| | | | | | |
|---------|---------|---------|---------|---------|---------|
| | 2-axial | 3-axial | 2-axial | 2-axial | |
| 3-axial | 3-axial | 2-axial | 3-axial | 3-axial | 2-axial |
| 2-axial | 2-axial | 3-axial | 3-axial | 2-axial | B |
| 2-axial | 2-axial | A | 3-axial | 2-axial | 2-axial |
| 3-axial | 3-axial | 2-axial | 2-axial | C | 3-axial |
| | D | 2-axial | 3-axial | 2-axial | |

Note: Letters A, B, C, and D denote the surrogate assemblies.

Figure 5-9. Locations of tri-axial and bi-axial accelerometers on the dummy assemblies.

5.3 Canister, Cask, and Trough Instrumentation

Canister (including basket), cask, and trough will be instrumented with accelerometers. This will allow for registering propagation of mechanical loads through all the elements of the test unit.

Two 3-accelerometer blocks separated by 90 degrees will be installed on the top and on the bottom of the canister. Two 3-accelerometer blocks will be installed on the vertical cask top separated by 180 degrees and on each end of one of the bottom flanges of the canister skid rails of the trough. Two uniaxial accelerometers will be installed on the top of the basket next to the accelerometers located on the top of the canister. The total number of uniaxial accelerometers will be 20. Figure 5-10 shows the locations of these accelerometers.

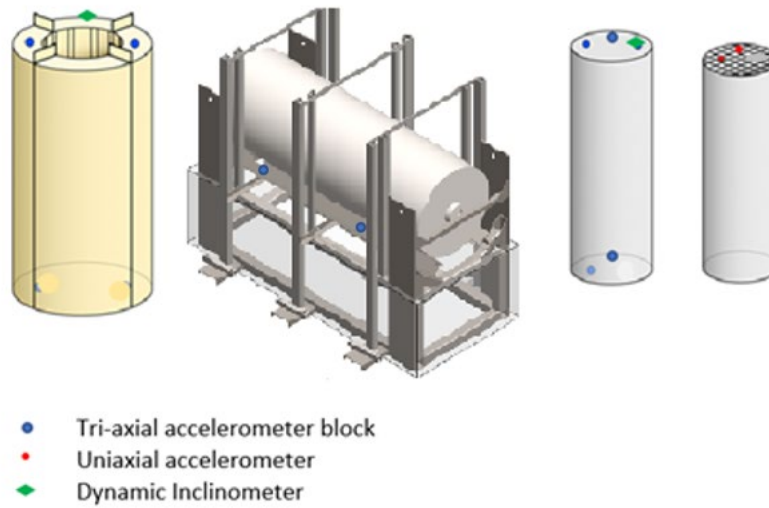


Figure 5-10. Sensor locations on the canister, vertical cask, and trough.

The inclination of the free-standing vertical cask during the tests will be recorded by dynamic inclinometers. The pre-test modeling suggested that the resolution should be $\sim 0.001^\circ$. The dynamic inclinometer that meets that requirement and is compatible with the data acquisition (DAQ) system is Althen Sensors&Controls LCF-3000 Digital Inclinometer (Figure 5-11). This model has three axis, resolution of 6×10^{-5} degrees, and ranges from $\pm 3.0^\circ$ to $\pm 90^\circ$. Operating temperature is from -40°C to $+80^\circ\text{C}$. The shock survival is 1000 g. One inclinometer will be placed on the top of the cask, and one will be placed on the top of the canister as shown in Figure 5-10.



Figure 5-11. Althen LCF-3000 digital inclinometer.

5.4 Instrumentation Summary

Table 5-2 provides the summary of the proposed instrumentation. The sensors listed in this table must be connected to the DAQ system. The total number of required channels is 268.

Table 5-2. Instrumentation summary.

| Instrumented Element | Location | Number |
|------------------------------|-----------------|---------------|
| Accelerometers | | |
| Dummy Assemblies (28) | top | 68 |
| Surrogate Assemblies (4) | tie plate | 12 |
| Surrogate Assemblies (4) | rods | 32 |
| Canister | top | 6 |
| Canister | bottom | 6 |
| Overpack (Cask or Trough) | top | 6 |
| Basket | top | 2 |
| Total | | 132 |
| Strain Gauges | | |
| Surrogate Assembly (2) | rods | 64 |
| Surrogate Assembly (2) | rods | 68 |
| Total | | 132 |
| Fiber Optic Sensors | | |
| Surrogate Assembly (2) | rods | 2 |
| Total | | 2 |
| Dynamic Inclinometers | | |
| Canister | Top | 1 |
| Cask | Top | 1 |
| Total | | 2 |
| TOTAL CHANNELS | | 268 |

5.5 Data Acquisition System

The LHPOST6 facility was recently equipped with a new DAQ system consisting of 13 nodes with 64 channels each (for a total of 832 measurement channels) at 24-bit analog-to-digital resolution, simultaneous sampling, and a sampling rate up to 25.6 kS/sec per channel. A photo of the DAQ system is shown in Figure 5-12. Each node consists of a chassis with a PXI Express backplane that houses the power supply, controller, timing and synchronization module, and the signal conditioning modules (Figure 5-13). The signal conditioning modules also support communicating with transducer electronic data sheets. Each DAQ node also includes three rack-mounted terminal blocks to connect sensors. Each terminal block supports connectivity to three signal conditioning modules allowing for the connection of up to 64 sensors per DAQ node. This DAQ provides superior aliasing rejection with user-configurable digital anti-aliasing filters and zero skew time between different channels due to simultaneous sampling, thus enabling accurate recordings from very small (ambient vibrations) to very large (seismic testing) motions.



Figure 5-12. New LHPOST data acquisition system.

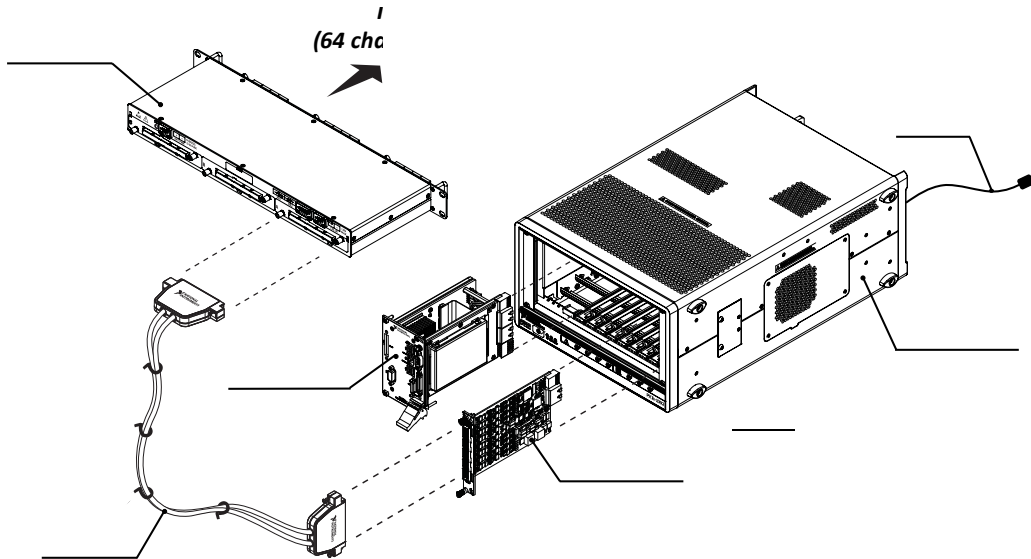


Figure 5-13. Schematic diagram of a single DAQ node.

The 13 DAQ nodes are networked locally through an intranet for synchronization. A trigger line from the shake table controller (MTS 469D) is connected to both the camera system and each DAQ node. When the shake table is operated during a test, a signal is sent to the camera system and the DAQ intranet network simultaneously triggering the recording of all connected sensors and cameras for a fully synchronized and automated data package. Figure 5-14 shows a simplified schematic of this trigger mechanism.

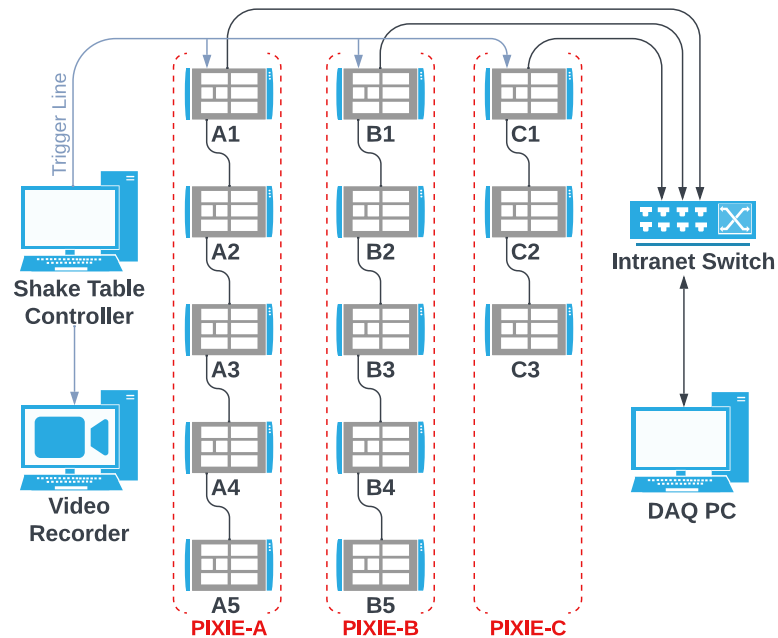


Figure 5-14. Triggering mechanism connecting the MTS 469D shake table controller to the video capture and DAQ systems.

LHPOST has calibration equipment for sensors and DAQ systems, as required for its ISO/IEC Standard 17025:2005 accreditation. The NHERI@UC San Diego Experimental Facility also has a fully configured, end-to-end, live video streaming production system with high resolution and low latency.

LHPOST has a number of different sensors, including accelerometers. However, their resolution is not sufficient. The accelerometers with required high resolution were purchased by SNL specifically for the shake table test.

The LHPOST also has a DJI Phantom 4 Pro (1) and DJI Mavic (1) drones capable of 4K video at 30 frames per second and an array of 1080p and 4K high definition (HD) video cameras running at 30 frames per second (fps) that are fully synchronized with the sensors. These include GoPros 4K (15), Axis 240Q/241Q video servers streaming (4), IQeye streaming/time-lapse video (3). The drones will be used in the shake table test. The high-speed cameras will be provided by SNL. Section 5.6 describes the photometric plan.

5.6 Photometrics

Overview

Non-contact optical measurements will be used to characterize the overall displacement of the cask as well as the fuel assemblies contained within during shake table tests at the UCSD LHPOST facility. The tests will be done for two configurations, vertical and horizontal. For both test setups, three primary high-speed cameras will be used: a Vision Research VEO 990 (4K resolution) camera will be used to quantify the relative movement of the fuel assemblies through an opening in the cask and two Vision Research T3610 cameras will be used to characterize the bulk motion of the cask throughout the shake tests.

Timing

An Irig-B time signal generator will be used to ensure the high-speed camera systems are synchronized to a common time code.

Calibration

Spatial camera and lens calibration procedures will be performed after the camera systems have been rigidly installed. These calibration files will be used for posttest analysis applications.

Communication

The cameras will be operated and armed remotely over an ethernet network.

Power

Each camera will rely on LHPOST facility power but will also be connected to an Uninterrupted Power Supply.

Trigger

All cameras will start their recording from a common TTL event-based trigger supplied by the facility. It is assumed that the facility will record the supplied trigger signal to establish a common start time that can be used to align the instrumentation and optical data.

Lighting

Camera exposures will primarily rely on available light, but artificial lighting will be supplied as deemed necessary to help fill in any harsh shadow areas.

Stills Documentation

Photometrics will document the Seismic Shake test set-up and any notable posttest observables.

The tests with the vertical cask will require the VEO 990 be mounted overhead so that it can see into the cask. It will be secured to a beam that is attached to a tower structure on each side of the shake table. The two T3610s will be at orthogonal locations to the test unit. A potential camera layout for the vertical tests is shown in Figure 5-15 to Figure 5-17.

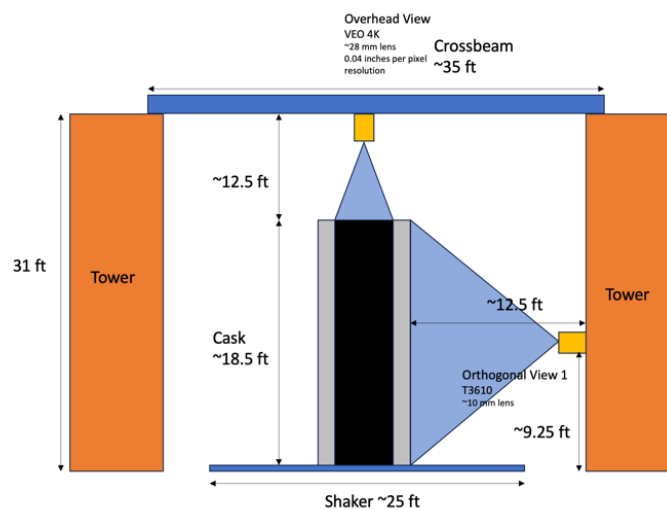


Figure 5-15. Setup for the vertical cask tests in north–south direction.

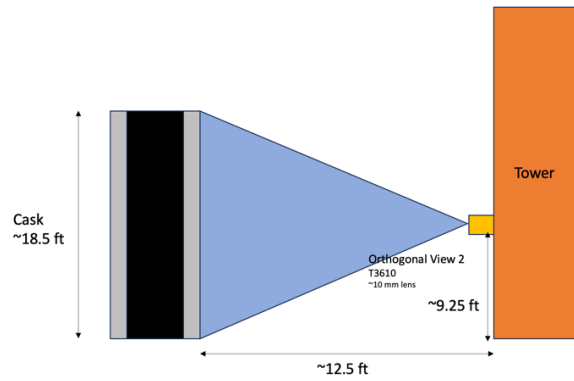


Figure 5-16. Setup for the vertical cask tests in west-east direction.

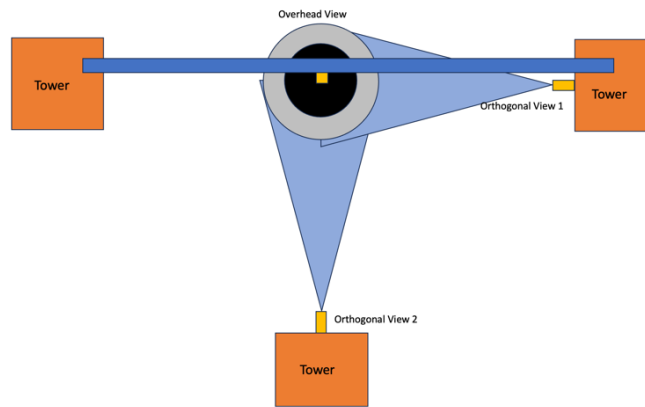


Figure 5-17. Overhead view of the vertical cask setup.

The tests with the trough will consist of the VEO 990 looking into the canister opening from the side position. The two T3610s will be mounted on towers and spaced about 15 degrees from one another so that their data can be triangulated in order to get 3-dimensional tracking of markings on the test unit. Figure 5-18 shows the configuration for the tests with the trough.

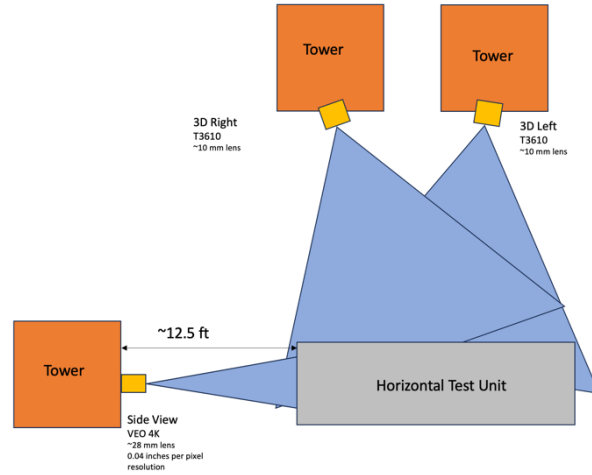


Figure 5-18. Overhead view of the trough setup.

The top ends of the dummy and surrogate assemblies facing the VEO 990 camera will be marked using stickers that are about ½ inch wide. The outside of the vertical cask will have stickers with white and black markings that are identifiable to "Track-eye" software in order to provide tracking of the overall motion. Because the trough does not have walls, the entire canister can be seen. Because of this, in the tests with the trough the stickers will be placed directly on the canister.

6. TEST ACTIVITIES AND SCHEDULE

Per preliminary agreement with LHPOST (UCSD), the start date of the test will be **April 8, 2024**. It is estimated that the test will take approximately 17 weeks to complete. The following sections provide the details of the pre-test and test activities and test schedule.

6.1 Pre-Test Activities

The pre-test activities described in this section include:

- Completing manufacturing of the trough
- Manufacturing of the safety rigging
- Manufacturing of the anchoring clamps for the vertical cask
- Manufacturing and installing restraining fixture on the canister for restricting the dummy and surrogate assembly movement in horizontal configuration when canister is in the trough
- Developing of the assembly, canister, cask, and trough handling procedures
- Surrogate assembly instrumentation
- Shipping canister and surrogate assemblies to LHPOST
- Coordination of SNL ES&H with LHPOST ES&H

Trough Manufacturing

The steel frame of the trough (Section 3.3.2) is being manufactured in Colorado Springs, CO. Per contract, the steel frame will be delivered to LHPOST in November 2023. The frame will be embedded in the concrete box at LHPOST by a concrete contractor. A few parts of the frame (vertical columns) will have to be bolted to the main frame after the concrete work is done. The trough is expected to be completed by the end of December 2023.

Safety Rigging Manufacturing

The pre-test modeling indicated limited sliding of the free-standing cask and no tip over. However, to meet the facility safety requirements, the safety rigging (Section 3.4) has to be used in the tests with the vertical cask. A contract for manufacturing the safety rigging will be placed in October 2023. The safety rigging will be delivered from the manufacturer (TBD) to LHPOST. The expected time of completion is February 2024.

Vertical Cask Anchoring Clamp Manufacturing

Anchoring the vertical cask to the shake table will require 4 clamps (Section 4.2). A contract for manufacturing the clamps will be placed in October 2023. The clamps will be delivered from the manufacturer (TBD) to LHPOST. The expected time of completion is February 2024.

Assembly Restraining Features

In the tests with the trough, the canister will be in a horizontal orientation. Because there is no lid on the canister, the assemblies will be able to move horizontally farther than they would if the lid were in place. The proposed assembly restraining fixture is shown in the diagram in Figure 6-1. It involves drilling and tapping 8 holes in the aluminum spacers at the edges of the basket and two holes in the stainless steel caps between basket tubes. Four sections of aluminum channel will be bolted to the end of the basket. The removable restraining fixture will be installed before the canister is shipped to LHPOST in March 2024.

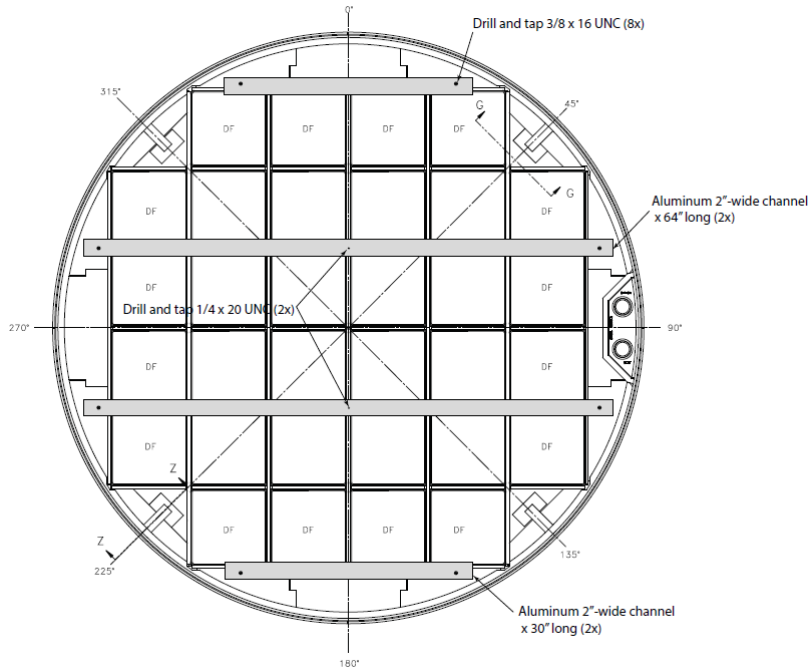


Figure 6-1. Assembly Restraining Fixture.

Handling Procedure Developing

The handling procedures will be developed in the fall of 2023 to describe all handling operations involved in preparing test units for the shake table test. These includes:

- Placing the empty canister in the vertical cask
- Loading dummy and surrogate assemblies into the canister
- Placing cask on the shake table
- Anchoring the cask to the table for selected tests
- Removing vertical cask from the shake table
- Extracting the canister from the cask
- Placing trough on the shake table
- Placing canister into the trough
- Anchoring trough to the shake table
- Removing trough from the shake table
- Extracting cask from the trough
- Removing surrogate assemblies from the canister

Developing of these procedures will require coordination with the crane operators. The LHPOST crane will not be sufficient for handling the majority of the handling operations. A contract with an external crane company will be required.

Surrogate Assembly Instrumentation

Three surrogate assemblies are located at SNL. The instrumentation of these assemblies in accordance with the instrumentation plan (Section 5.2.1) will begin in fall of 2023 and will be completed at the end of February 2024. The fourth surrogate assembly is expected to be delivered at SNL in mid-March 2024 where it will be instrumented.

Shipping Canister and Surrogate Assemblies to LHPOST

The canister and instrumented surrogate assemblies will be shipped to LHPOST in early April 2024.

Coordination of SNL ES&H with LHPOST ES&H

Most activity work will be performed by LHPOST personnel. The SNL staff members will be present at the LHPOST mostly to observe and to guide the activity work. SNL staff will perform some activity work, such as installation of instrumentation and cameras and wiring these to appropriate recording/triggering equipment. Therefore, the coordination with SNL ES&H will be required.

6.2 Test Activities

Per the preliminary agreement with LHPOST (UCSD) the shake table test starting date is April 1, 2024. This is when the use of the LHPOST starts (usage fees begin to apply). The last date of the test is when the shake table is returned to its original conditions (the last day when the usage fees apply). This section describes the activities during this period of time starting with day one rather than April 1, 2024. This will allow for an easy way to adjust time if needed. However, the project schedule (Section 6.3) starts on April 1, 2024.

6.2.1 Prerequisites

The following test hardware will be at the LHPOST before the start of the test:

- Vertical cask
- Trough
- NUHOMS 32 PTH2 canister
- 30 dummy assemblies
- three (or four) instrumented surrogate assemblies (except pressure paper and accelerometers on the top nozzle).
- Safety rigging
- four anchoring clamps for the vertical cask

The PNNL surrogate assembly (4th assembly) may arrive at LHPOST shortly after the beginning of the test. This depends on its delivery time to SNL for instrumentation.

6.2.2 Activity Details

Twenty-two test activities were defined. The details are provided below. The required number of weeks to complete the test is 17.

Activity 1: Installation of concrete slab on the shake table

- Starts on Day 1
- Ends on Day 13

- Duration: 13 days

The concrete slab specifications and configuration are described in Section 4. A contract will be placed with an external concrete contractor in March 2024 to perform this work. The contractor will use studs, wire mesh, anchors, and embedded paraphernalia to secure the connection between the concrete slab and the shake table. The shake table holes located within the concrete slab and required for anchoring the vertical cask and trough will be left open (not filled with concrete). Table 6-1 provides the activity details.

Table 6-1. Concrete slab installation activities.

| NN | Activity | Number | Number per day | Days | Range in Days | |
|-----|--|--------|----------------|------|---------------|------|
| | | | | | Starts | Ends |
| 1.1 | Studs | 40 | 20 | 2 | 1 | 2 |
| 1.2 | Wire mesh, anchors, embedded paraphernalia | - | - | 3 | 3 | 5 |
| 1.3 | Concrete pouring | - | - | 1 | 6 | 6 |
| 1.4 | Concrete curing | - | - | 7 | 7 | 13 |

Activity 2: Shake Table Training

- Starts on Day 11
- Ends on Day 28
- Duration: 18 days

The details regarding this activity are provided in Section 2.5. The estimated number of THs per day during the table training is three. Consequently, it will take 17 days to run 53 THs defined in Sections 2.2-2.4. The training can start on Day 11 when the concrete slab will be sufficiently cured.

Activity 3: Pressure Paper Installation and installing accelerometers on the bottom of the canister.

- Starts on Day 22
- Ends on Day 23
- Duration: 2 days

The pressure paper has to be placed between the surrogate assembly rods within the two long spans (next to top and bottom nozzles) of each of four surrogate assemblies (Section 3.2.2). The 4th surrogate assembly must be delivered to LHPOST prior to the start of this activity. Once the canister is loaded into the vertical cask, the location where the two triaxial accelerometer blocks will not be accessible.

Activity 4: Assembling Vertical Cask Test Unit

- Starts on Day 24
- Ends on Day 25
- Duration: 2 days

This activity can be performed after Activity 1 is completed (the site is clear from the concrete contractor machinery and tools). The Activity 3 must be also completed. It can be performed during the time when Activity 2 takes place.

The vertical cask will remain on the concrete pad next to the shale table for this activity. Assembling the vertical cask test unit starts with placing the canister into the vertical cask and then placing dummy and instrumented surrogate assemblies, including pressure paper, into the canister. The assemblies must be placed in accordance with the loading map described in Section 3.2.3.

This activity may require placing a contract with an external crane company. The handling and loading procedures will be developed in the fall of 2023.

Activity 5: Installing Additional Sensors

- Starts on Day 26
- Ends on Day 27
- Duration: 2 days

This activity has to be performed after Activity 4 is completed. The activity will consist of installing:

- 3- and 2-axial accelerometer blocks on the top of 28 dummy assemblies and 3-axial accelerometer blocks on the top plate of 4 surrogate assemblies (Section 5.2).
- 3-axial accelerometer blocks on the vertical cask and canister and uniaxial accelerometers on the canister basket (Section 5.3).
- Dynamic inclinometers on the vertical cask and canister (Section 5.3).

Activity 6: Placing Vertical Cask on the Shake Table

- Starts on Day 28
- Ends on Day 28
- Duration: 1 day

This activity has to be performed after Activity 2 and Activity 5 are completed. During this activity, the vertical cask loaded with canister and assemblies will be moved from the concrete pad to the shake table. It will be placed in the center of the concrete pad on the shake table.

This activity will require placing a contract with an external crane company. The handling and loading procedures will be developed in the fall of 2023.

Activity 7: Installing Safety Rigging

- Starts on Day 29
- Ends on Day 30
- Duration: 2 days

This activity has to be performed after Activity 6 is completed.

The safety rigging described in Section 3.4 will be installed on the shake table after the vertical cask is placed on the shake table and before the actual tests begin. The parts of the safety rigging will be bolted to the table outside of the concrete slab.

Activity 8: Connecting Sensors to the LHPOST DAQ

- Starts on Day 31
- Ends on Day 39

- Duration: 9 days

This activity can be performed after Activity 7 is completed and in parallel with Activity 8. During this activity, 268 sensors (Section 5.4) will be connected to the LHPOST DAQ. The system will be tested. The estimated time required for connecting and testing is 30 sensors per day. Consequently, 9 days will be needed.

Activity 9: Preparing Photometrics Setup

- Starts on Day 38
- Ends on Day 39
- Duration: 1 days

This activity can be performed after Activity 7 is completed. During this activity, 3 restraining towers will be placed around the shake table as described in Section 5.6. A beam connecting two towers will be placed. The camera locations will be setup and tested.

Activity 10: Tests with Vertical Cask

- Starts on Day 40
- Ends on Day 51
- Duration: 12 days

This activity has to be performed after Activity 9 is completed.

The number of THs proposed for the tests with the vertical cask is 53 (Section 2.2). The estimated number of THs that can be performed per day is five. One day will be required to anchor the vertical cask to the shake table using 4 clamps for the last series of tests. One day will be required for the tests with the anchored cask. Consequently, the duration of this activity is 12 days.

Activity 11: Disconnecting Sensors from the LHPOST DAQ

- Starts on Day 52
- Ends on Day 56
- Duration: 5 days

This activity can be performed after Activity 10 is completed. During this activity, 268 sensors (Section 5.4) will be disconnected from the LHPOST DAQ. The estimated time required for disconnecting is 60 sensors per day. Consequently, 5 days will be needed.

Activity 12: Removing Safety Rigging from the Shake Table

- Starts on Day 53
- Ends on Day 53
- Duration: 1 day

This activity has to be performed after Activity 10 is completed. It can be done in parallel with Activity 11. During this activity the safety rigging will be removed from the shake table.

Activity 13: Removing Vertical Cask from the Shake Table

- Starts on Day 57

- Ends on Day 57
- Duration: 1 day

This activity has to be performed after Activity 11 is completed. During this activity the anchoring clamps will be removed. The vertical cask loaded with canister and assemblies will be moved from the shake table to the concrete pad next to the shake table.

This activity will require placing a contract with an external crane company. The handling and loading procedures will be developed in the fall of 2023.

Activity 14: Loading Canister into the Trough and Placing Trough on the Shake Table

- Starts on Day 58
- Ends on Day 58
- Duration: 1 day

This activity has to be performed after Activity 13 is completed. During this activity the trough will be placed on the shake table and bolted to the table. The assembly restraining fixture (Figure 6-1) will be installed on the canister top. The canister with the assemblies will be pulled from the vertical cask and placed inside the trough.

This activity will require placing a contract with an external crane company. The handling and loading procedures will be developed in the fall of 2023.

Activity 15: Connecting Sensors to the LHPOST DAQ

- Starts on Day 60
- Ends on Day 68
- Duration: 9 days

This activity has to be performed after Activity 14 is completed and in parallel with Activity 15. During this activity, 268 sensors (Section 5.4) will be connected to the LHPOST DAQ. The system will be tested. The estimated time required for connecting and testing is 30 sensors per day. Consequently, 9 days will be needed.

Activity 16: Preparing Photometrics Setup

- Starts on Day 67
- Ends on Day 68
- Duration: 1 day

This activity has to be performed after Activity 14 is completed. During this activity, the restraining towers will be placed in positions required for the tests with the trough (Section 5.6). The camera locations will be setup and tested.

Activity 17: Tests with Trough

- Starts on Day 69
- Ends on Day 76
- Duration: 8 days

This activity has to be performed after Activity 16 is completed.

The number of THs proposed for the tests with the vertical cask is 38 (Section 2.2). The estimated number of THs that can be performed per day is five. Consequently, the duration of this activity is 8 days.

Activity 18: Disconnecting Sensors from the LHPOST DAQ

- Starts on Day 77
- Ends on Day 81
- Duration: 5 days

This activity can be performed after Activity 17 is completed. During this activity, 268 sensors (Section 5.4) will be disconnected from the LHPOST DAQ. The estimated time required for disconnecting is 60 sensors per day. Consequently, 5 days will be needed.

Activity 19: Removing Trough from the Shake Table

- Starts on Day 82
- Ends on Day 82
- Duration: 1 days

This activity has to be performed after Activity 18 is completed. During this activity the trough anchoring system will be removed. The trough with the canister and assemblies will be moved from the shake table to its location next to the shake table. The canister loaded with the assemblies will be extracted from the trough and placed on the ground in a designated location.

This activity will require placing a contract with an external crane company. The handling and loading procedures will be developed in the fall of 2023.

Activity 20: Shake Table Restoration

- Starts on Day 83
- Ends on Day 86
- Duration: 4 days

This activity has to be performed after Activity 19 is completed. This activity will require a contract with a concrete contractor and with a painting contractor. During this activity the concrete contractor will demolish the concrete slab and will remove studs from the table. The painting contractor will perform grinding of the shake table surface and will paint it.

Activity 21: Vertical Cask and Trough Demolishing

- Starts on Day 85
- Ends on Day 87
- Duration: 3 days

This activity can start two days after Activity 20, after the concrete slab is demolished. This activity will require a contract with a concrete contractor. During this activity the contractor will demolish the cask and the trough and will remove their debris and the safety structure from the LHPOST.

Activity 22: Shipping Canister and Assemblies

- Starts on Day 83
- Ends on Day 85
- Duration: 3 days

This activity can be performed in parallel with Activity 20. During this activity, the surrogate assemblies will be extracted from the canister and will be placed in the shipping containers. One surrogate assembly will be shipped to SNL, one surrogate assembly will be shipped to PNL, and two surrogate assemblies will be shipped to KNF. The canister with the dummy assemblies will be shipped to SNL.

This activity may require placing a contract with an external crane company. The handling and loading procedures will be developed in the fall of 2023.

6.3 Test Schedule

The shake table test schedule generated based on the activities described in Section 6.2 is shown in Figure 6-2. The test starts on Monday, April 8, 2024, and ends on Tuesday, August 6. The test duration is approximately 17 weeks. The important test dates are:

- **Test with the vertical cask:** Tuesday, **May 30, 2024**, to Friday, **June 14, 2024**.
- **Test with the trough:** Thursday, **July 11, 2024**, to Monday, **July 22, 2024**.

The schedule will be adjusted to accommodate the changes in the test and or individual activity start dates (if any) and activity durations.

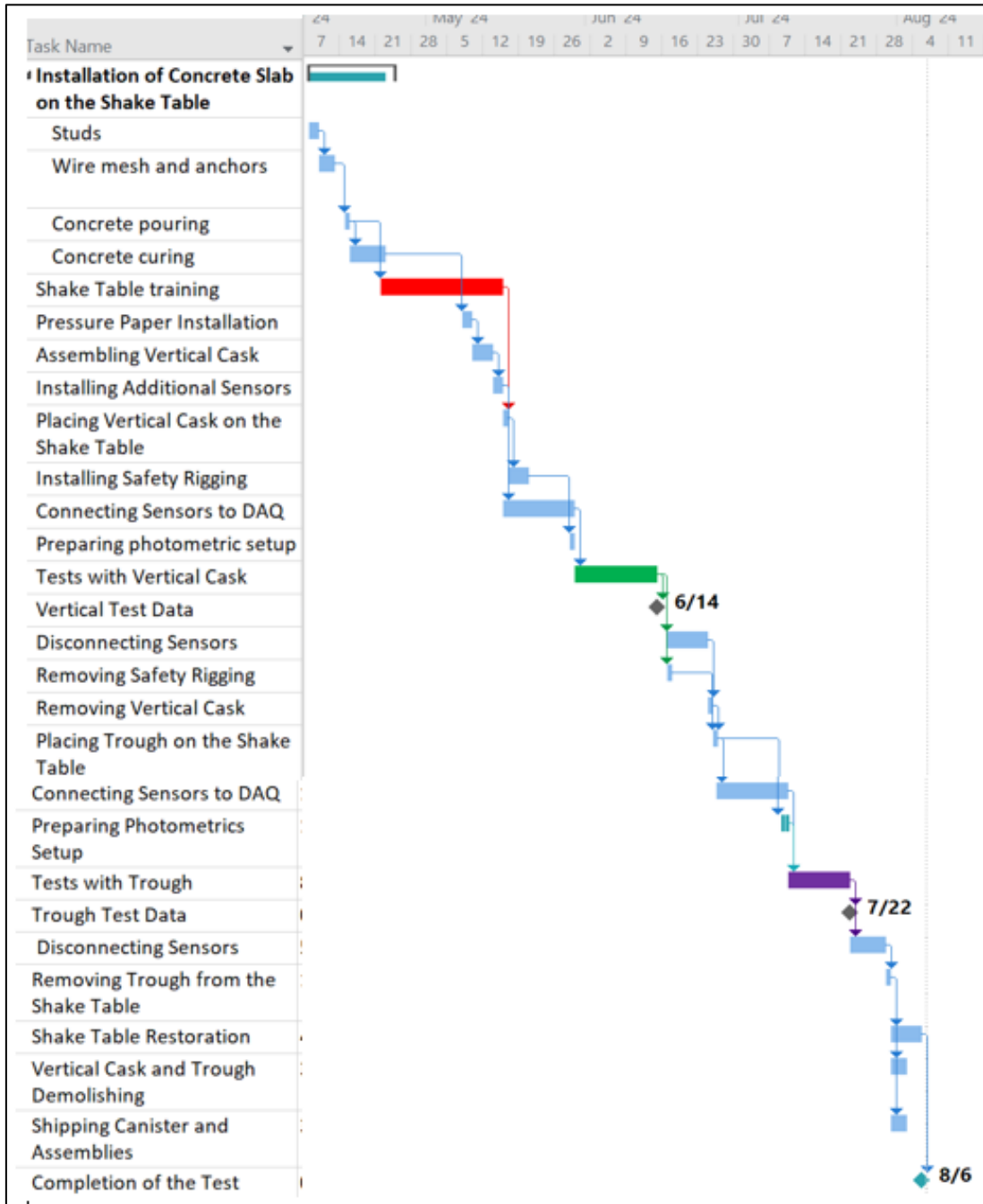


Figure 6-2. Shake table test schedule.

7. REFERENCES

- [1] E. Kalinina and D. Ammerman, "Shake Table Test Plan," Sandia National Laboratory, Albuquerque, 2020.
- [2] N. Gregor and L. A. Atik, "Ground Motions for Shake-Table Testing of Dry Casks," SC Solutions, 2021.
- [3] E. Kalinina, L. Lujan, N. Gregor and L. Al Atik, "Ground Motion Inputs for the Seismic Shake Table Test," Sandia National Laboratories, Albuquerque, 2021.
- [4] E. Kalinina, D. Ammerman and L. Lujan, "Seismic Shake Table Test Plan," Sandia National Laboratories, Albuquerque, NM, 2021.
- [5] J. Garcia, "Soil Structure Interaction (SSI) Report Supporting Shake Table Testing of Dry Storage Casks," SC Solutions, 2021.
- [6] J. Garcia, H. Hayati, L. Lujan and W. R. Johnson, "Soil Structure Interaction (SSI) Simulations Supporting Shake Table Testing of Dry Storage Casks," SC Solutions, Inc., 2022.
- [7] E. Kalinina, D. Ammerman, L. Lujan and G. Flores, "Updated Seismic Shake Table Test Plan," Sandia National Laboratories, 2022.
- [8] M. Taha, "Concrete Surface Friction Testing," UNM, Albuquerque, NM, 2022.
- [9] W. Johnson, "Soil Structure Interaction Simulations for Shake Table Testing of Horizontal Storage Modules," Savannah River National Laboratory, Jackson, SC, 2023.
- [10] E. Kalinina, W. Johnson and L. Lujan, "Response of the Pad with Horizontal Storage Modules with Account for Soil-Structure Interaction," Sandia National Laboratories, Albuquerque, NM, 2023.
- [11] N. Klymyshyn, K. Kadooka, J. Fitzpatrick and C. Spitz, "Modeling a Spent Nuclear Fuel Cask Seismic," in *ASME PVP-2023*, Atlanta, GA, 2023.
- [12] N. K. K. S. C. M. T. B. N. S. L. W. W. Klymyshyn, "Spent Nuclear Fuel Seismic Pre-Test Modeling, Part 2, PNNL-35000," Pacific Northwest National Laboratory, Richland, WA, 2023.
- [13] E. Kalinina and L. Lujan, "Friction Experiment Data Analysis," Sandia National Laboratories, Albuquerque, NM, 2023.
- [14] N. Klymyshyn, P. Ivanusa, C. Spitz, K. Kadooka, C. T. Mason, B. Jensen, J. A. Bamberger, C. Campbell and D. K. Fagan, "Modeling and Analysis for Spent Nuclear Fuel Seismic Testing," PNNL, 2021.
- [15] N. Klymyshyn, K. Kadooka, T. Mason, C. Spitz, J. Fitzpatrick, N. Barrett, A. Rigato, P. Ivanusa, A. Lynch, B. Hanson and S. Ross, "Spent Nuclear Fuel Seismic Pre-Test Modeling, Part 1," Pacific Northwest National Laboratory, Richland, WA, 2022.
- [16] Y. Bozorgnia, N. Abrahamson, L. Atik, T. Ancheta, G. Atkinson, J. Baker, A. Baltay, D. Boore, K. Campbell, B. Chiou, R. Darragh, D. Day, R. Graves, N. Gregor, T. Hanks, I. Idriss, R. Kamai, T. Kishida and A. Kottke, "NGA-West2 Program," *Earthquake Spectra*, Vols. Vol. 30., pp. pp. 973-987, 2014.

- [17] U.S. Nuclear Regulatory Commission, "A Performance Based Approach to Define the Site-Specific Earthquake Ground Motion," Regulatory Guide 1.208, 2007.
- [18] D. Bhargava, D. Heacock and E. Hendrixson, "MINERAL, VIRGINIA USA MW 5.8 EARTHQUAKE OF 2011: RESPONSE," in *SMiRT-23*, Manchester, UK, 2023.
- [19] B. Widrow and P. Stearns, Adaptive Signal Processing 1st edition by Widrow, Bernard, Stearns, Peter N., Prentice Hall, 1985.
- [20] J. Bondre, "A Complete NUHOMS® Solution for Storage and Transport of High Burnup Spent Fuel," in *14th International Symposium on the Packaging and Transportation of Radioactive Materials, PATRAM-2004*, Berlin, Germany, 2004.
- [21] C. Mason, "Dummy Assembly Drawings," PNNL, 2021.
- [22] E. Kalinina, D. Ammerman, C. Grey and M. W. C. F. G. S. S. Arviso, "Surrogate Assembly 30 cm Drop Test," Sandia National Laboratories, SAND2019-15256 R, Albuquerque, NM, 2019.
- [23] T. Mason, "Vertical Cask Drawings," PNNL, 2021.
- [24] V. Luk, B. Spencer, I. Lam and R. Dameron, "Parametric Evaluation of Freestanding Spent Fuel," Sandia National laboratories, Albuquerque, 2005.
- [25] H. International, "Final Safety Analysis Report for the HI-STORM 100 Cask System rev 11," NRC, Waashington, D.C., 2013.
- [26] E. Corportion, "Grand Gulf Nuclear Station Unit 3 Combined License Application Final Safety Analysis Report," NRC, Washington, D.C., 2008.
- [27] P. Baltay and A. Gjelsvik, "Coefficient of friction for steel on concrete at high normal stress," *Journal of Materials in Civil Engineering*, vol. 2, no. 1, pp. 46-49, 1990.
- [28] B. Rabbat and H. Russell, "Friction coefficient of steel on concrete or grout.," *Journal of Structural Engineering*, vol. 111, no. 3, pp. 505-515, 1985.
- [29] J. McCormick, T. Nagae, M. Ikenaga, P.-C. Zhang, M. Katsuo and M. Nakashima, "Investigation of the sliding behavior between steel and mortar," *Earthquake Engineering & Structural Dynamics*, vol. 38, no. 12, p. 1401–1419, 2009.
- [30] E. Ahmeta and B. Tuncan, "Determination of Friction Behaviour between Concrete and Steel Tubre Interaction," in *EUROSTEEL 2014*, Naples, Italy, 2014.
- [31] E. Kalinina, C. Wright, L. Lujan, N. Gordon, S. Saltzstein and K. Norman, "Data Analysis of ENSA/DOE Rail Cask Tests,," Sandia National laboratories, Albuquerque, NM, 2018.
- [32] K. Kaddoka, N. Klymyshyn, J. Fitzpatrick and N. Barrett, "Spent Nuclear Fuel Modeling Methods for Seismic Loads," Pacific Northwest national Laboratory, 2022.
- [33] E. A. Kalinina, D. Ammerman, C. Grey, G. Flores, L. Lujan, S. Saltzstein and D. Michel, "Surrogate Assembly 30 cm Drop Test," SAND2020-10498 R, Sandia National Laboratories, Albuquerque, NM, 2020.
- [34] Luna, "ODiSI Fiber Optic Sensor Installation Guide," Luna, 2017.